Electronic Supplementary Material (ESI) for Dalton Transactions.

Potent and Selective Anticancer Activity of Half-Sandwich Ruthenium and Osmium Complexes with Modified Curcuminoid Ligands

Noemi Pagliaricci,[a] Riccardo Pettinari,[a] Fabio Marchetti,[b] Claudio Pettinari,[a] Loredana Cappellacci,[a] Alessia Tombesi,[a] Massimiliano Cuccioloni,[c] Mouna Hadiji,[d] Paul J. Dyson.[d]**

[a]School of Pharmacy, [b]School of Science and Technology and [c]School of Biosciences and Veterinary Medicine, University of Camerino, via Madonna delle Carceri (ChIP), 62032 Camerino, Italy. [d]Institut des Sciences et Ingénierie Chimiques, École Polytechnique Fédérale de Lausanne (EPFL), 1015 Lausanne, Switzerland.

Supporting Information

Index

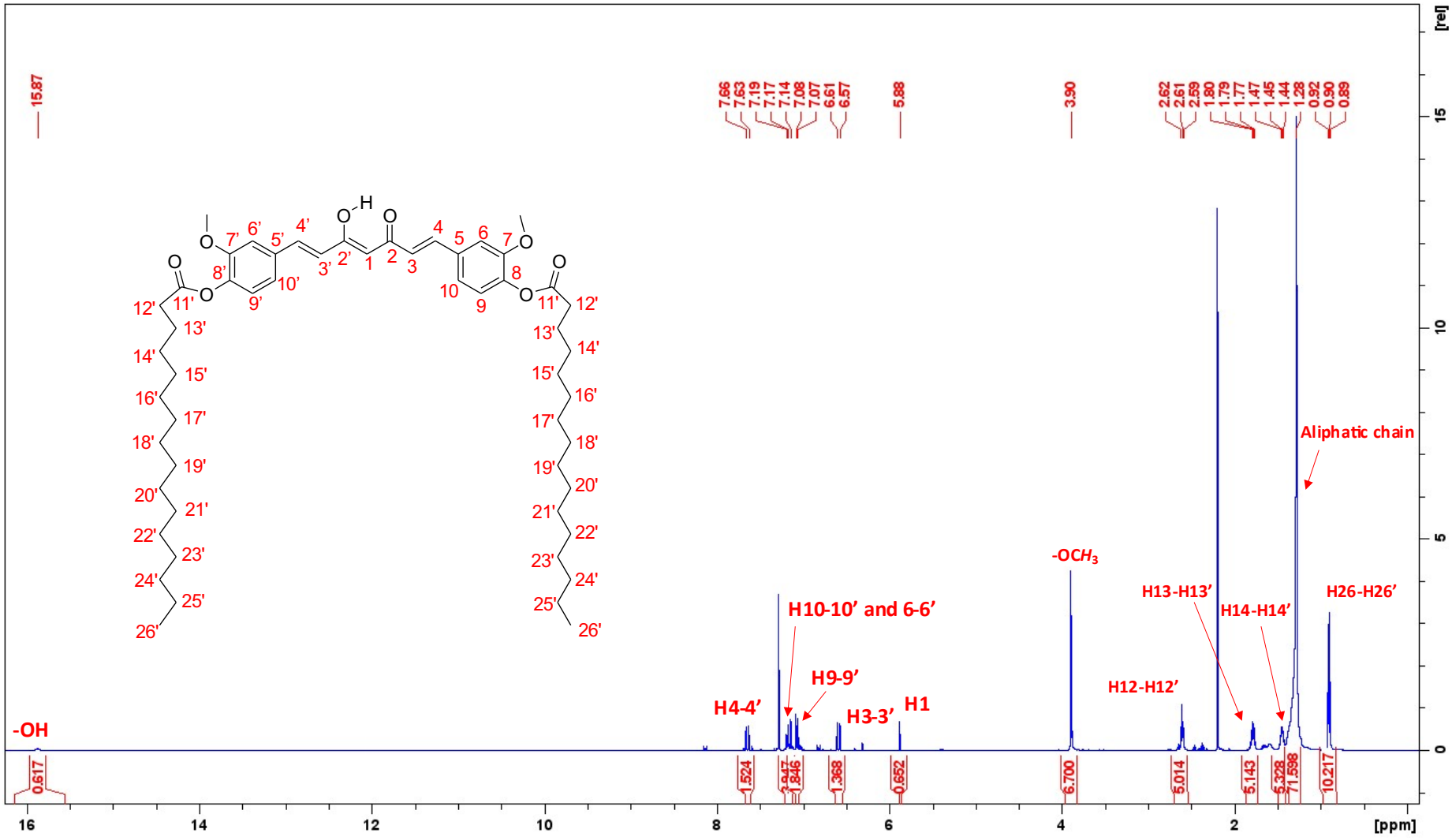

Figure S1. ^{1}H-NMR of p-curcH in $CDCl_3$ at 293 K

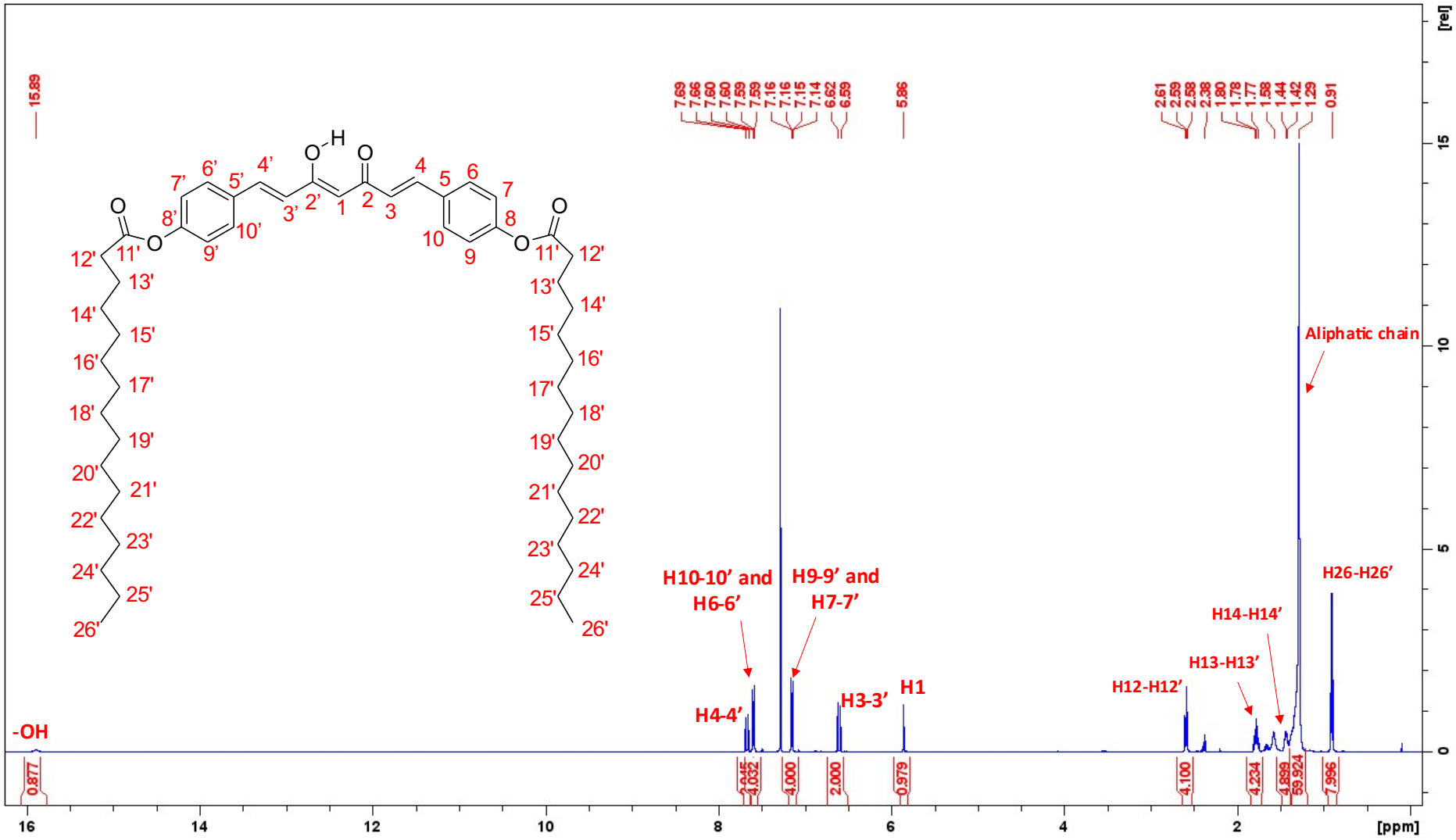

Figure S2. ^{1}H-NMR of p-bdcurcH in $CDCl_3$ at 293 K

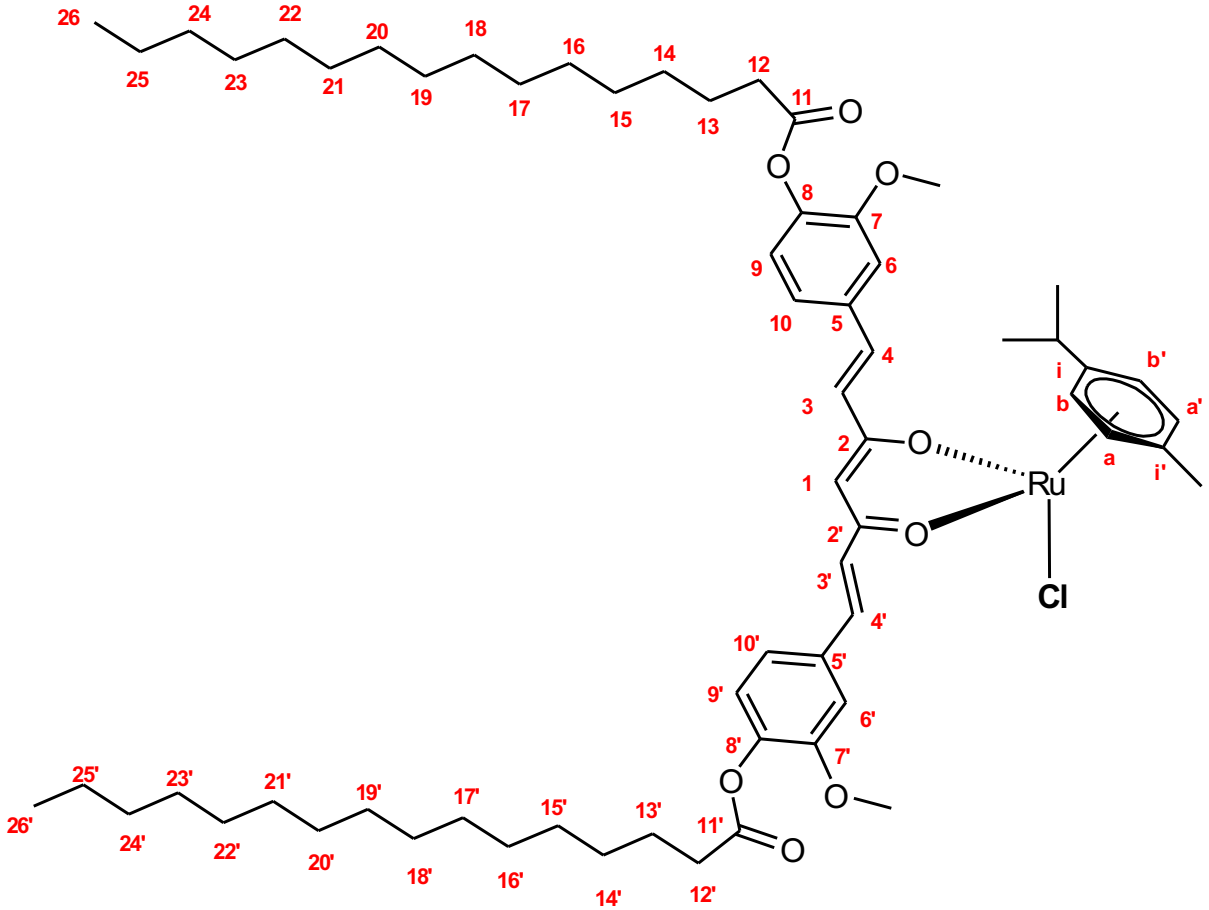
26
24
22
20
18
16
14
12
11
25
23
21
19
17
15
13
O
O
8
7
9
6
10
5
4
3
2
1
O
Ru
2'
O
3'
4'
10'
5'
9'
6'
8'
7'
O
O
Cl
i
b'
b
a'
a
i'
25'
23'
21'
19'
17'
15'
13'
11'
26'
24'
22'
20'
18'
16'
14'
12'
O

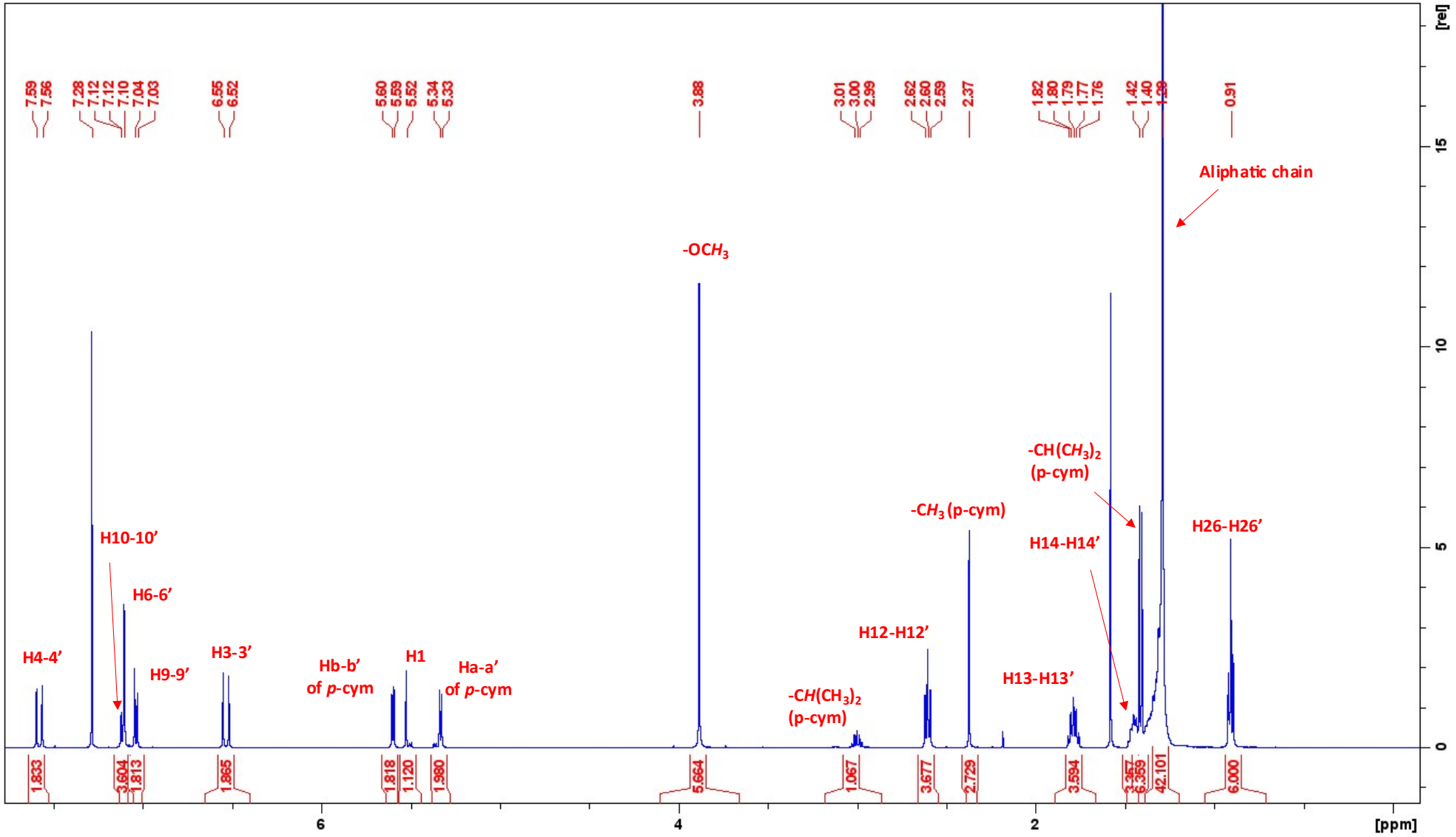

Figure S3. ^{1}H-NMR of **1** in $CDCl_3$ at 298 K

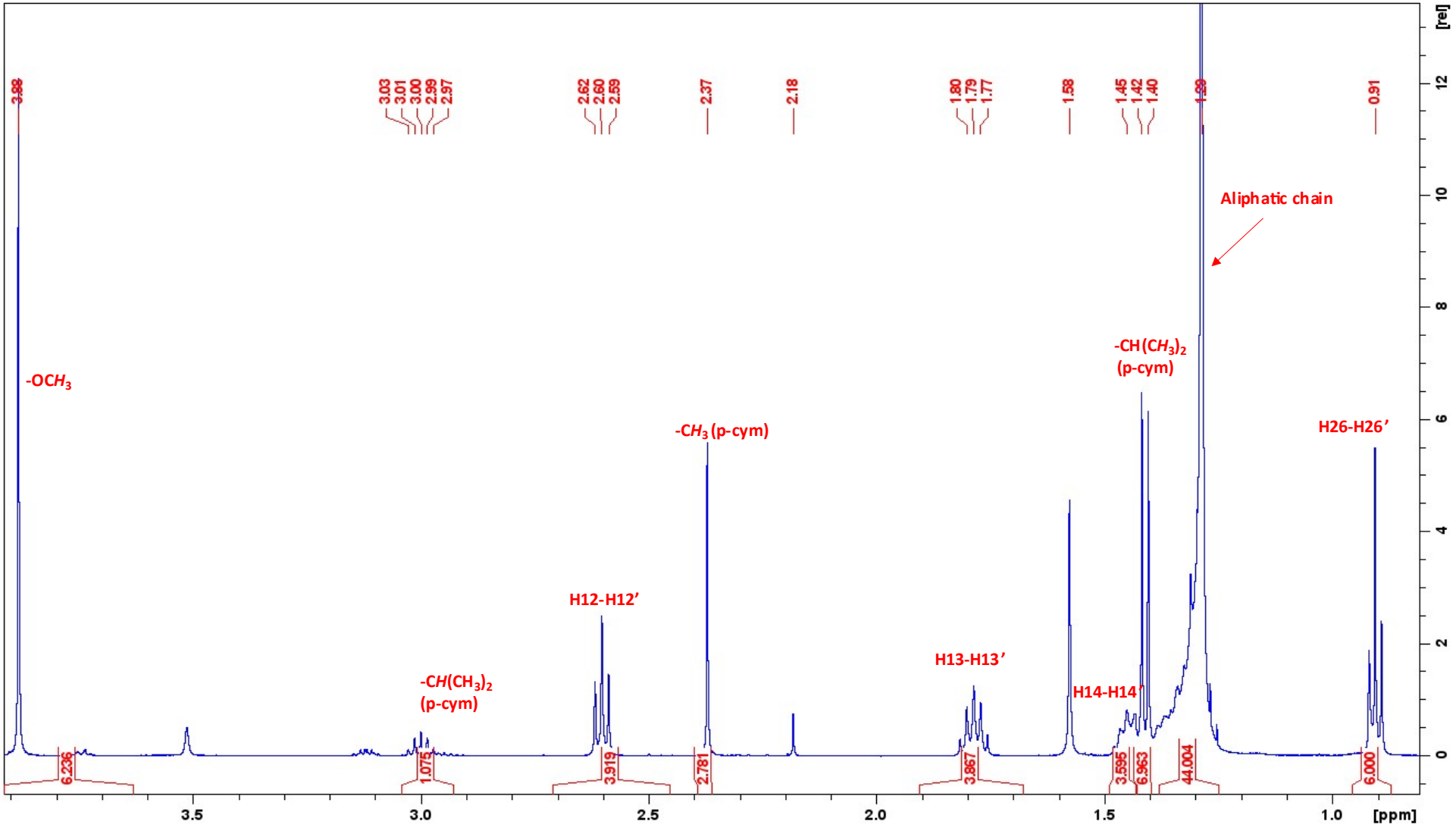

Figure S3 (a). Magnification of ^{1}H-NMR (range 1-4 ppm)

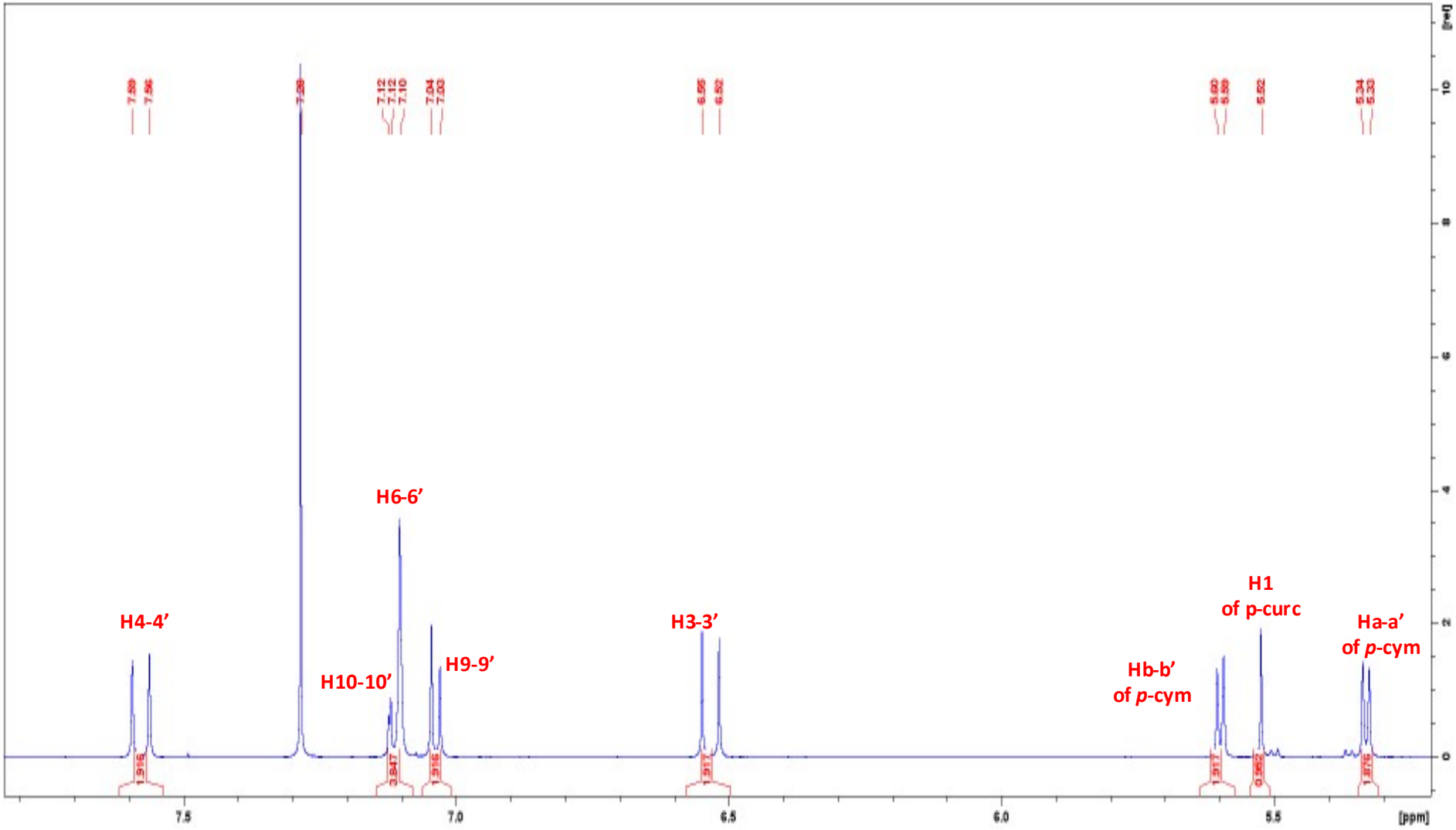

Figure S3 (b). Magnification of ^{1}H-NMR (range 4-8 ppm)

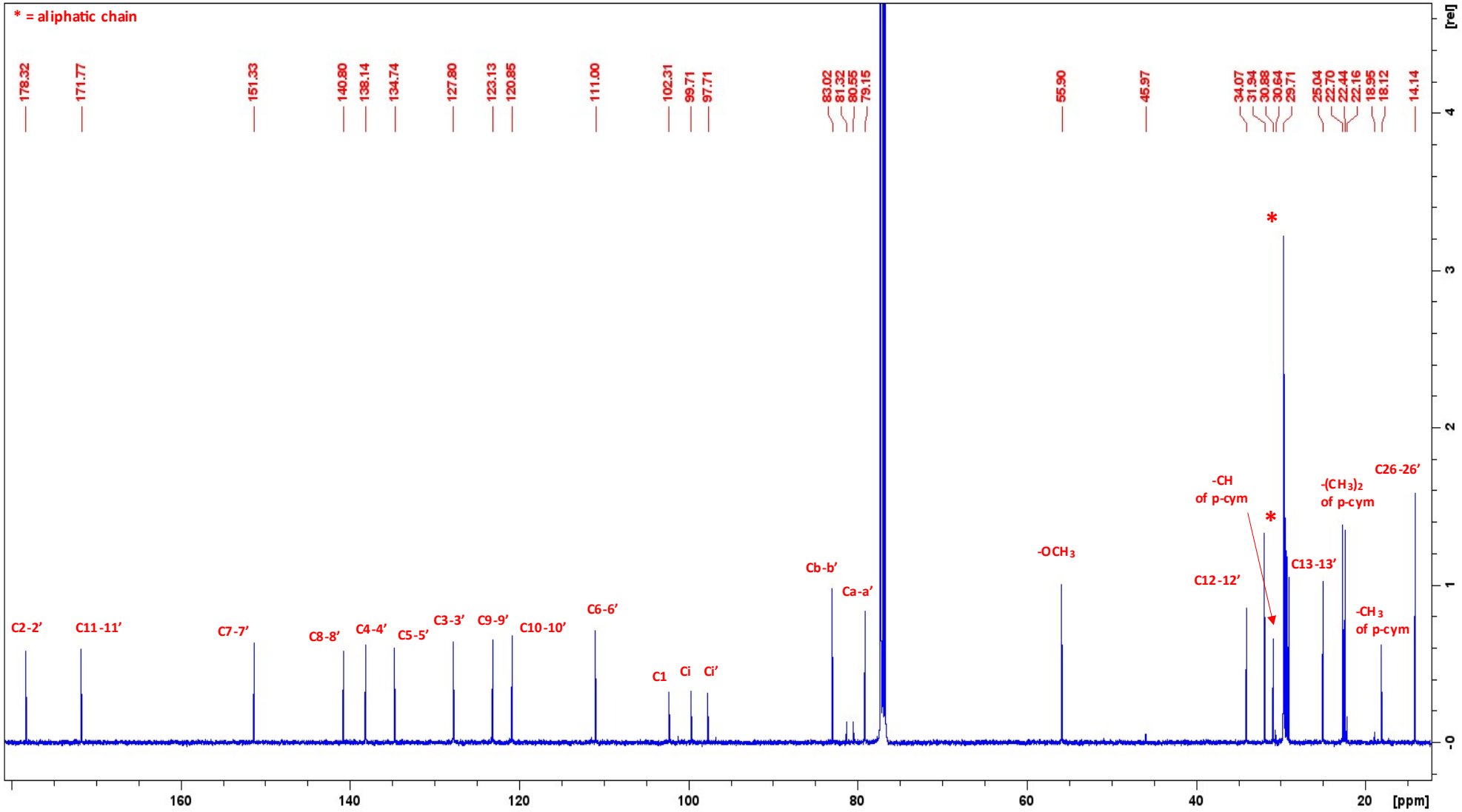

Figure S4. ^{13}C-NMR of **1** in $CDCl_3$ at 293 K

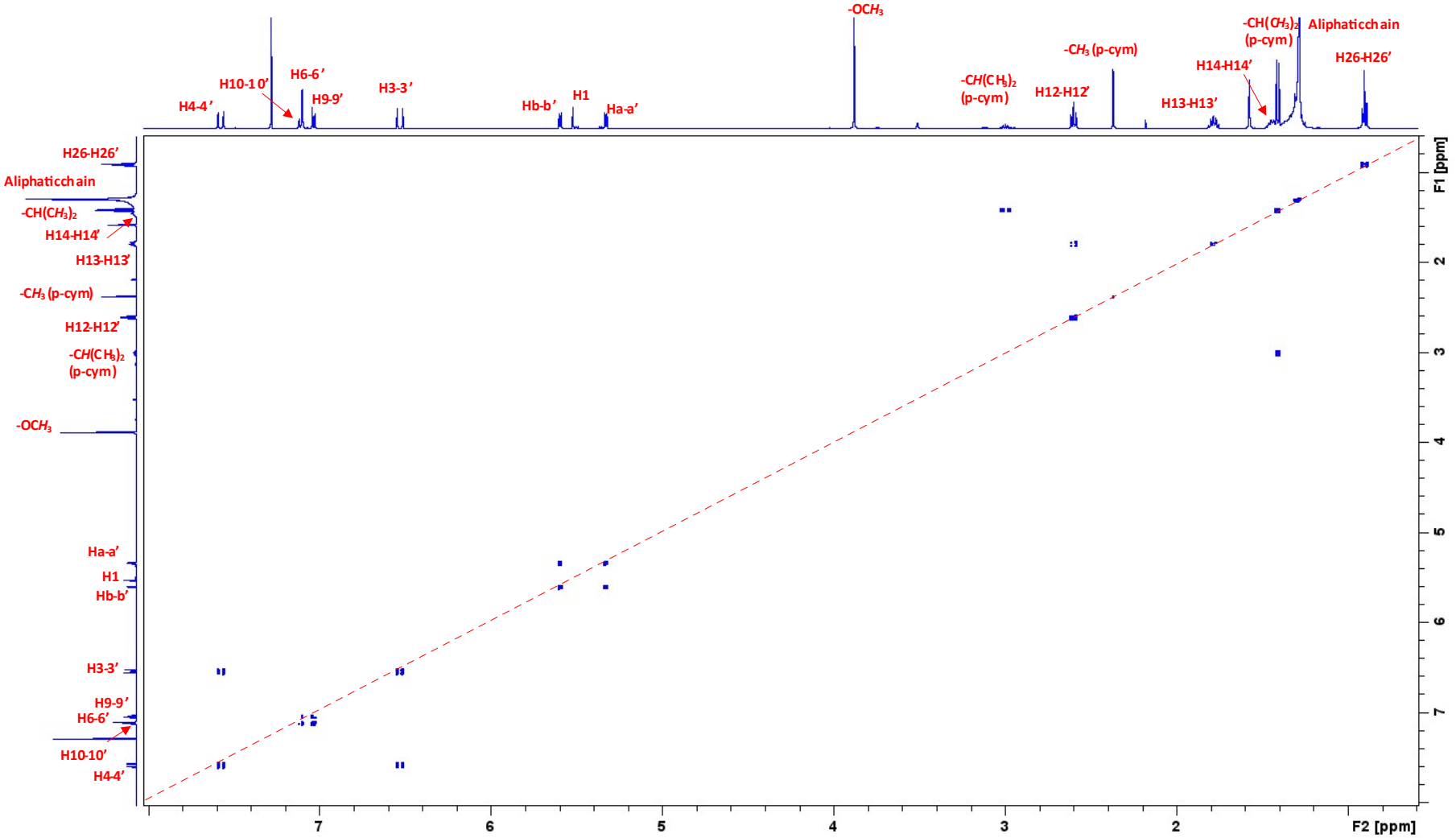

Figure S5. {^{1}H-^{1}H}-COSY NMR of **1** in $CDCl_3$ at 293 K

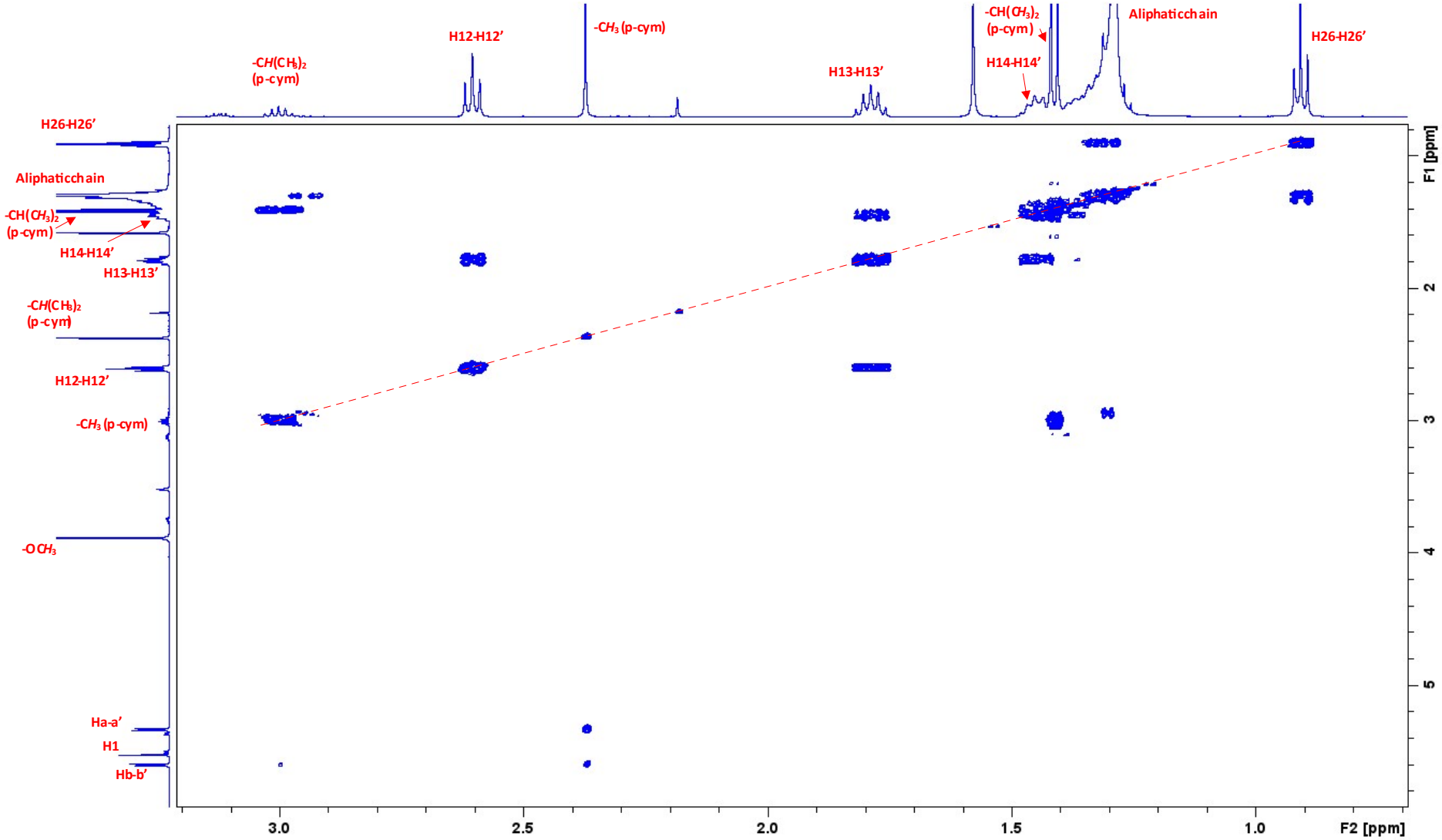

Figure S5 (a). Magnification of {^{1}H-^{1}H}-COSY NMR

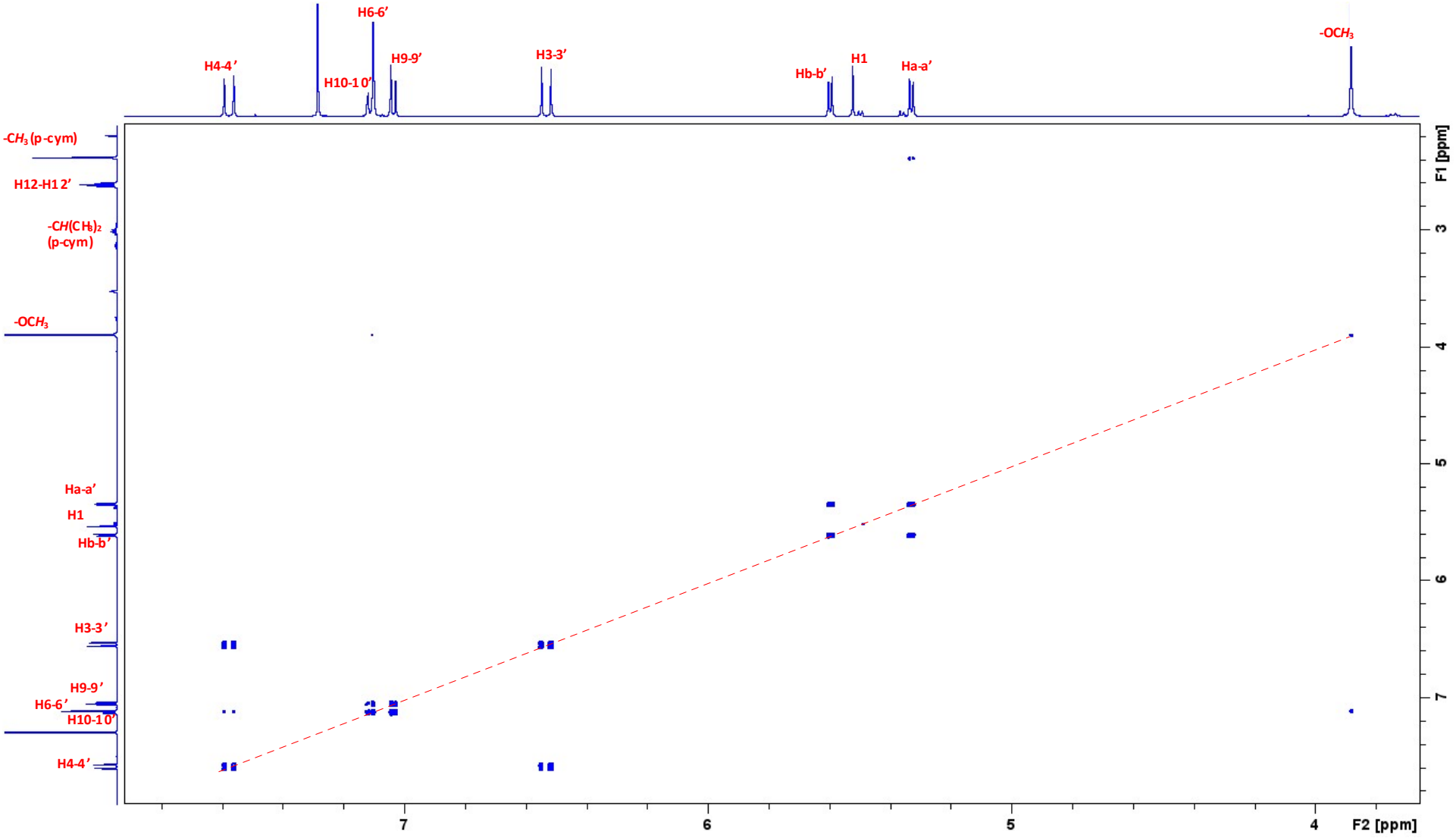

Figure S5 (b). Magnification of {^{1}H-^{1}H}-COSY NMR

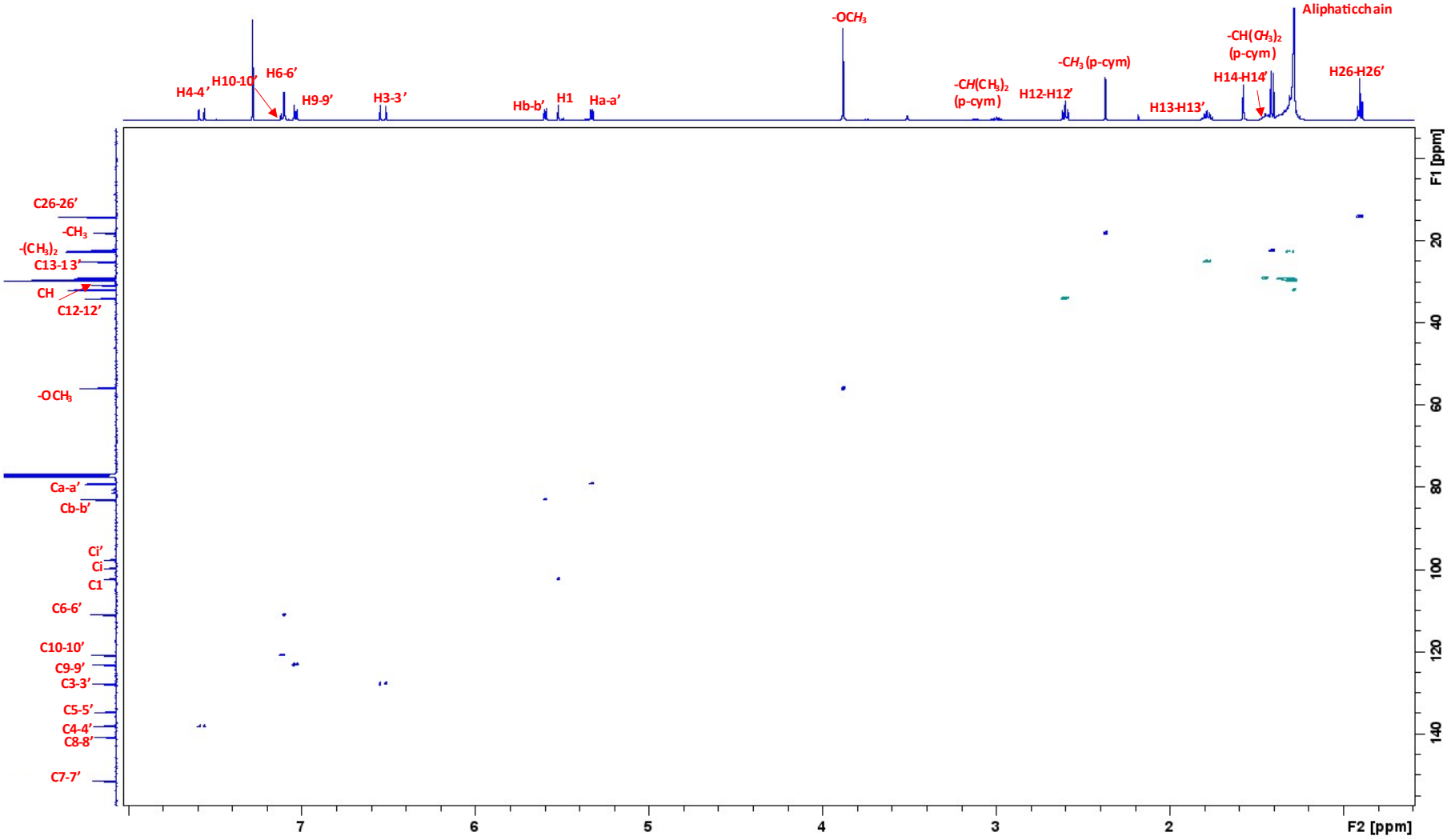

Figure S6. {^{1}H-^{13}C}-HSQC NMR of **1** in $CDCl_3$ at 293 K

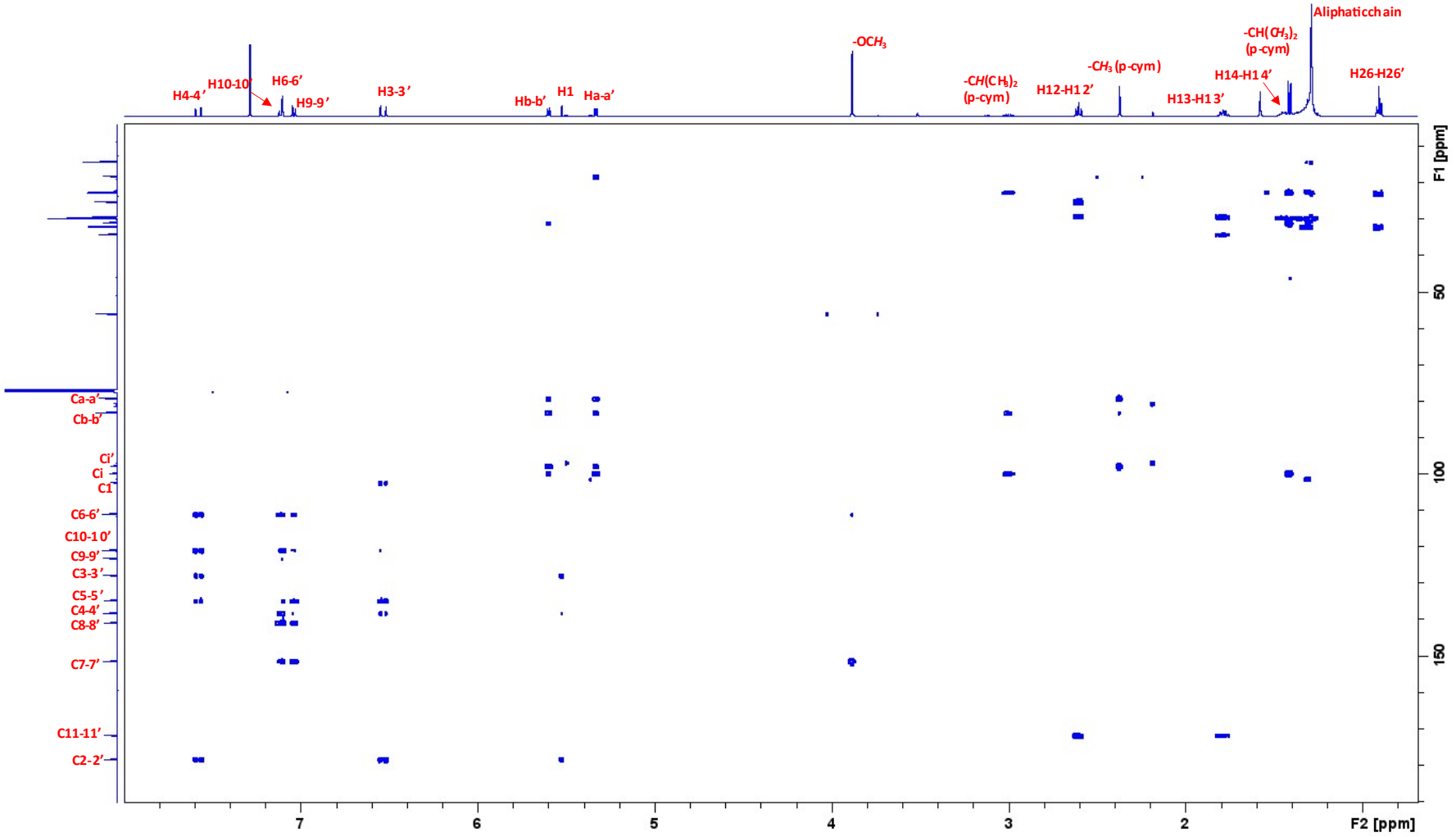

Figure S7. {^{1}H-^{13}C}-HMBC NMR of **1** in $CDCl_3$ at 293 K

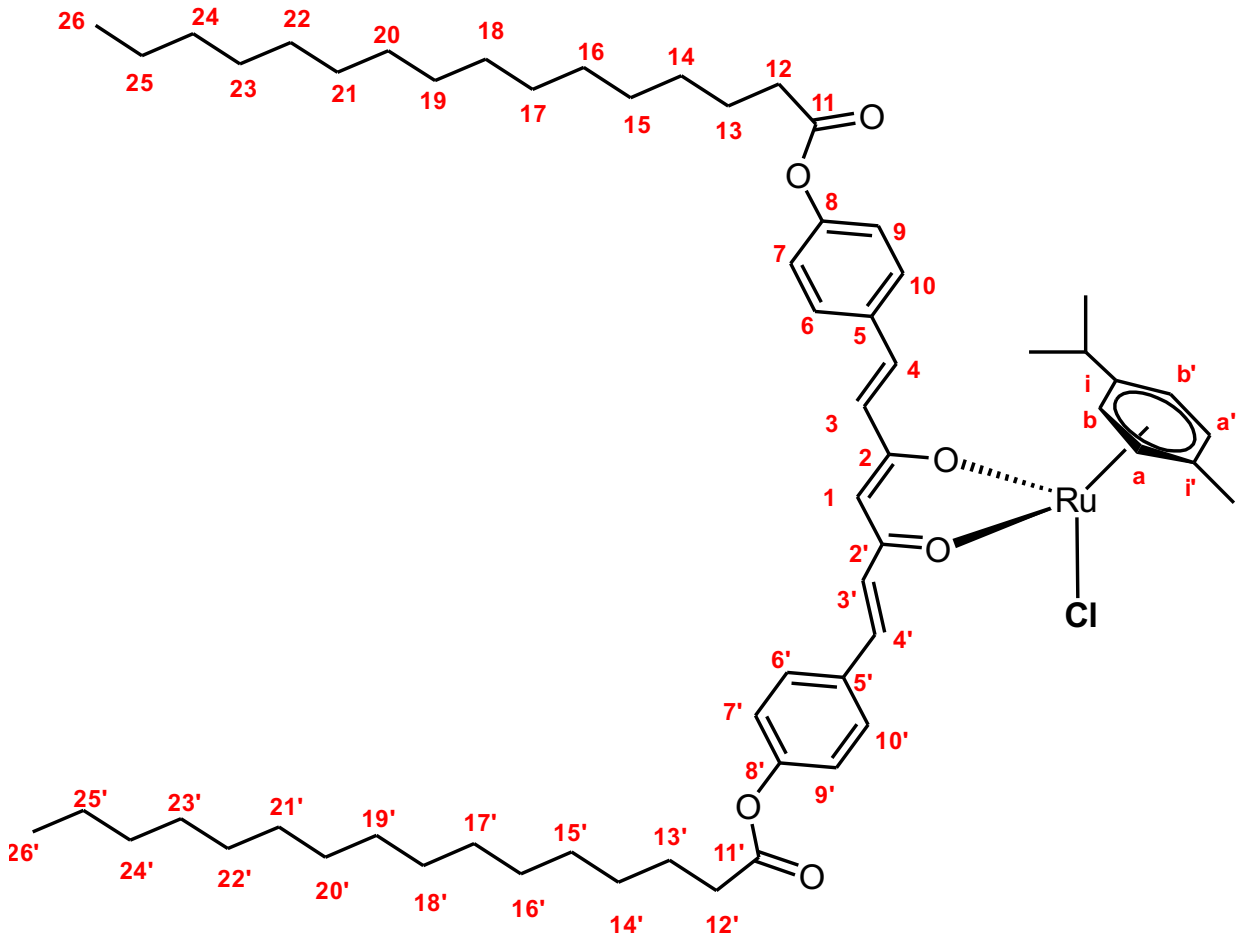
26
24
22
20
18
16
14
12
11
O
25
23
21
19
17
15
13
O
8
9
7
10
6
5
4
3
2
O
1
Ru
2'
O
3'
4'
6'
5'
7'
10'
8'
9'
O
26'
25'
23'
21'
19'
17'
15'
13'
11'
O
24'
22'
20'
18'
16'
14'
12'
i
b'
b
a'
a
i'
Cl

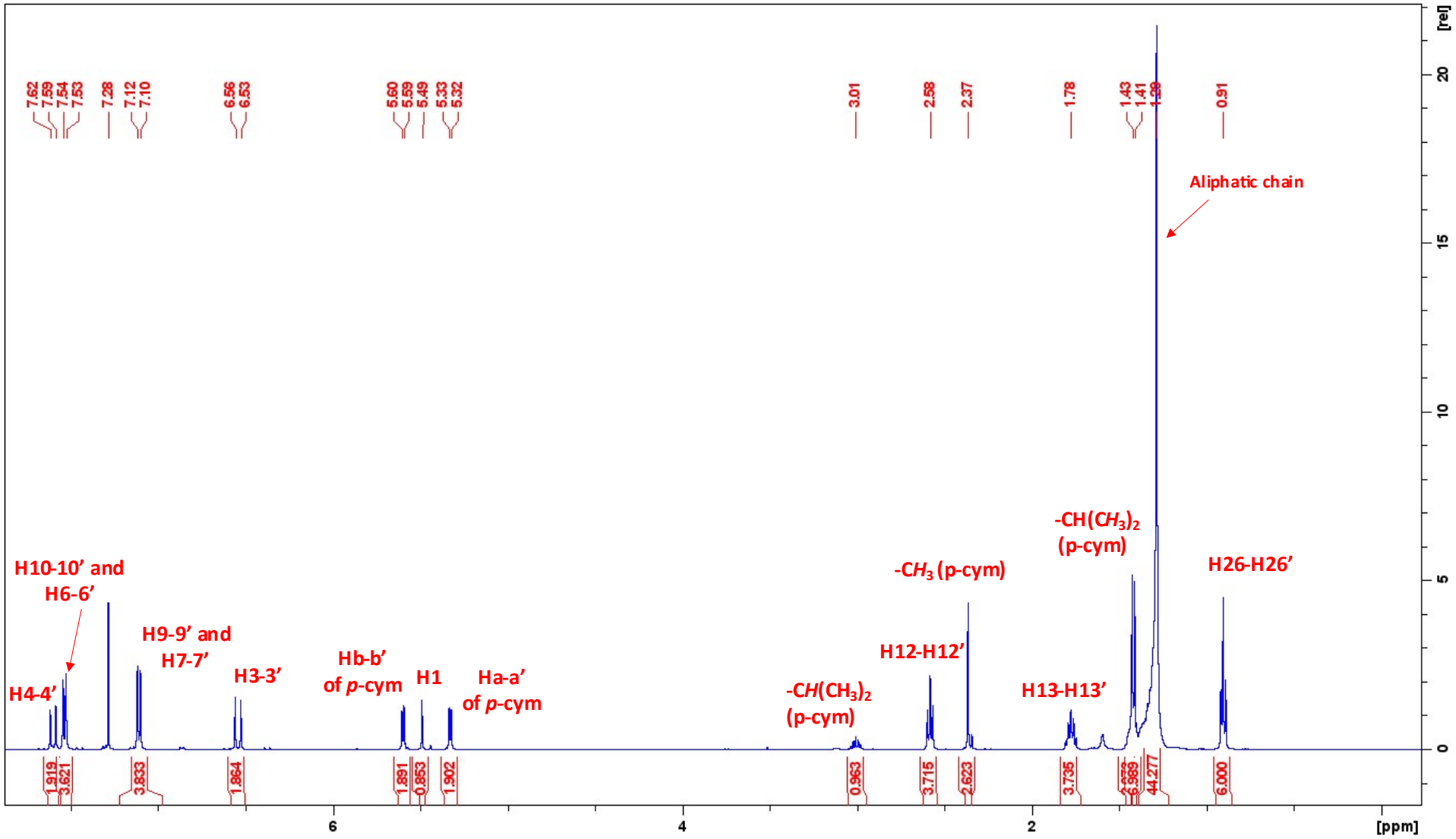

Figure S8. ^{1}H-NMR of **2** in $CDCl_3$ at 293 K

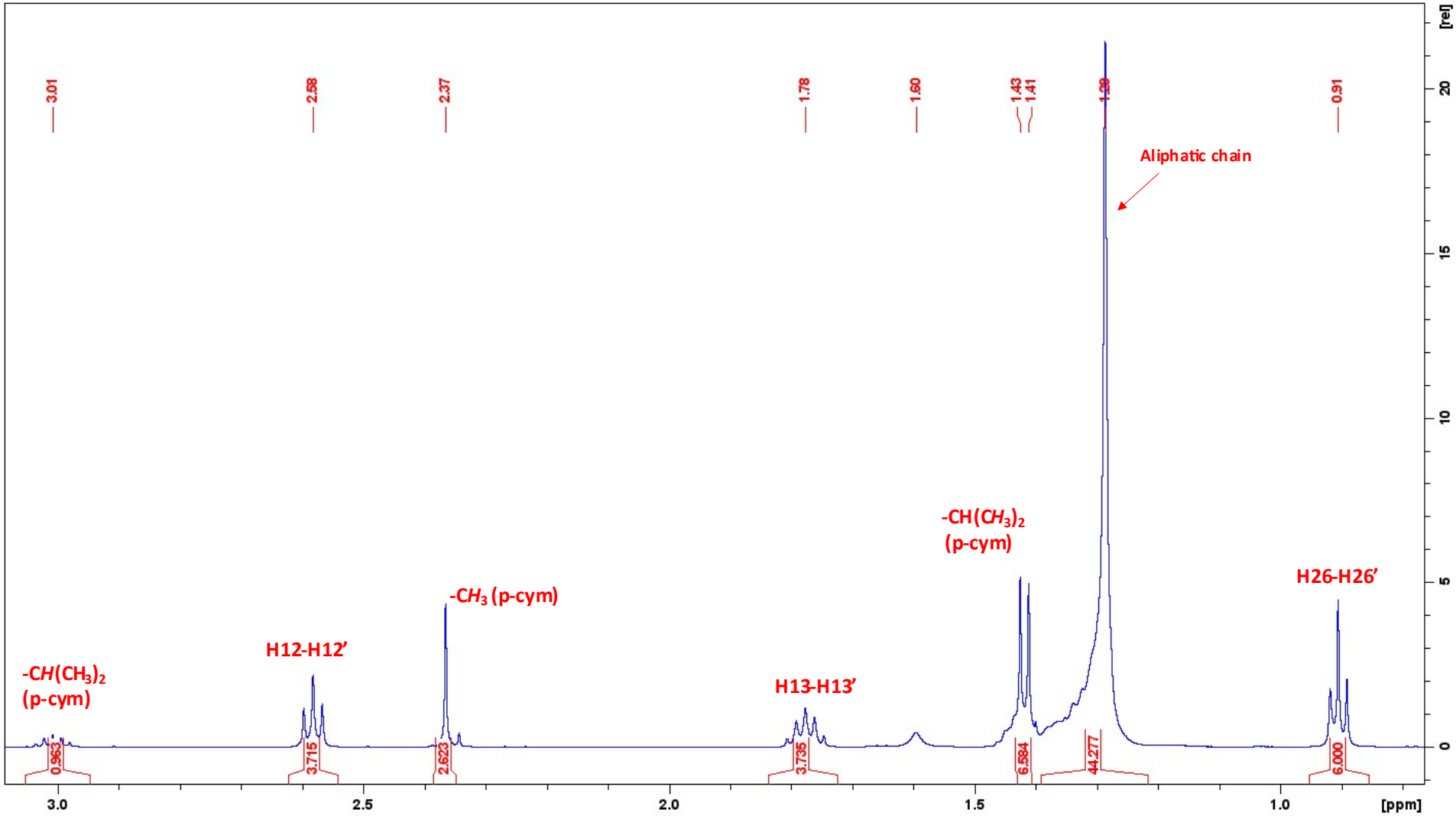

Figure S8 (a). Magnification of ^{1}H-NMR (1-3 ppm)

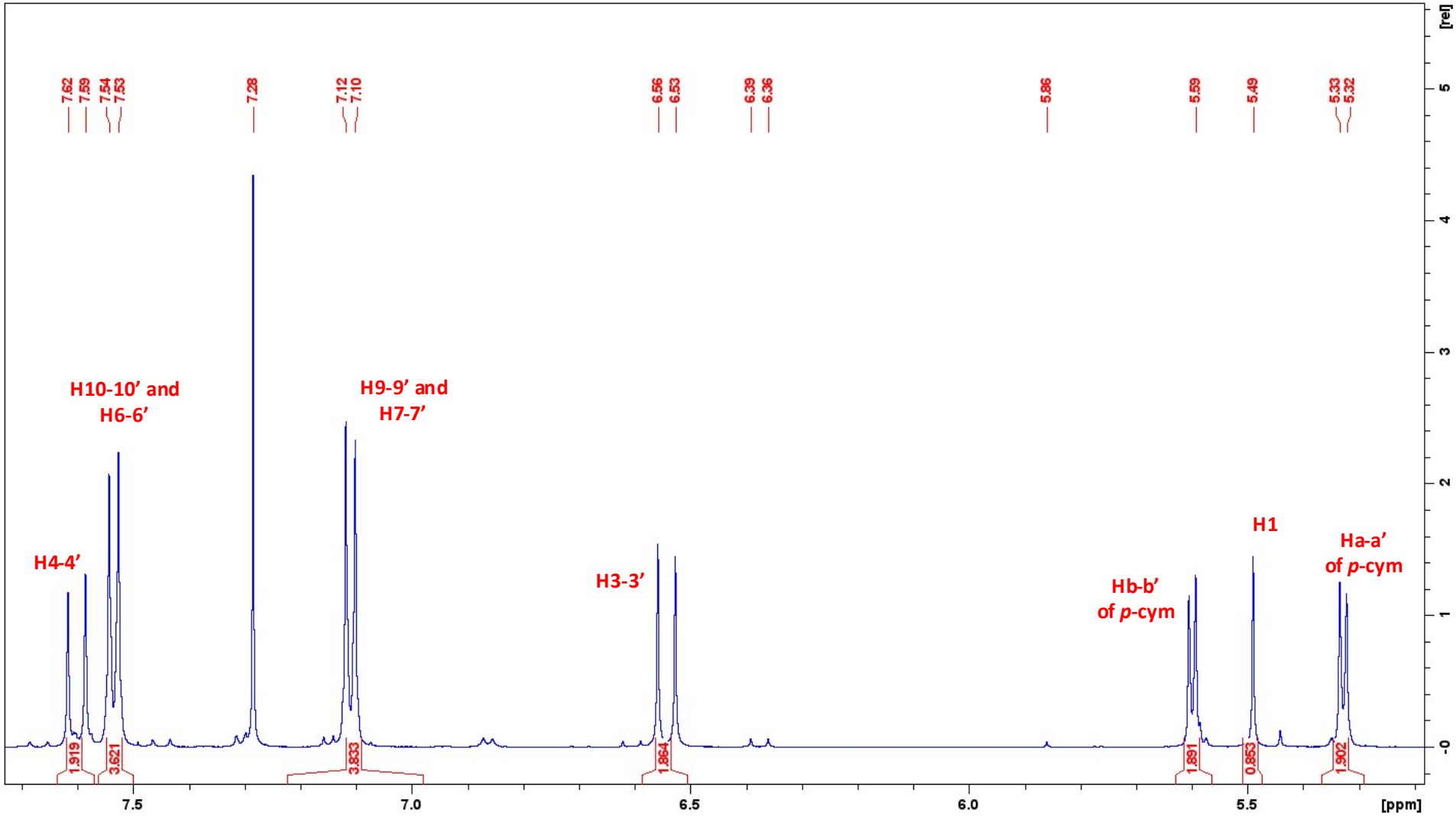

Figure S8 (b). Magnification of ^{1}H-NMR (4-8 ppm)

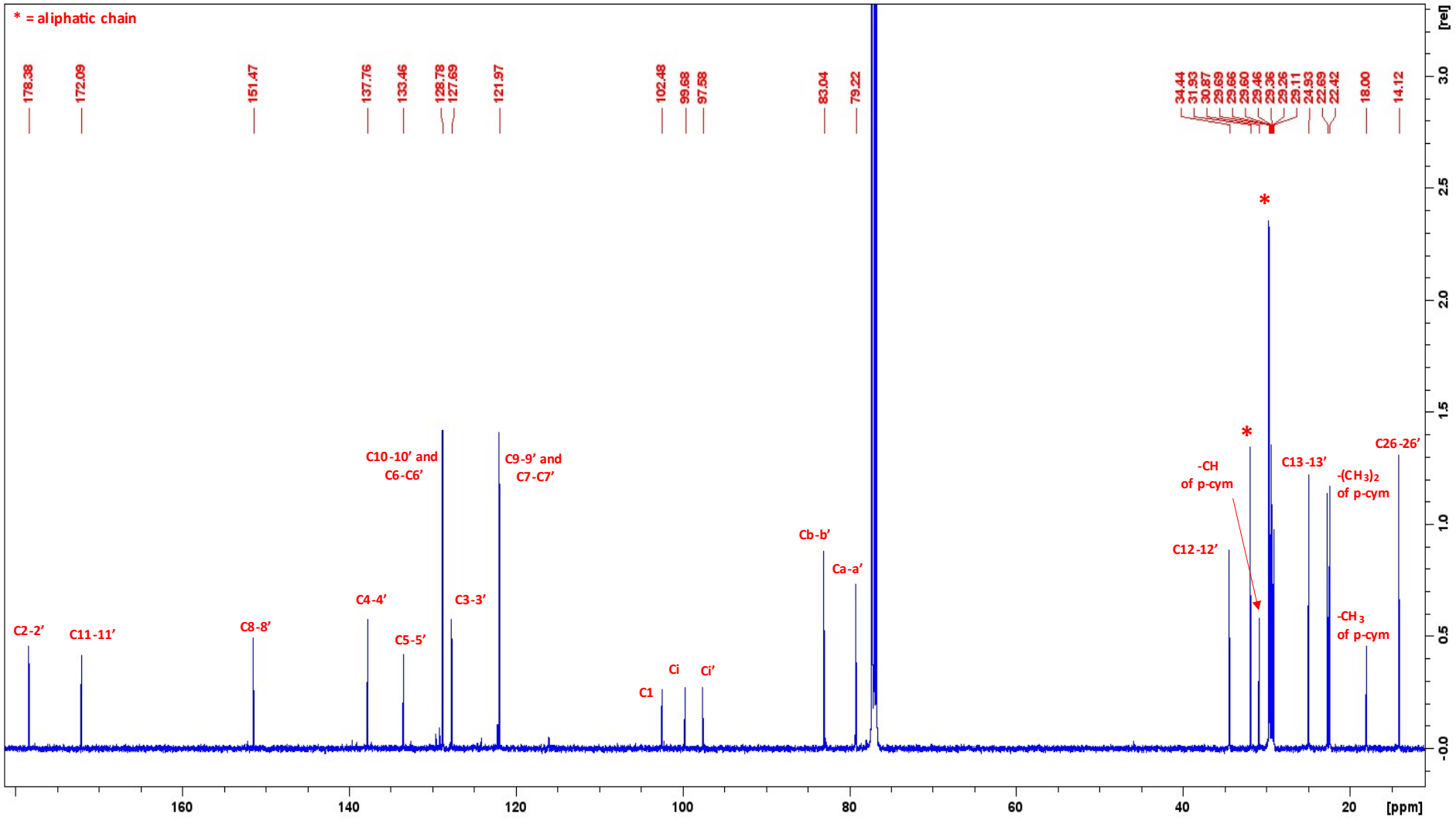

Figure S9. ^{13}C-NMR of **2** in $CDCl_3$ at 293 K

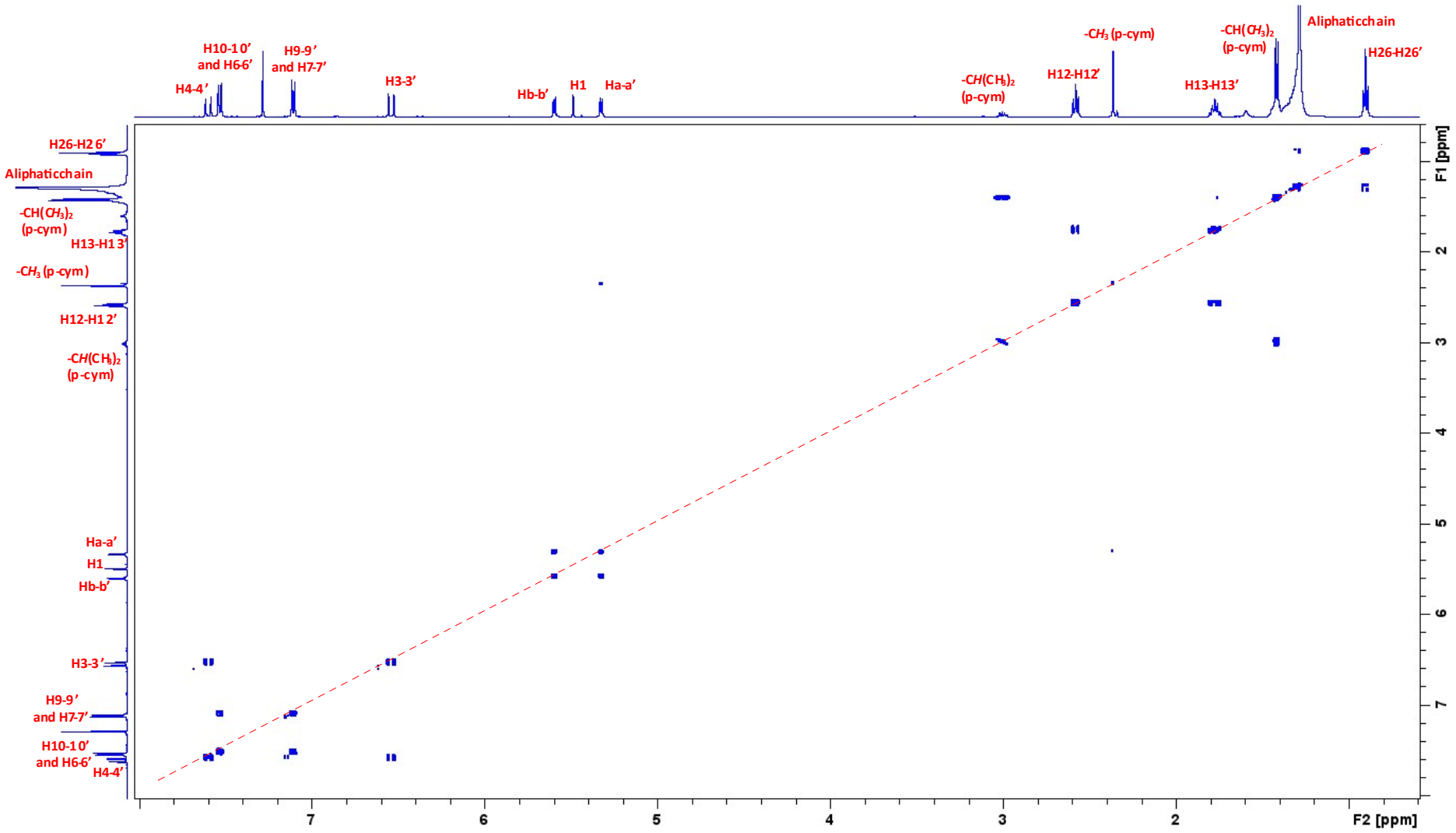

Figure S10. {^{1}H-^{1}H}-COSY NMR of **2** in $CDCl_3$ at 293 K

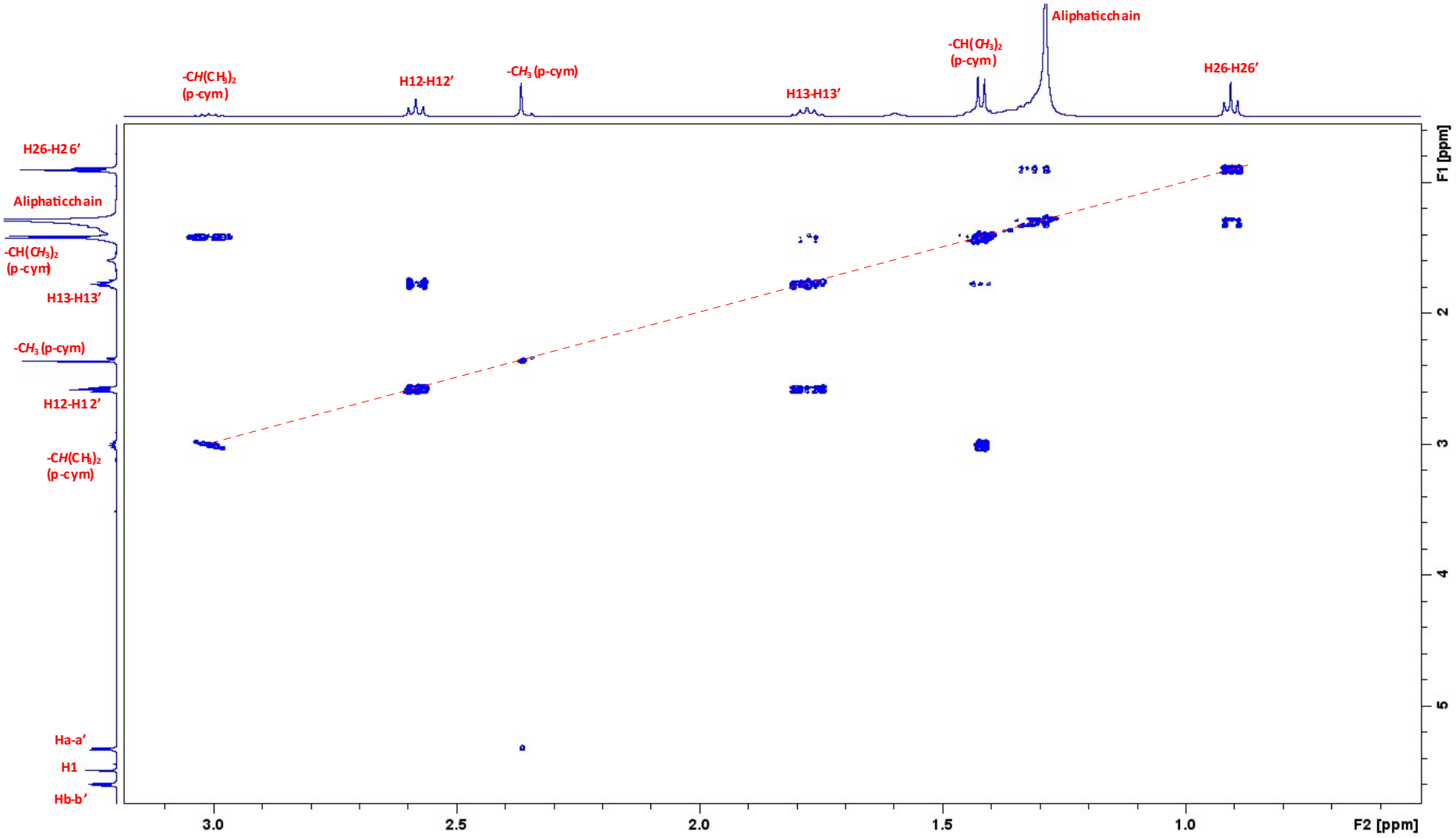

Figure S10 (a). Magnification of {^{1}H-^{1}H}-COSY NMR

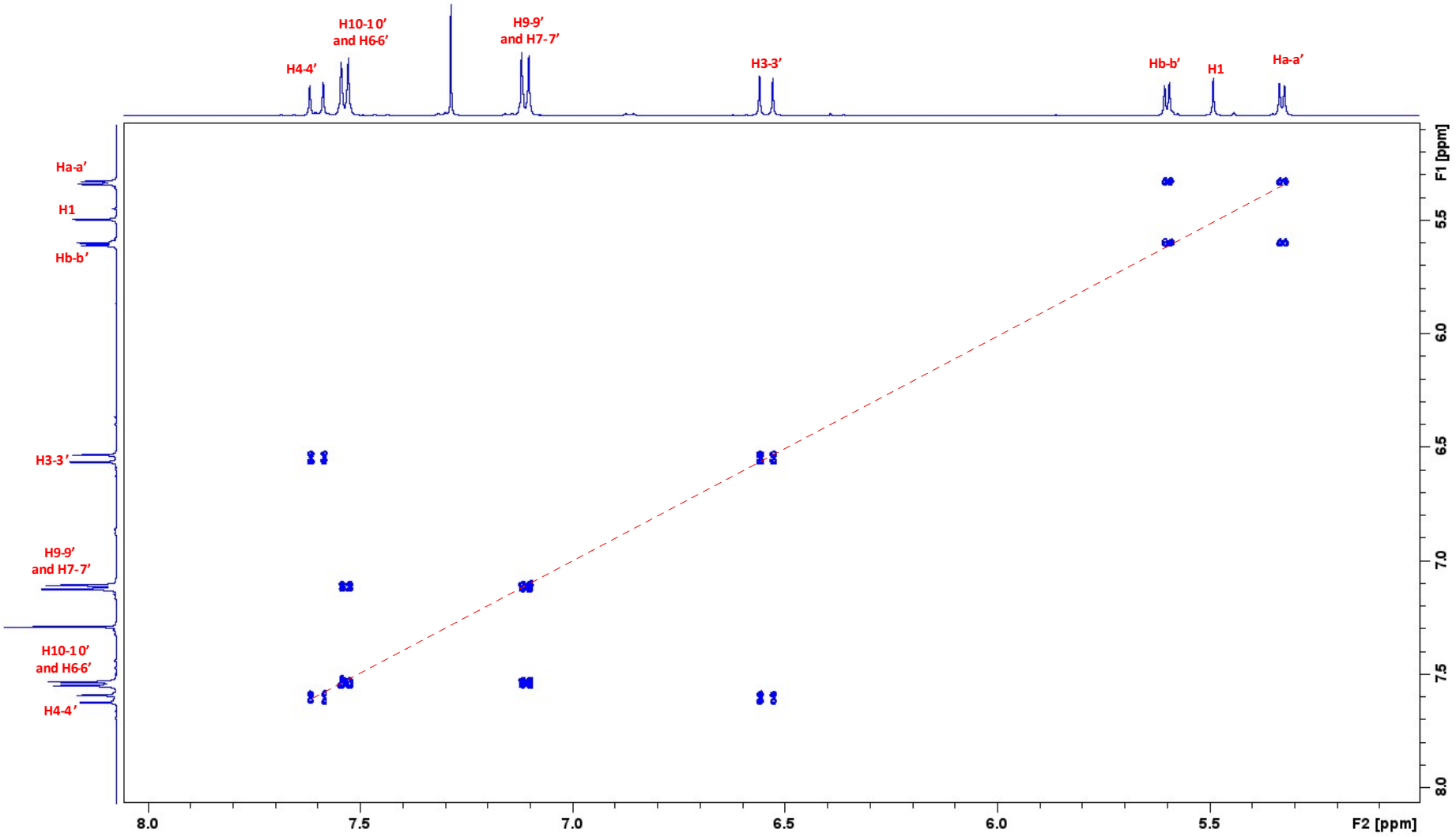

Figure S10 (b). Magnification of {^{1}H-^{1}H}-COSY NMR

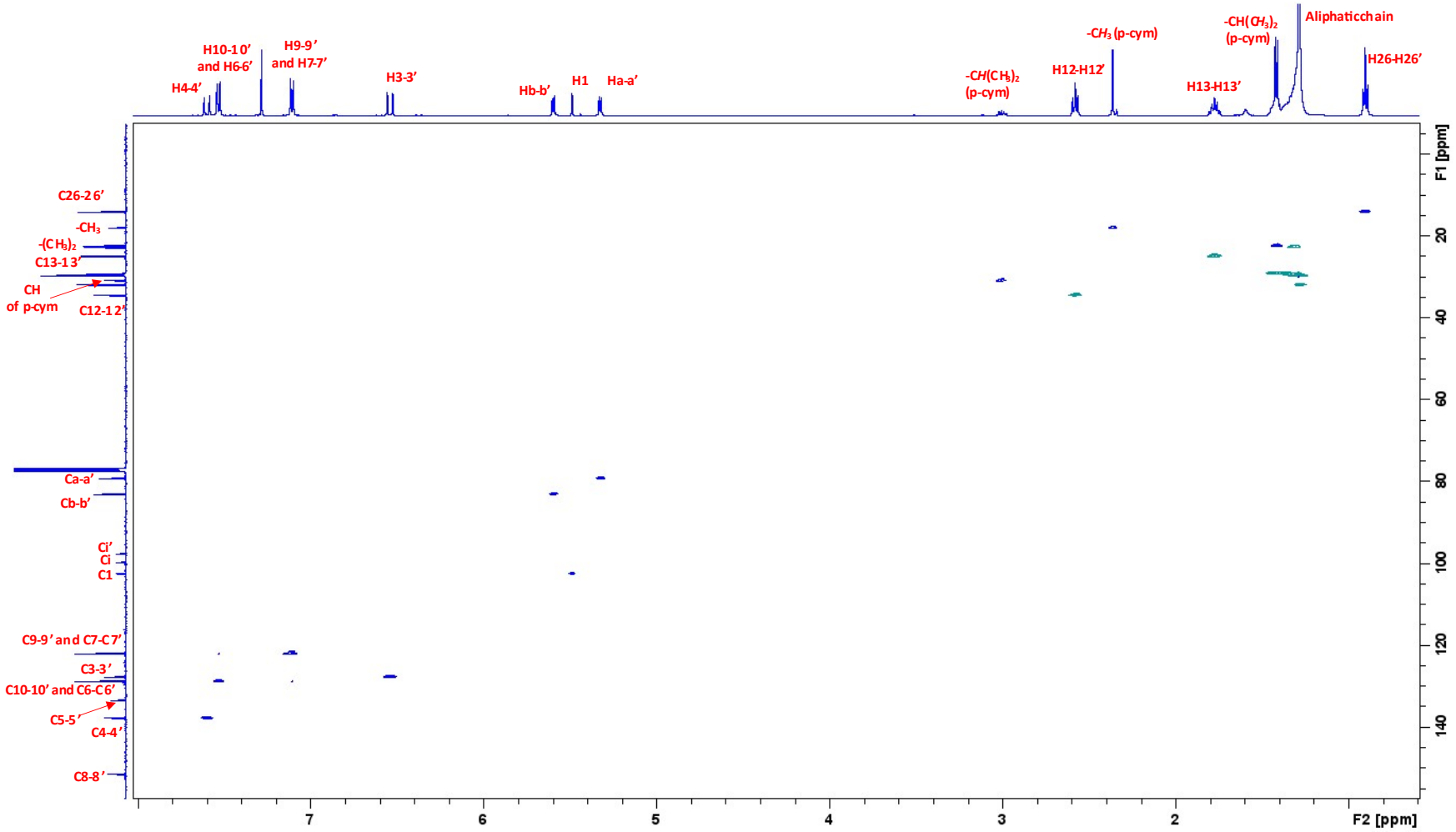

Figure S11. {^{1}H-^{13}C}-HSQC NMR of **2** in $CDCl_3$ at 293 K

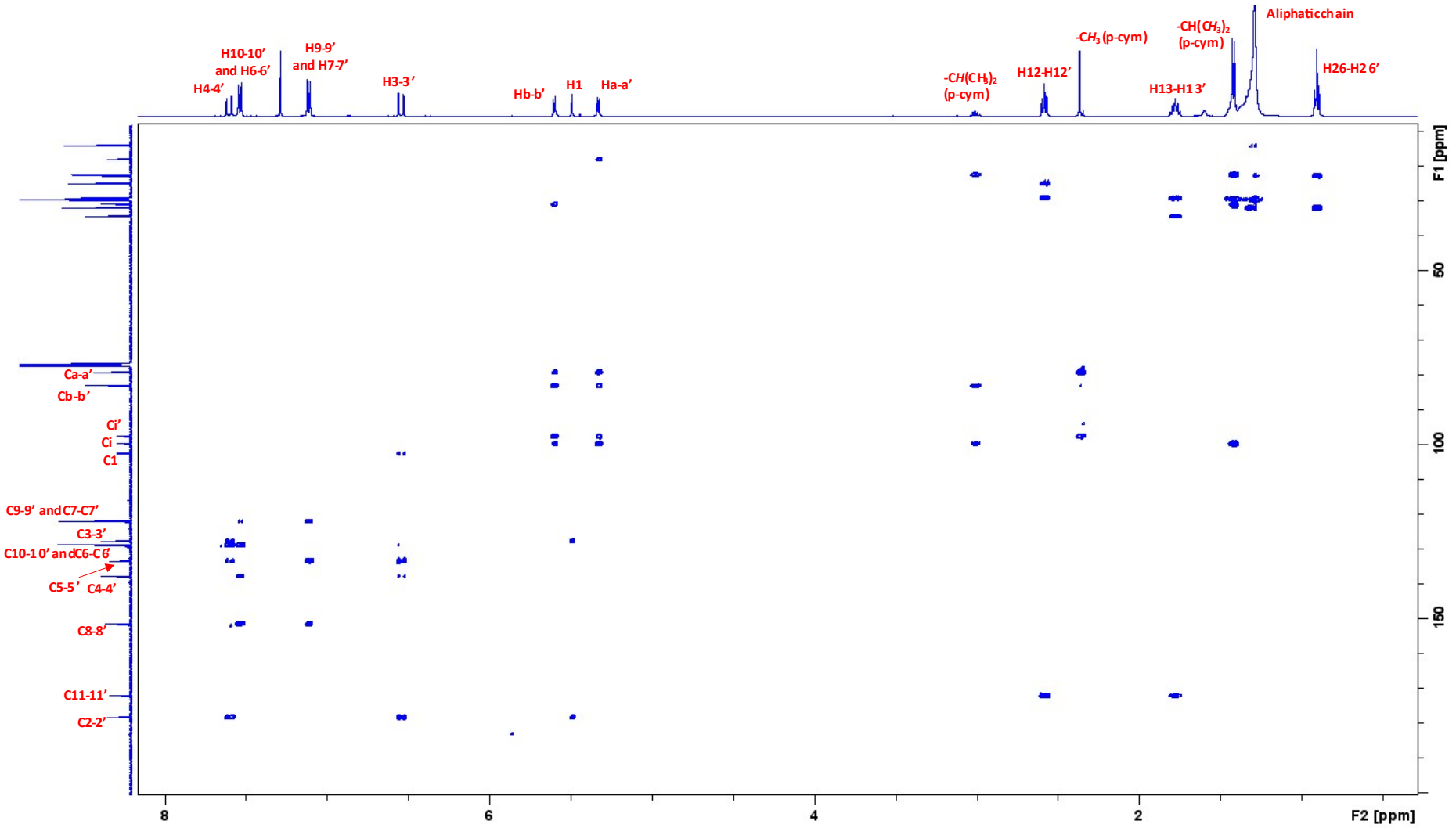

Figure S12. {^{1}H-^{13}C}-HMBC NMR of **2** in $CDCl_3$ at 293 K

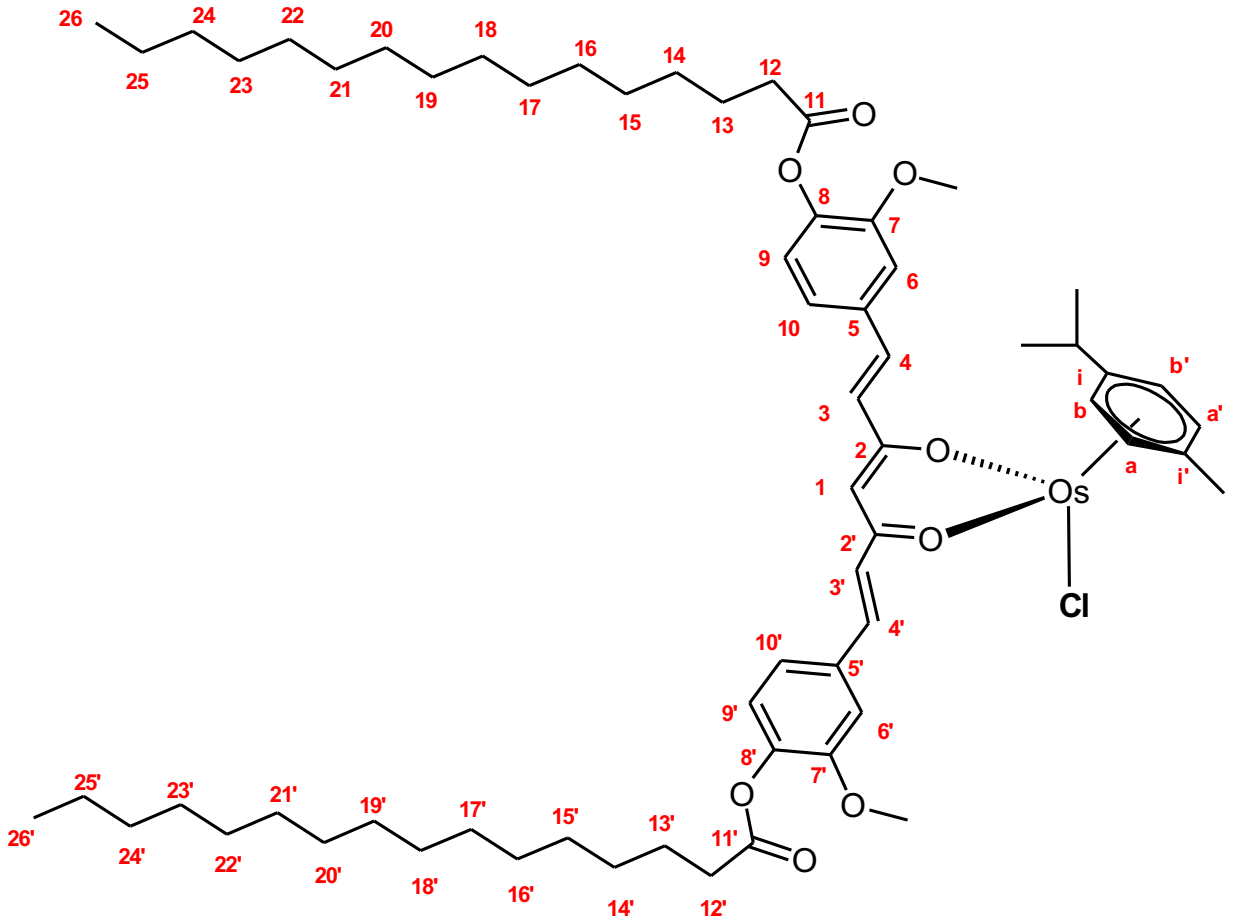
26
24
22
20
18
16
14
12
11
25
23
21
19
17
15
13
O
O
O
8
7
9
6
10
5
4
3
2
1
O
Os
O
2'
3'
4'
10'
5'
9'
6'
8'
7'
O
O
Cl
i
b'
b
a'
a
i'
25'
23'
21'
19'
17'
15'
13'
11'
26'
24'
22'
20'
18'
16'
14'
12'

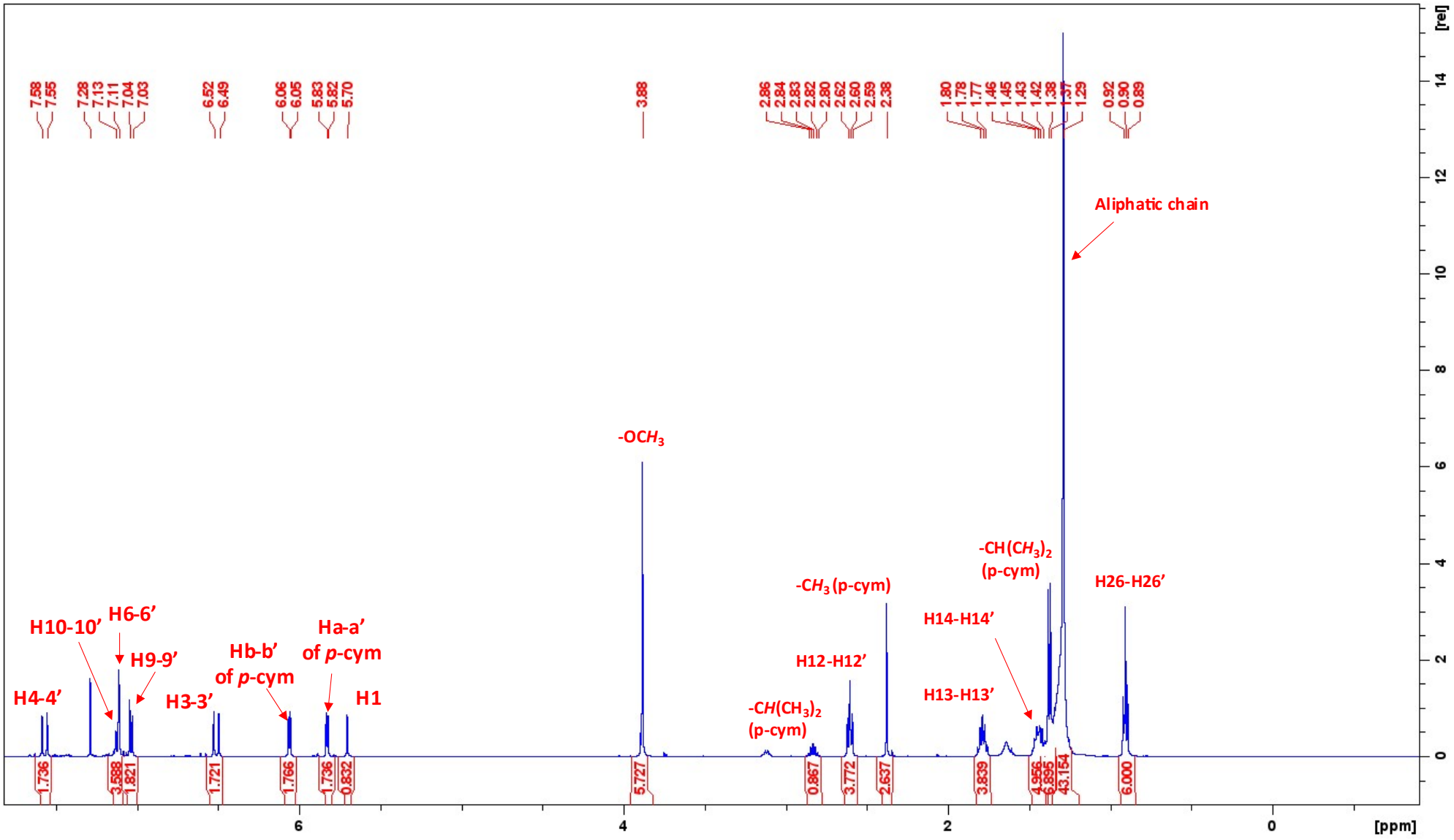

Figure S13. ^{1}H-NMR of **3** in $CDCl_3$ at 293 K

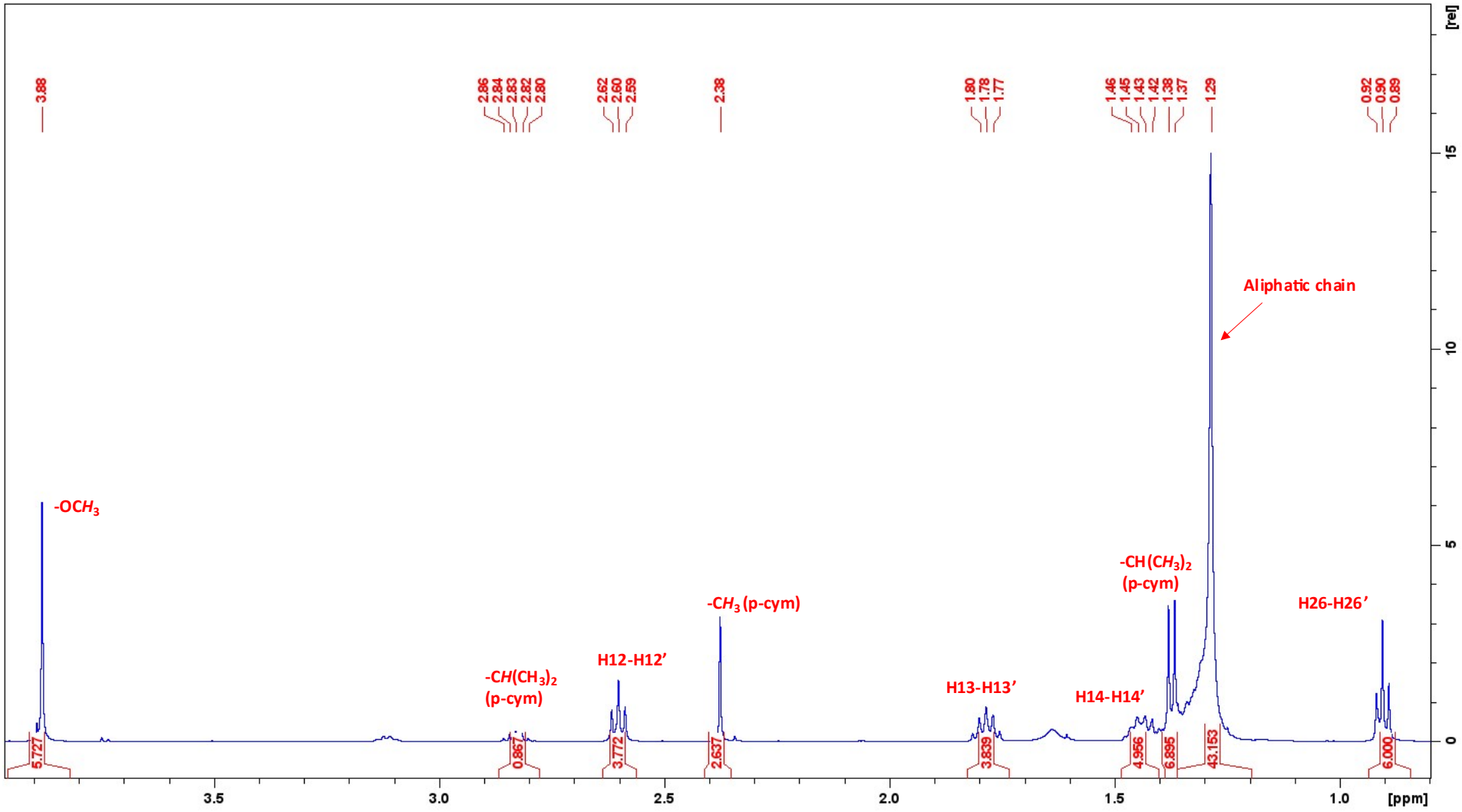

Figure S13 (a). Magnification of ^{1}H-NMR (1-4 ppm)

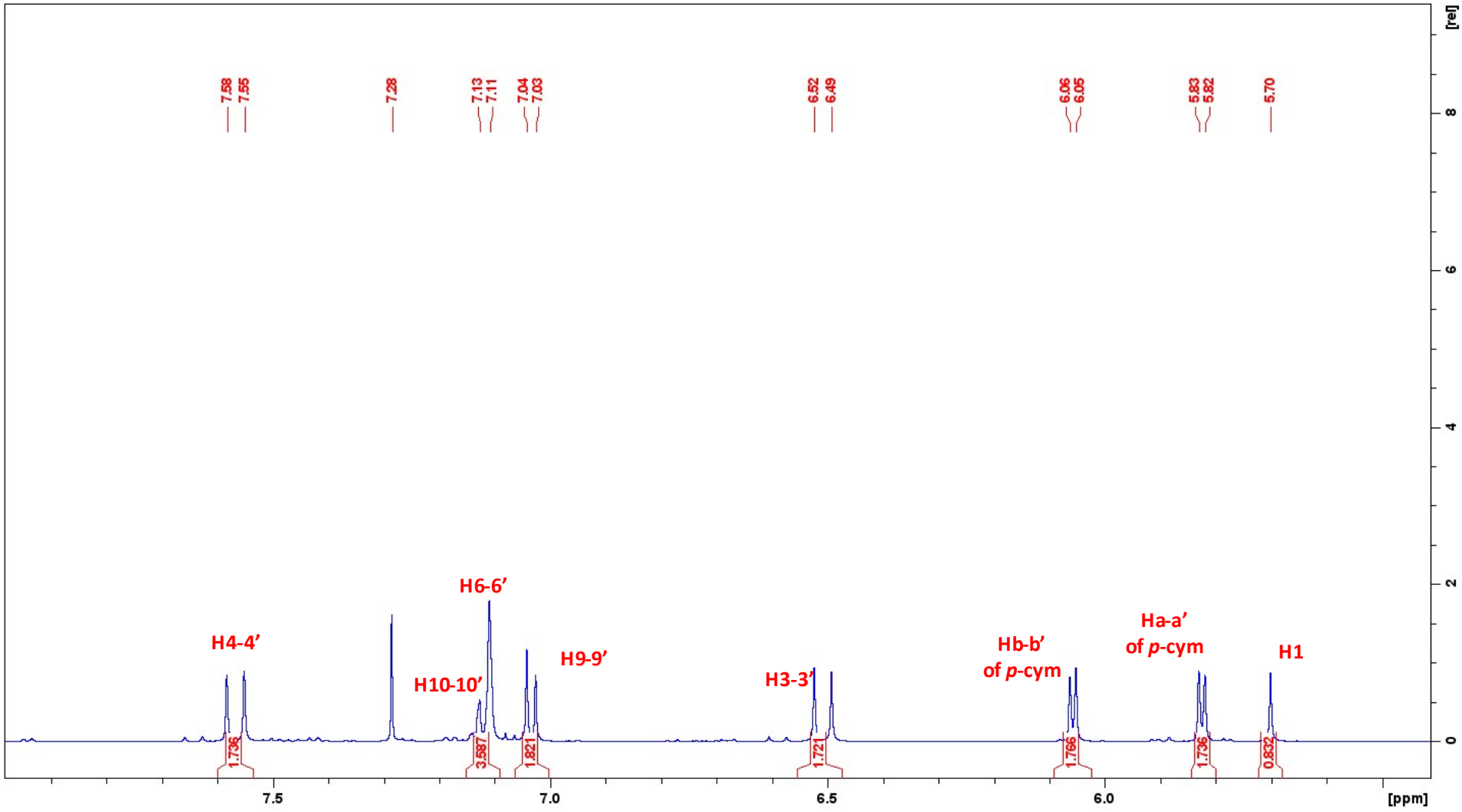

Figure S13 (b). Magnification of ^{1}H-NMR (1-8 ppm)

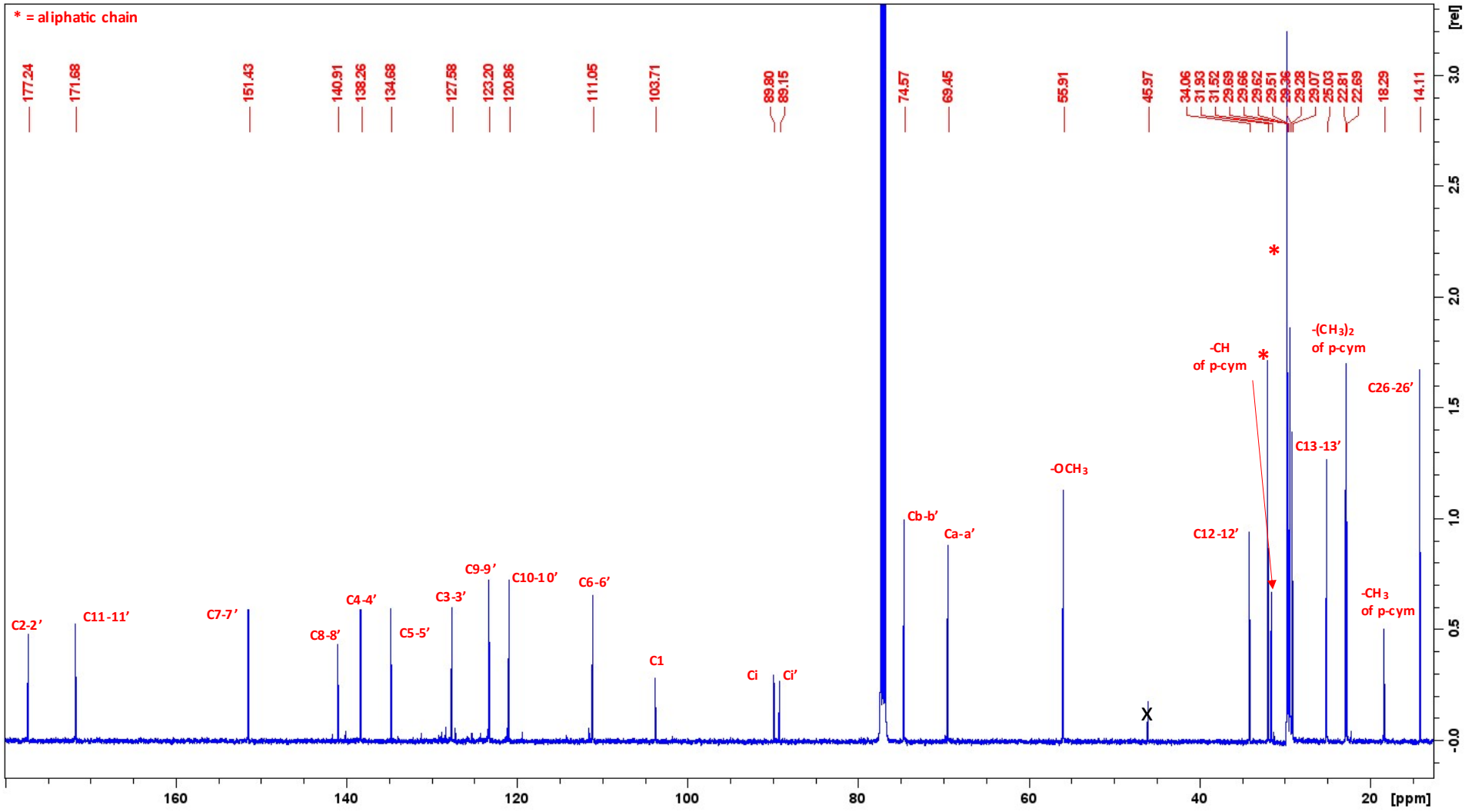

Figure S14. ^{13}C-NMR of **3** in $CDCl_3$ at 293 K

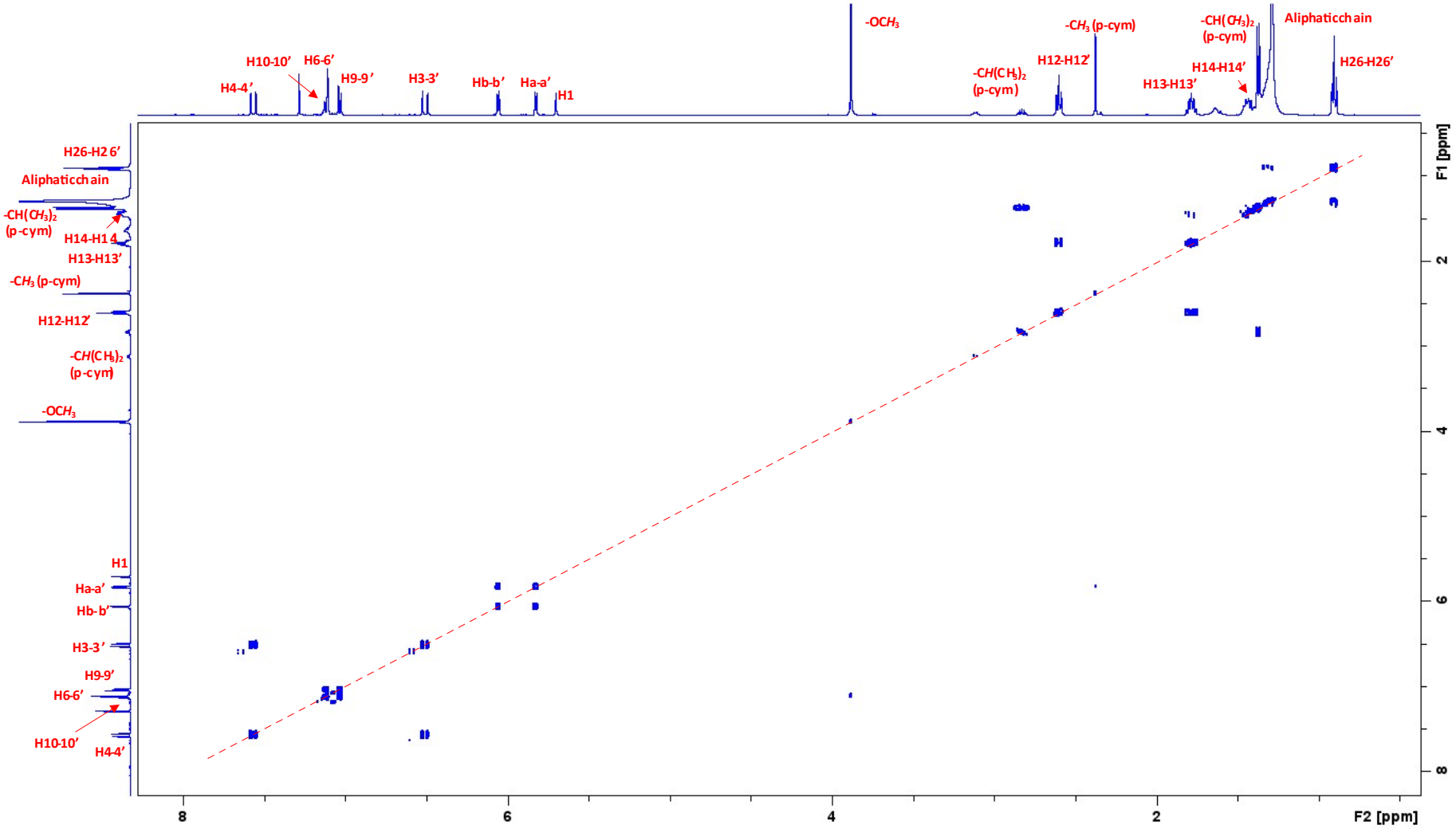

Figure S15. {^{1}H-^{1}H}-COSY NMR of **3** in $CDCl_3$ at 293 K

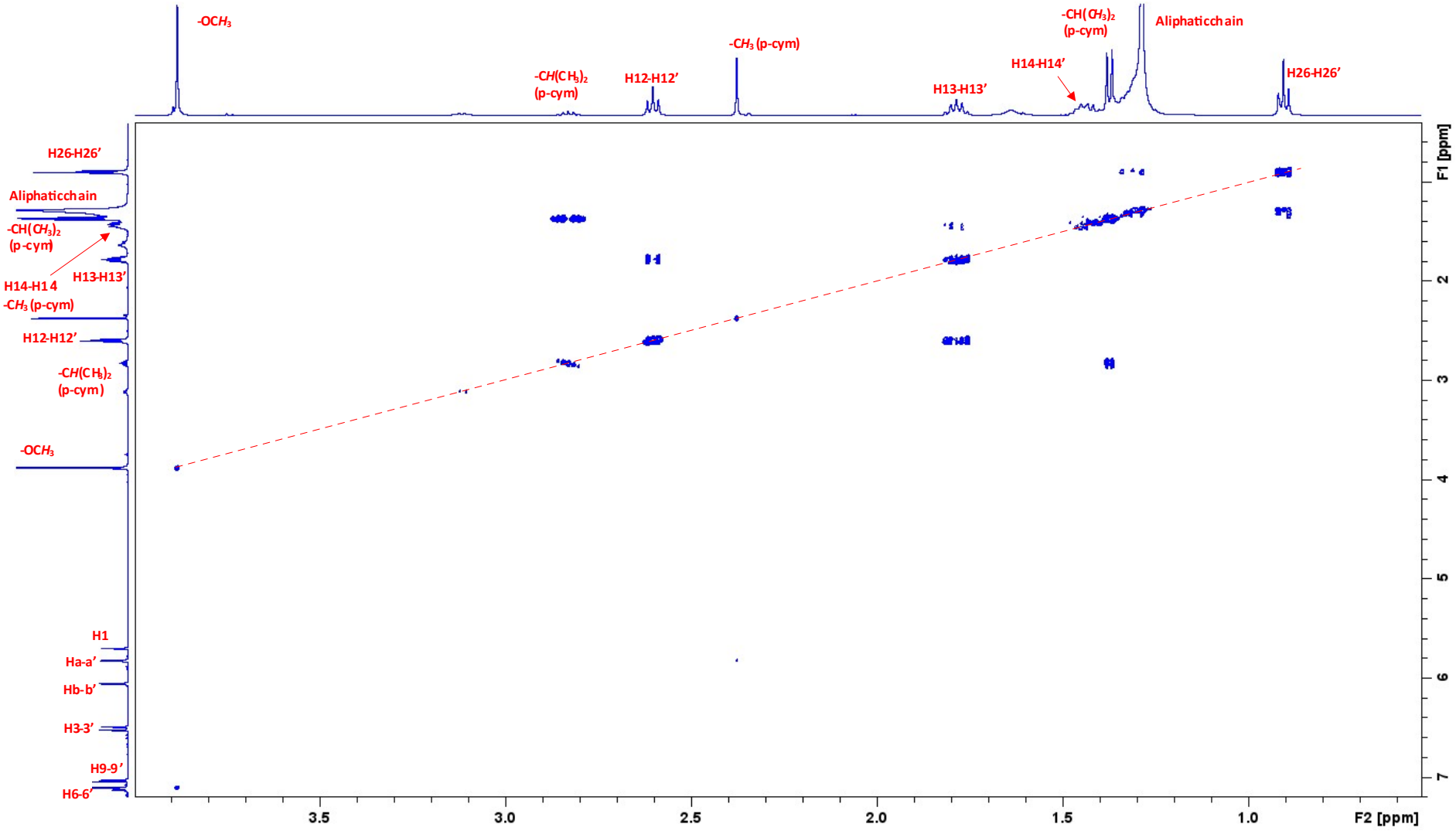

Figure S15 (a). Magnification of {^{1}H-^{1}H}-COSY NMR

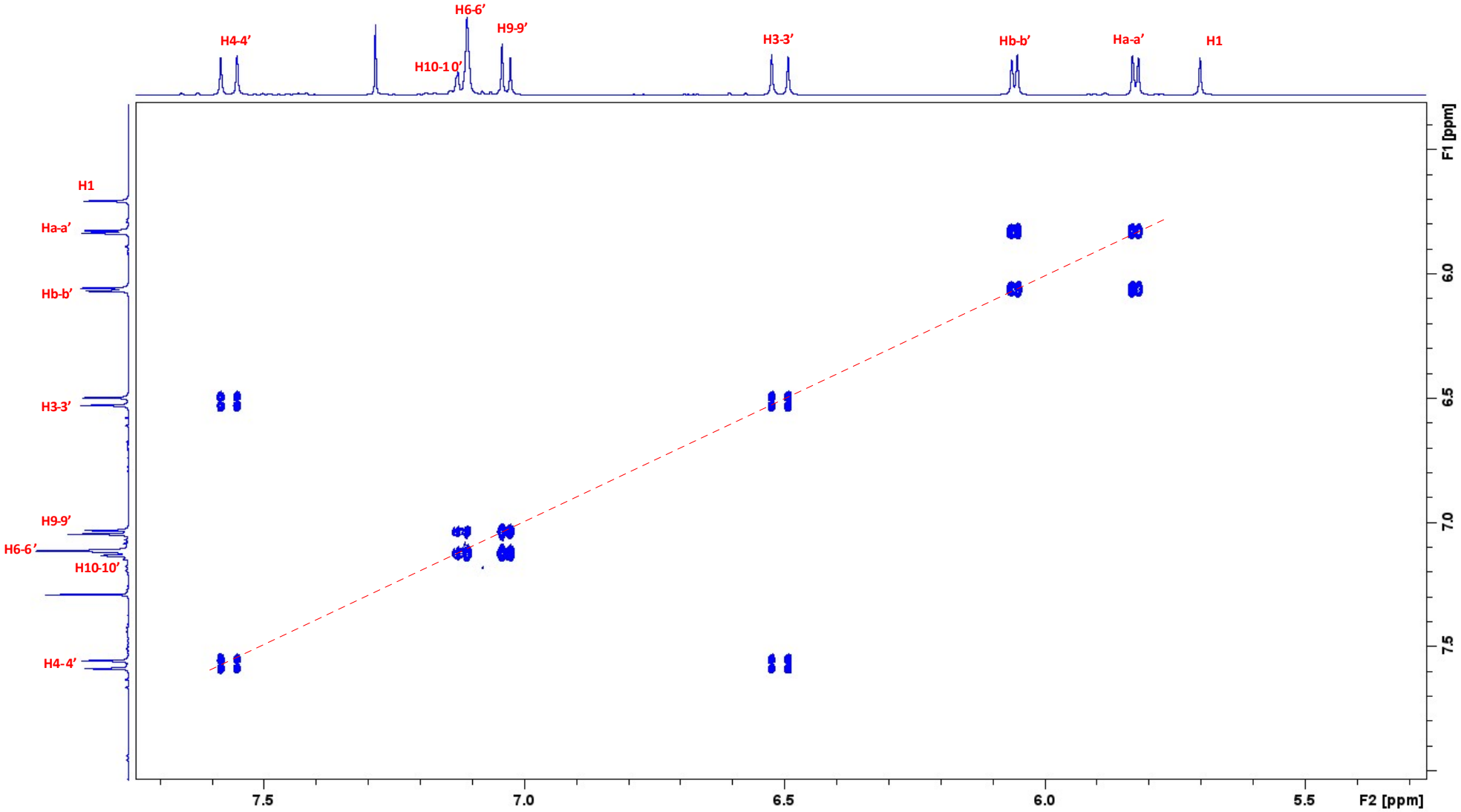

Figure S15 (b). Magnification of {^{1}H-^{1}H}-COSY NMR

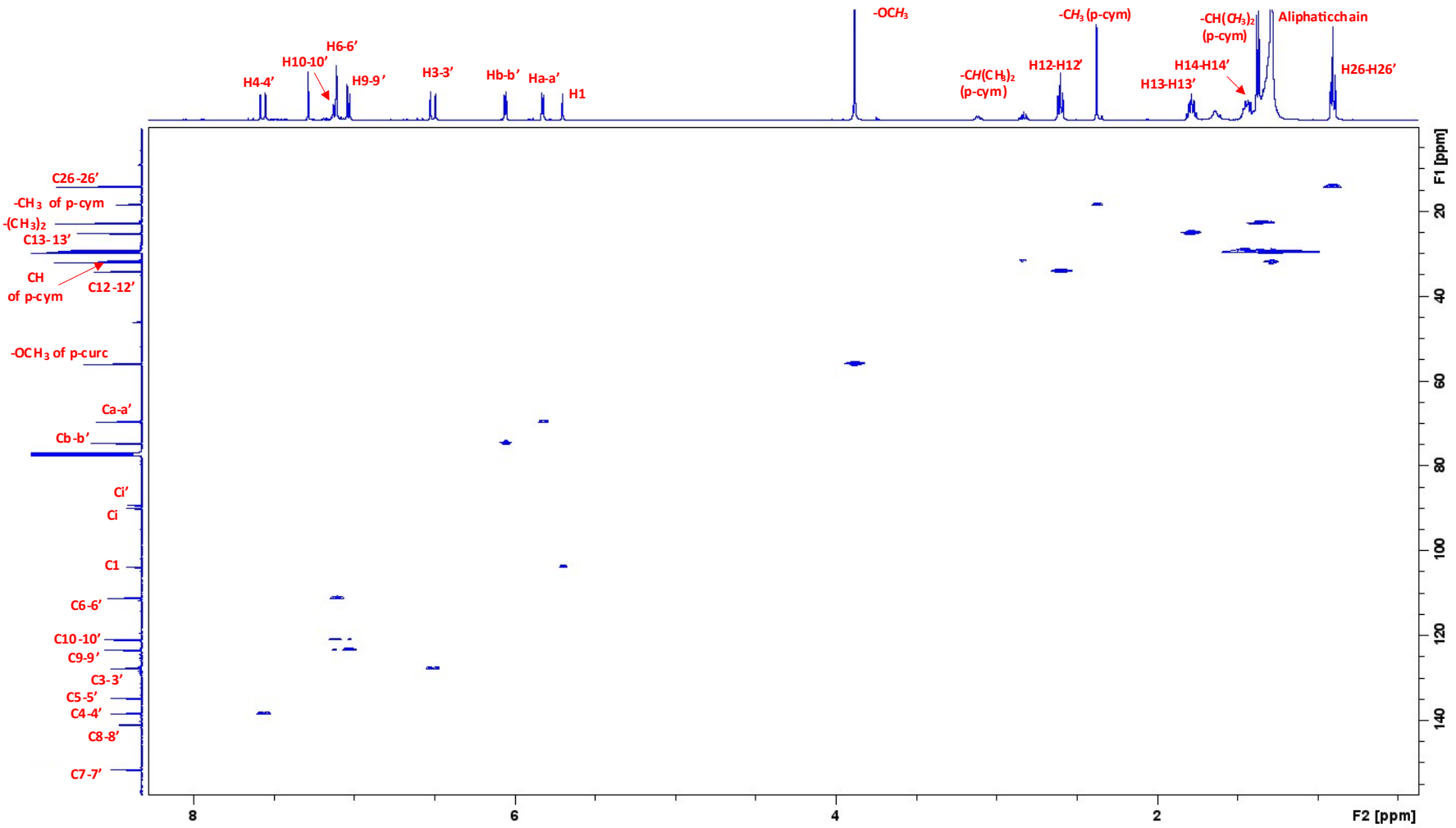

Figure S16. {^{1}H-^{13}C}-HSQC NMR of **3** in $CDCl_3$ at 293 K

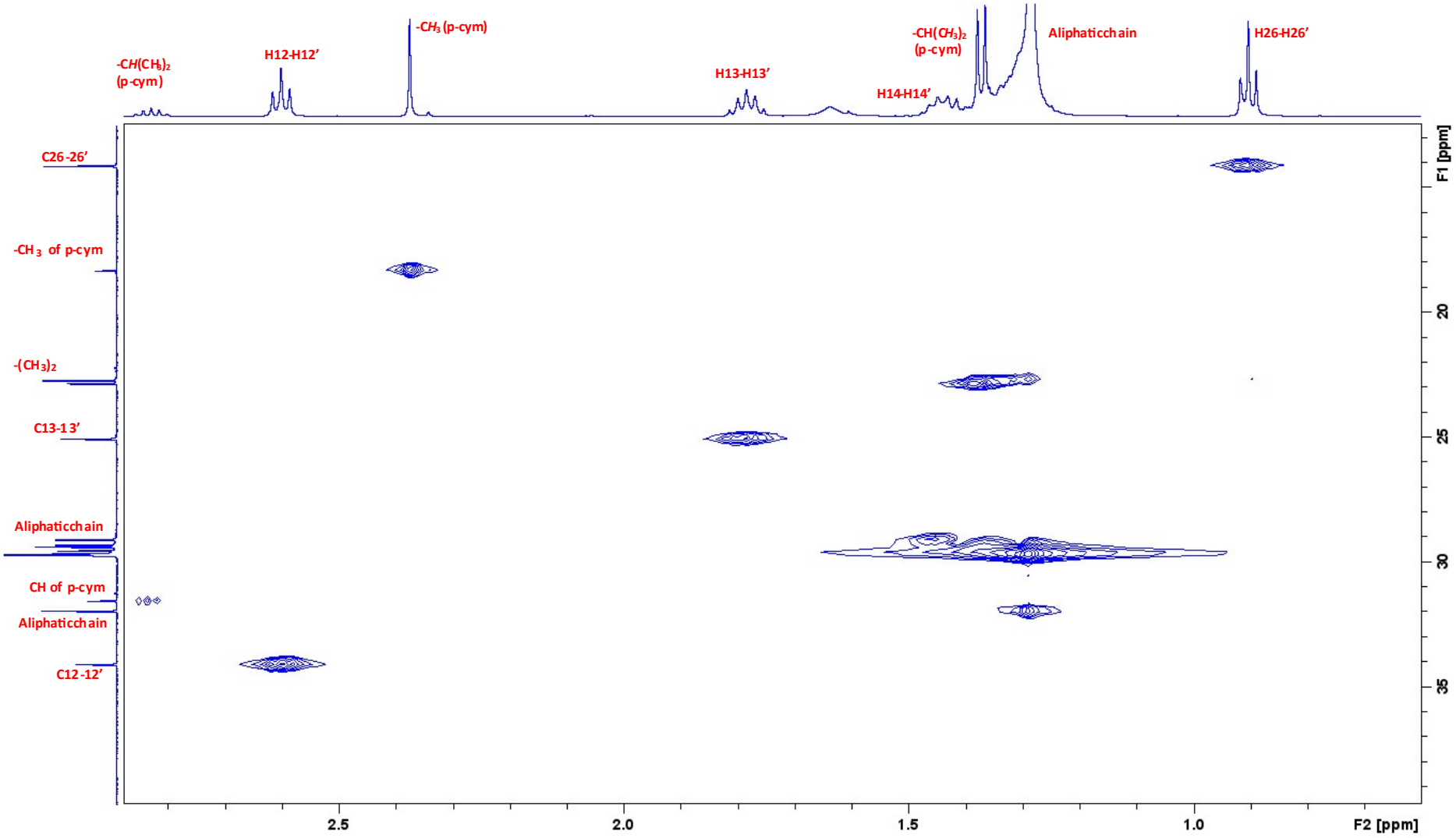

Figure S16 (a). Magnification of {^{1}H-^{13}C}-HSQC NMR

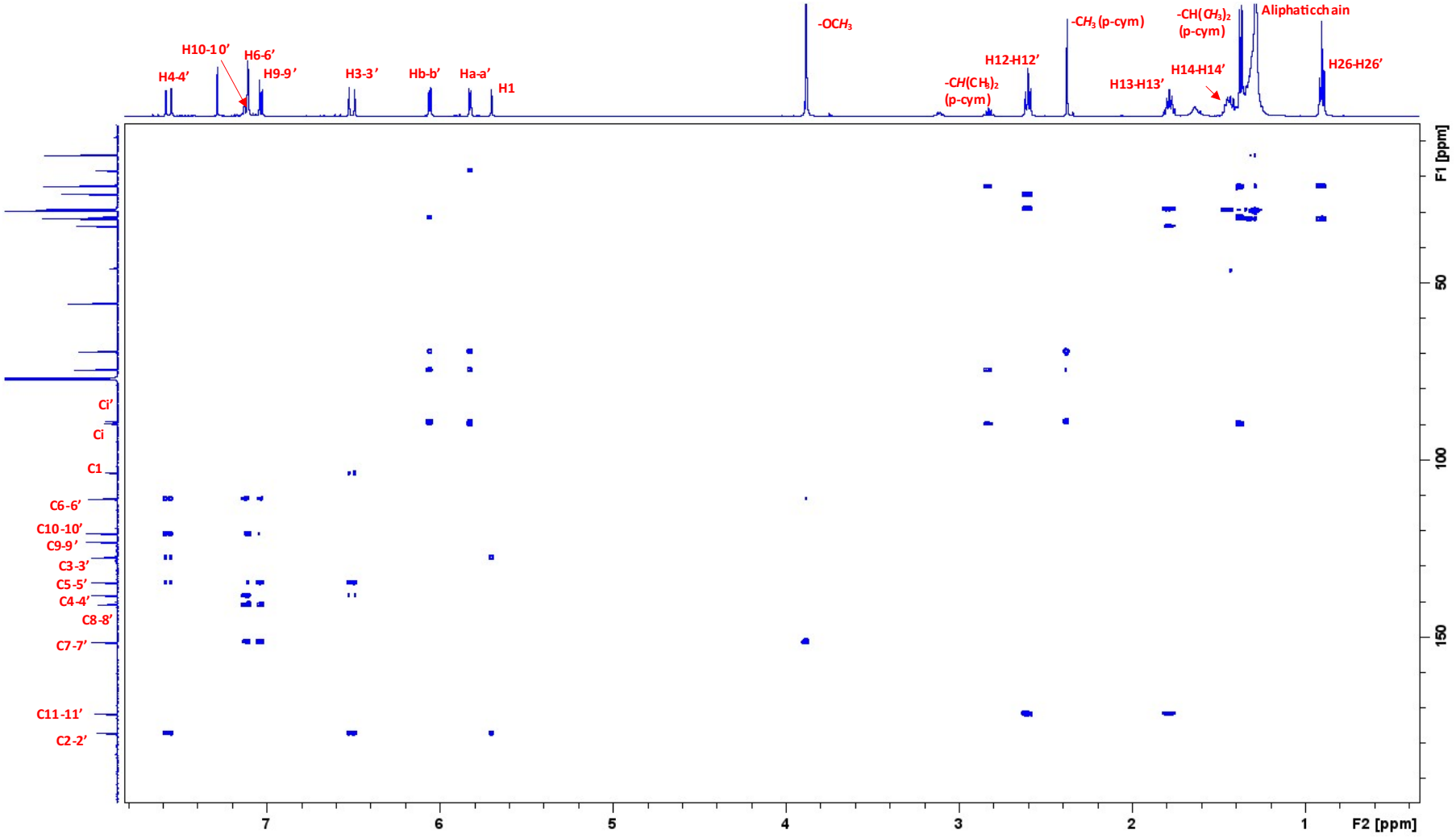

Figure S17. {^{1}H-^{13}C}-HMBC NMR of **3** in $CDCl_3$ at 293 K

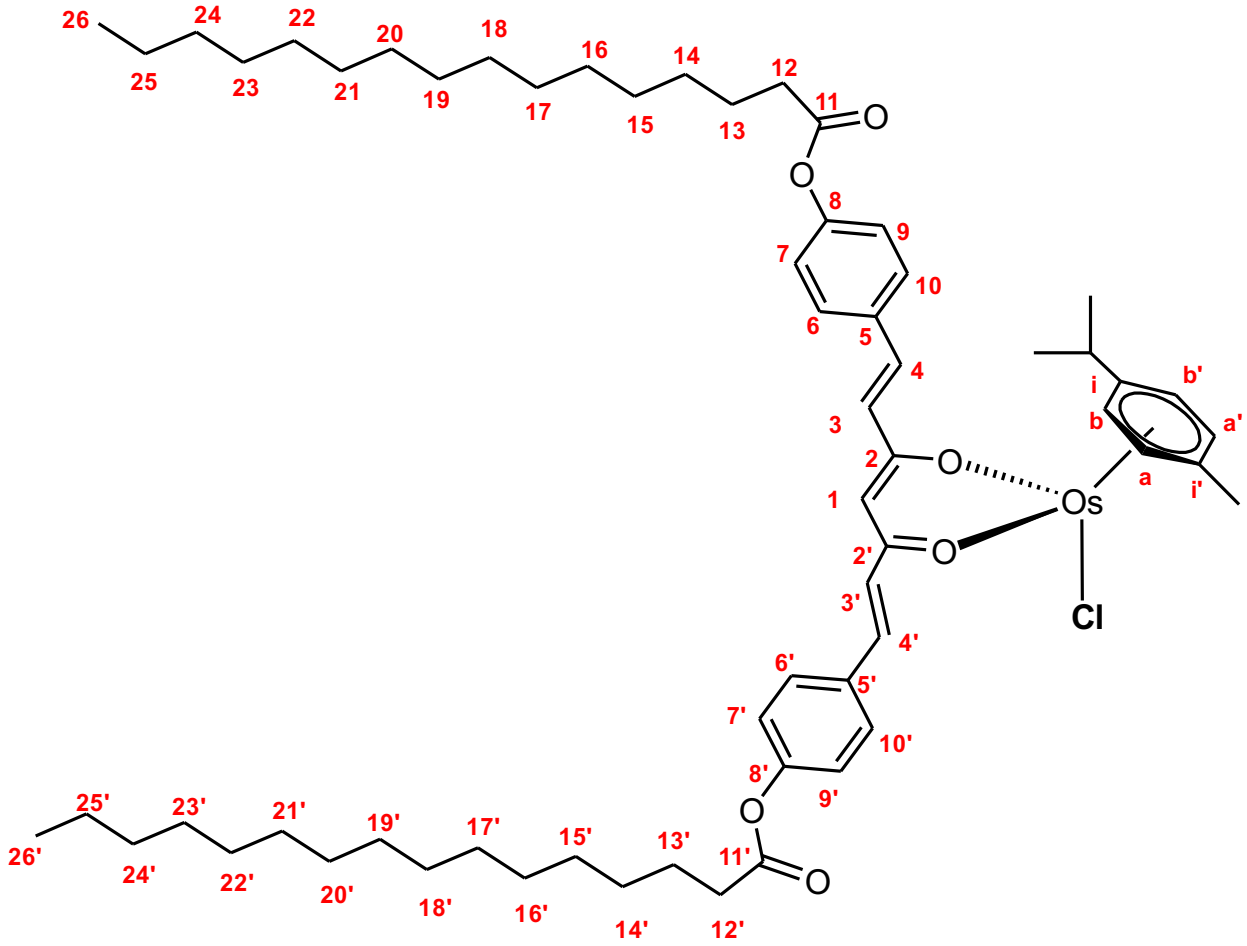
26
24
22
20
18
16
14
12
11
O
25
23
21
19
17
15
13
O
8
9
7
10
6
5
4
3
2
1
O
Os
2'
O
3'
4'
Cl
i
b'
b
a'
a
i'
6'
5'
7'
10'
8'
9'
O
25'
23'
21'
19'
17'
15'
13'
11'
26'
24'
22'
20'
18'
16'
14'
12'
O

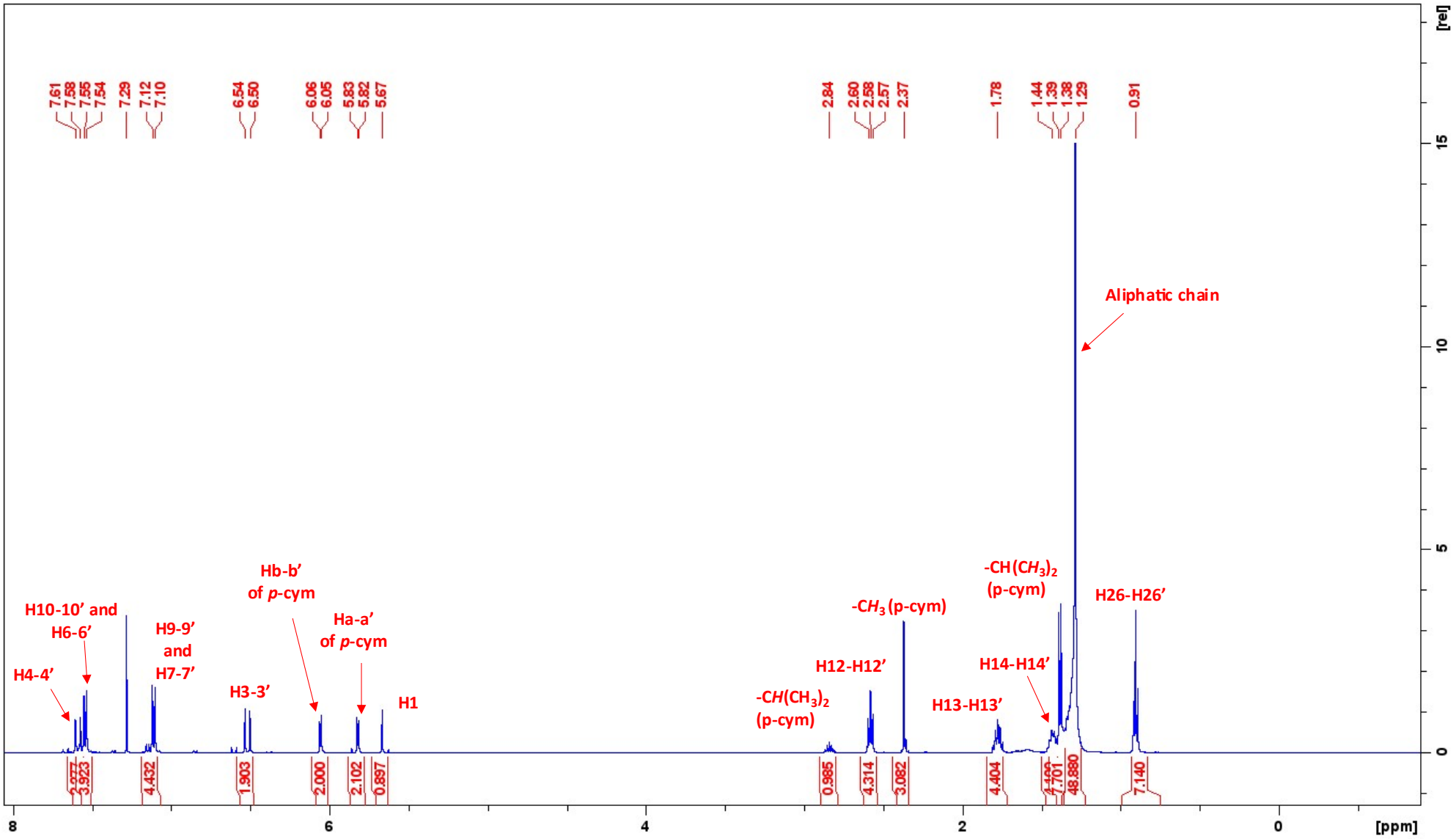

Figure S18. ^{1}H-NMR of **4** in $CDCl_3$ at 298 K

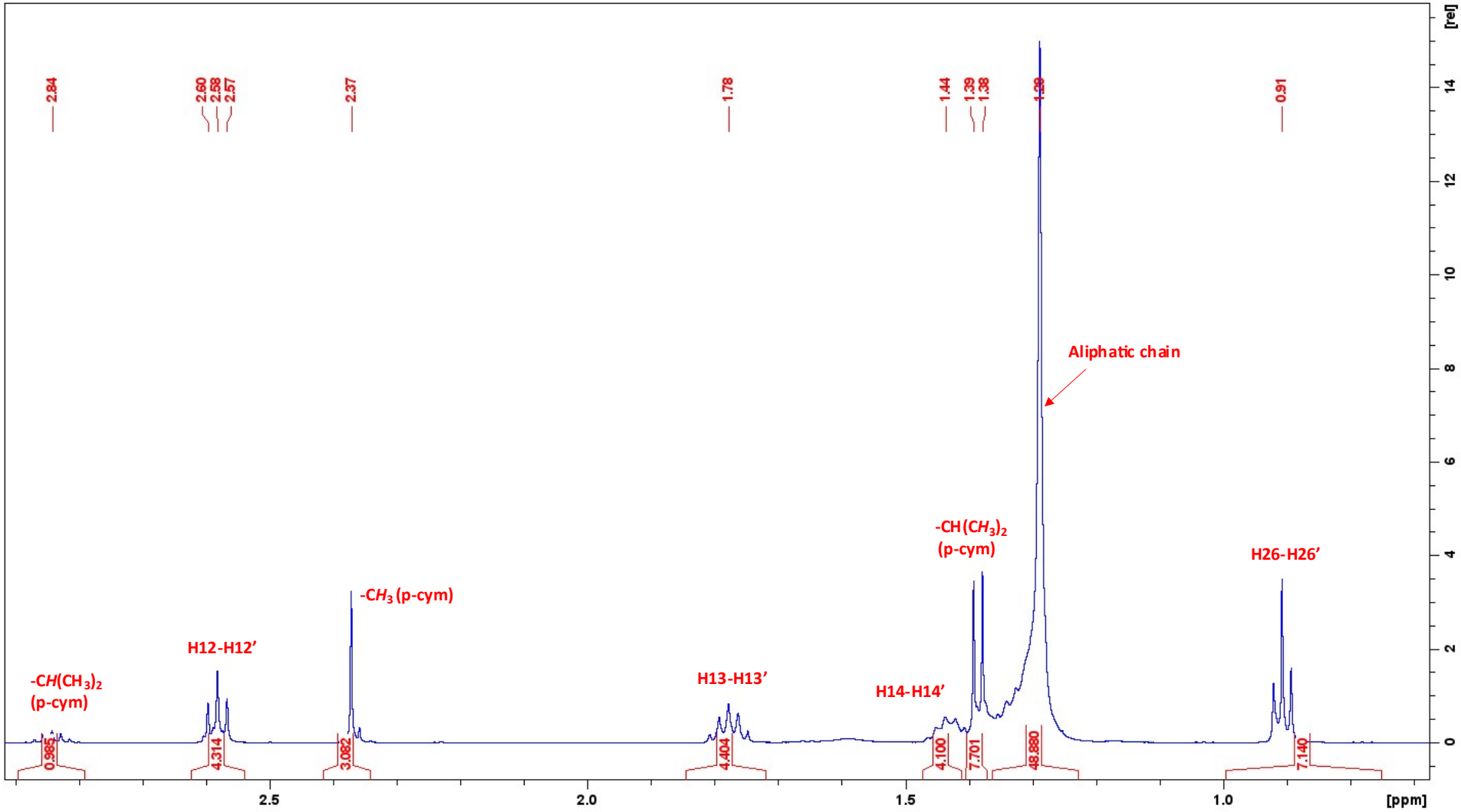

Figure S18 (a). Magnification of ^{1}H-NMR (1-3 ppm)

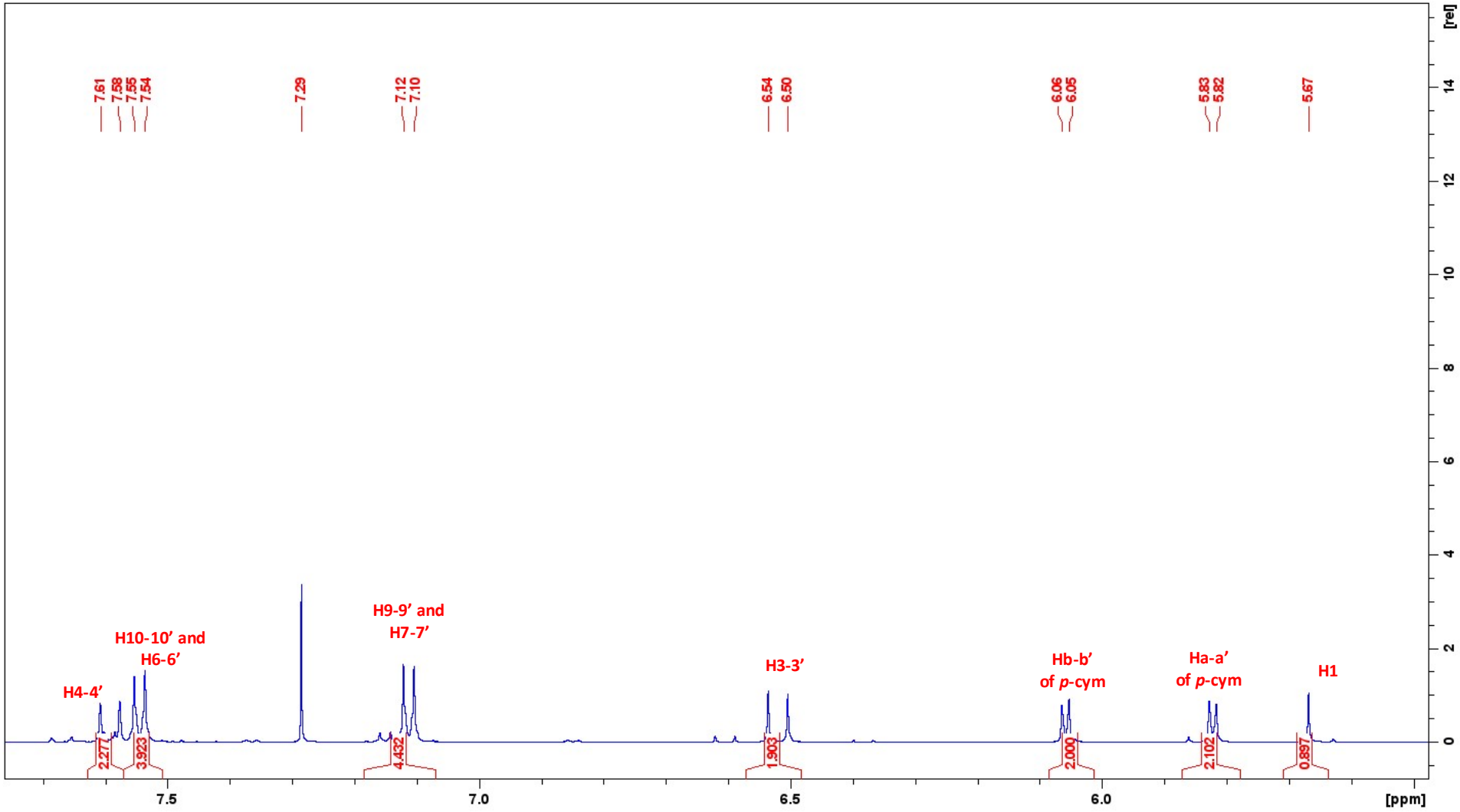

Figure S18 (b). Magnification of ^{1}H-NMR (4-8 ppm)

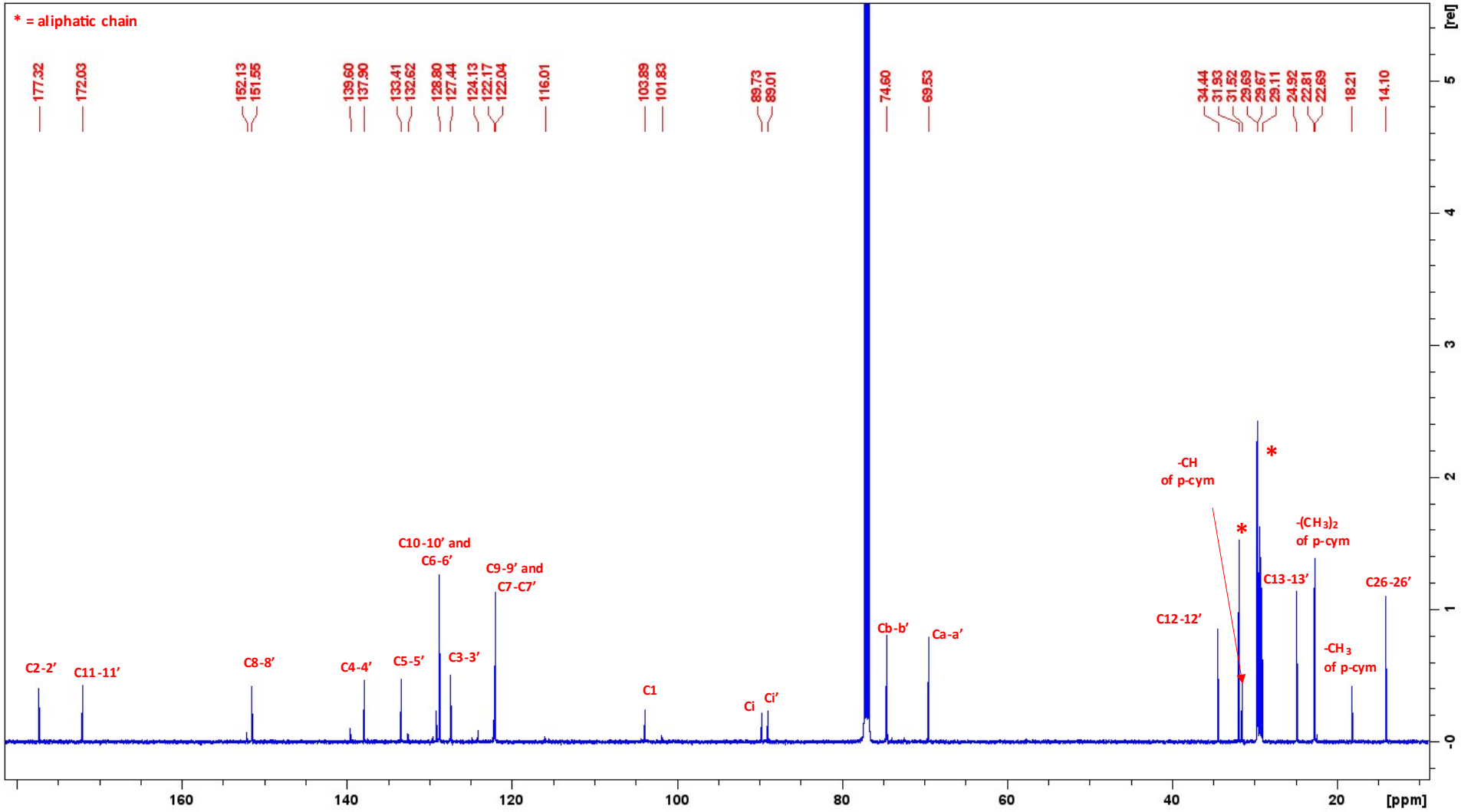

Figure S19. ^{13}C-NMR of **4** in $CDCl_3$ at 298 K

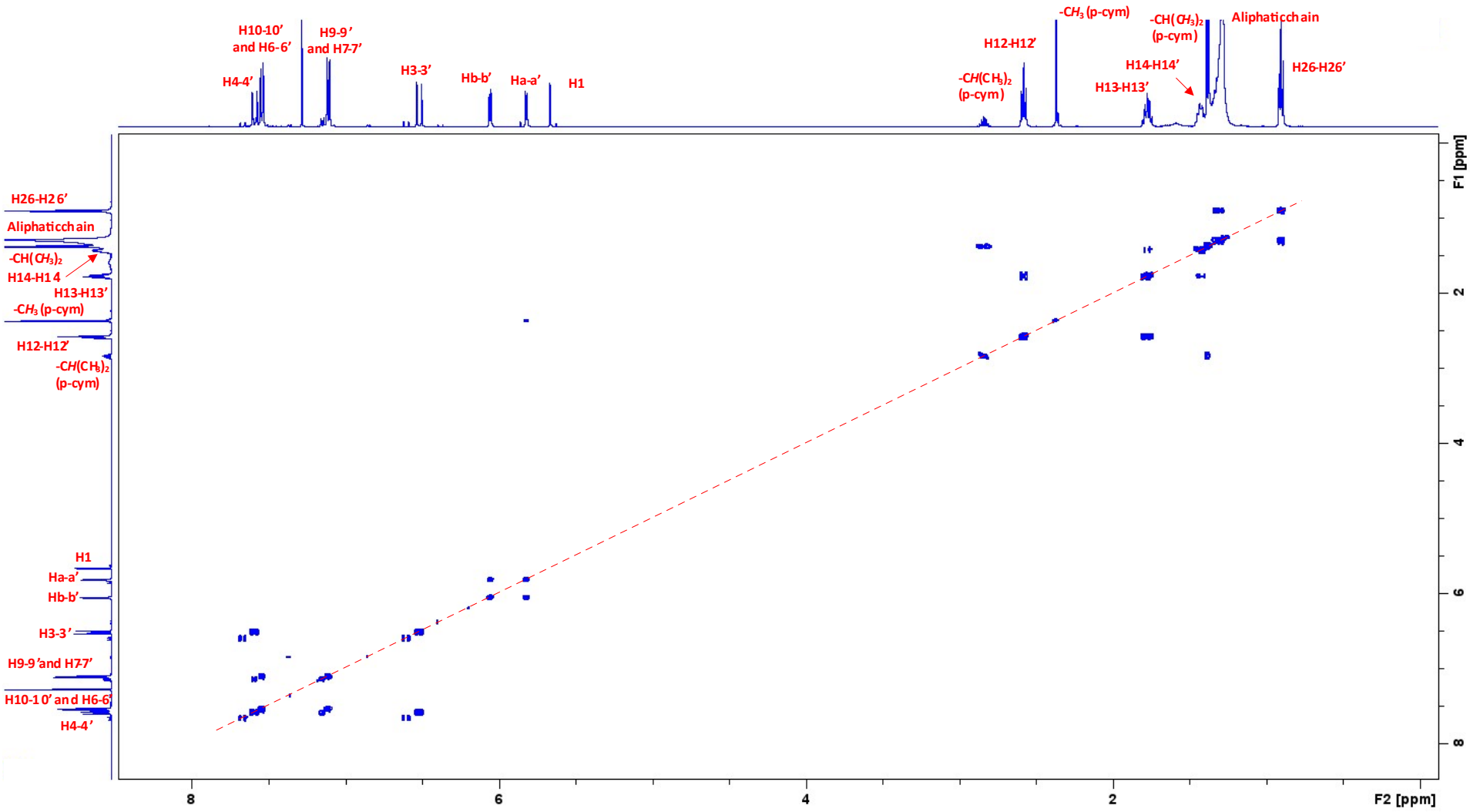

Figure S20. {^{1}H-^{1}H}-COSY NMR of **4** in $CDCl_3$ at 293 K

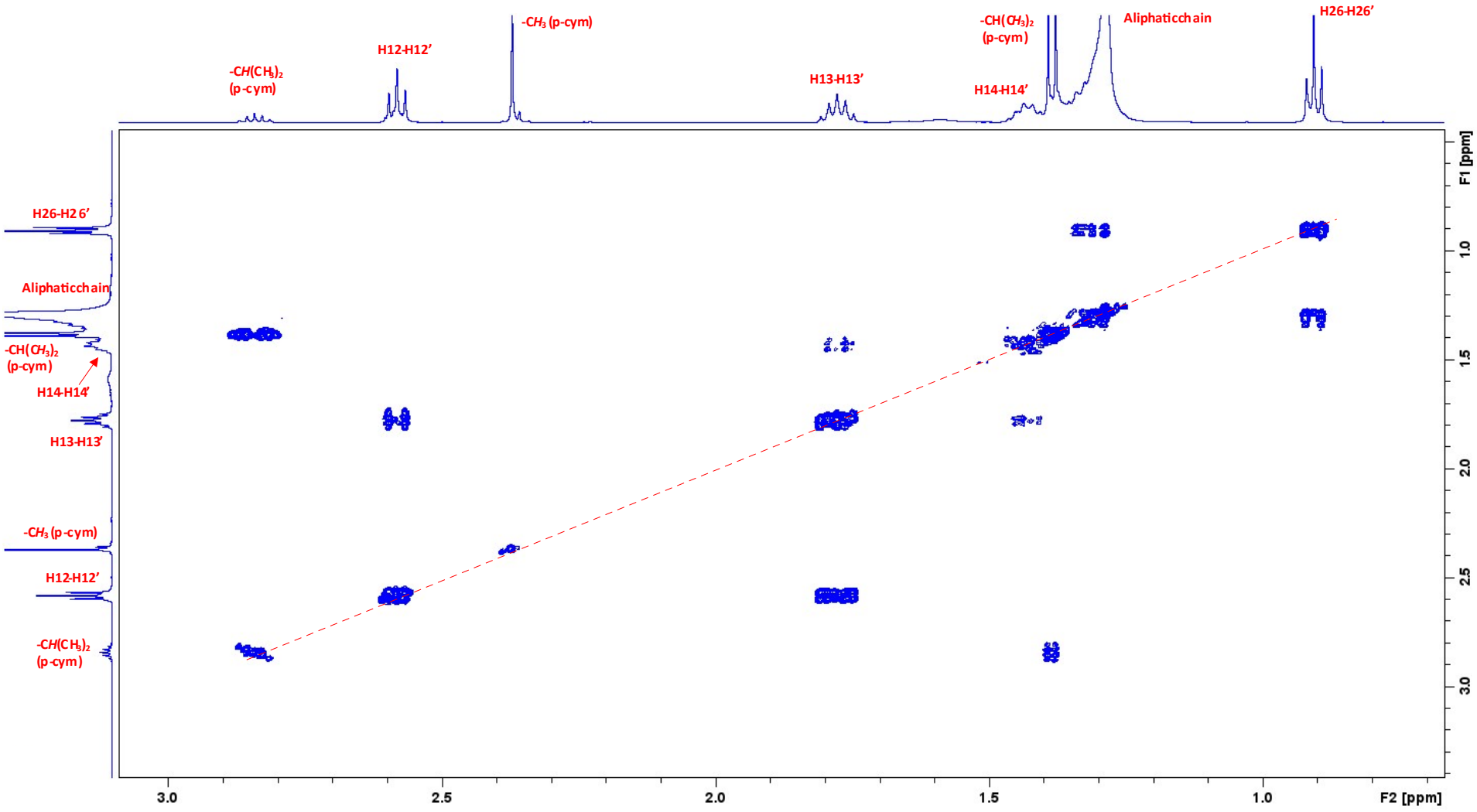

Figure S20 (a). Magnification of {^{1}H-^{1}H}-COSY NMR

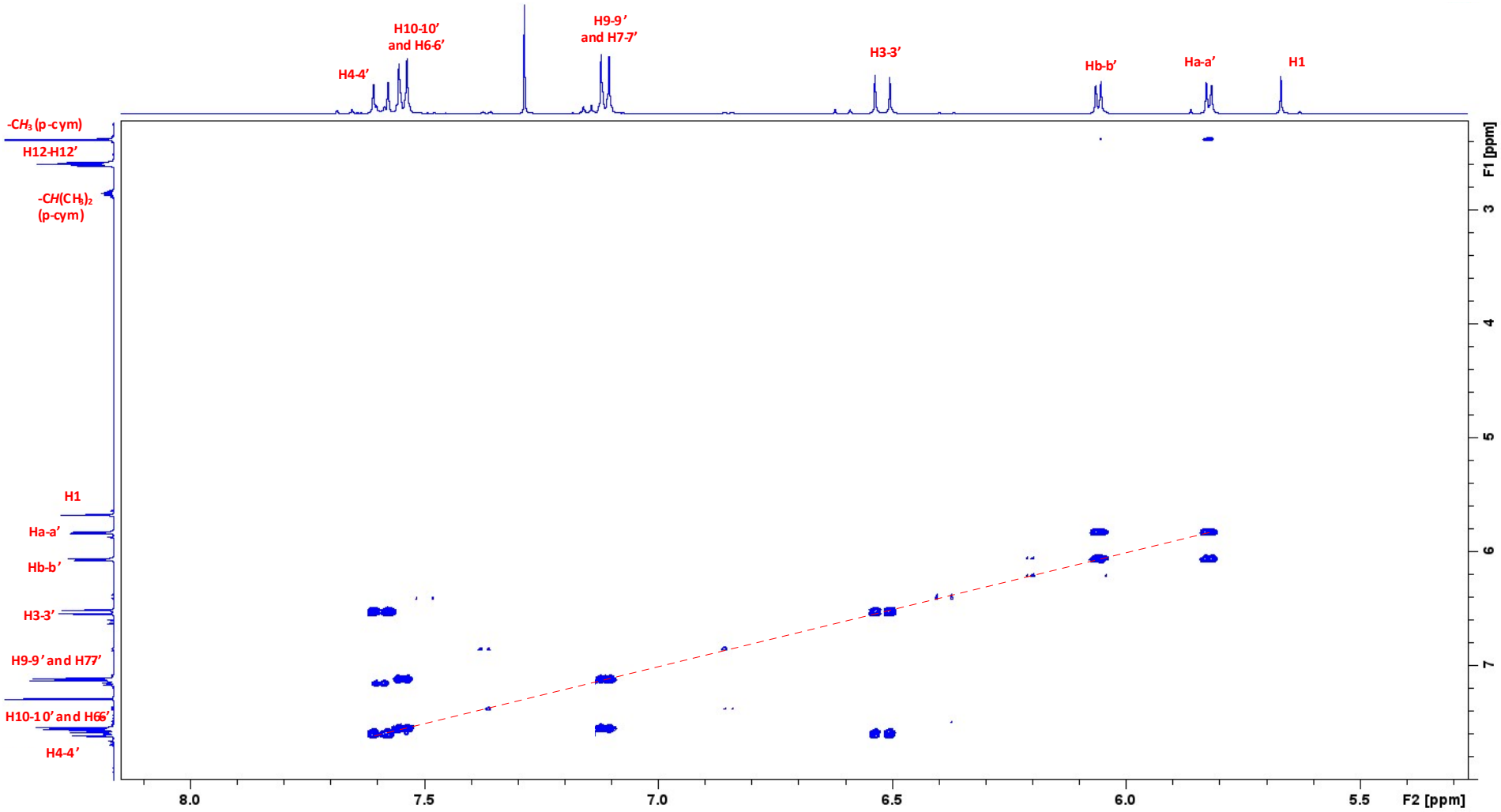

Figure S20 (b). Magnification of {^{1}H-^{1}H}-COSY NMR

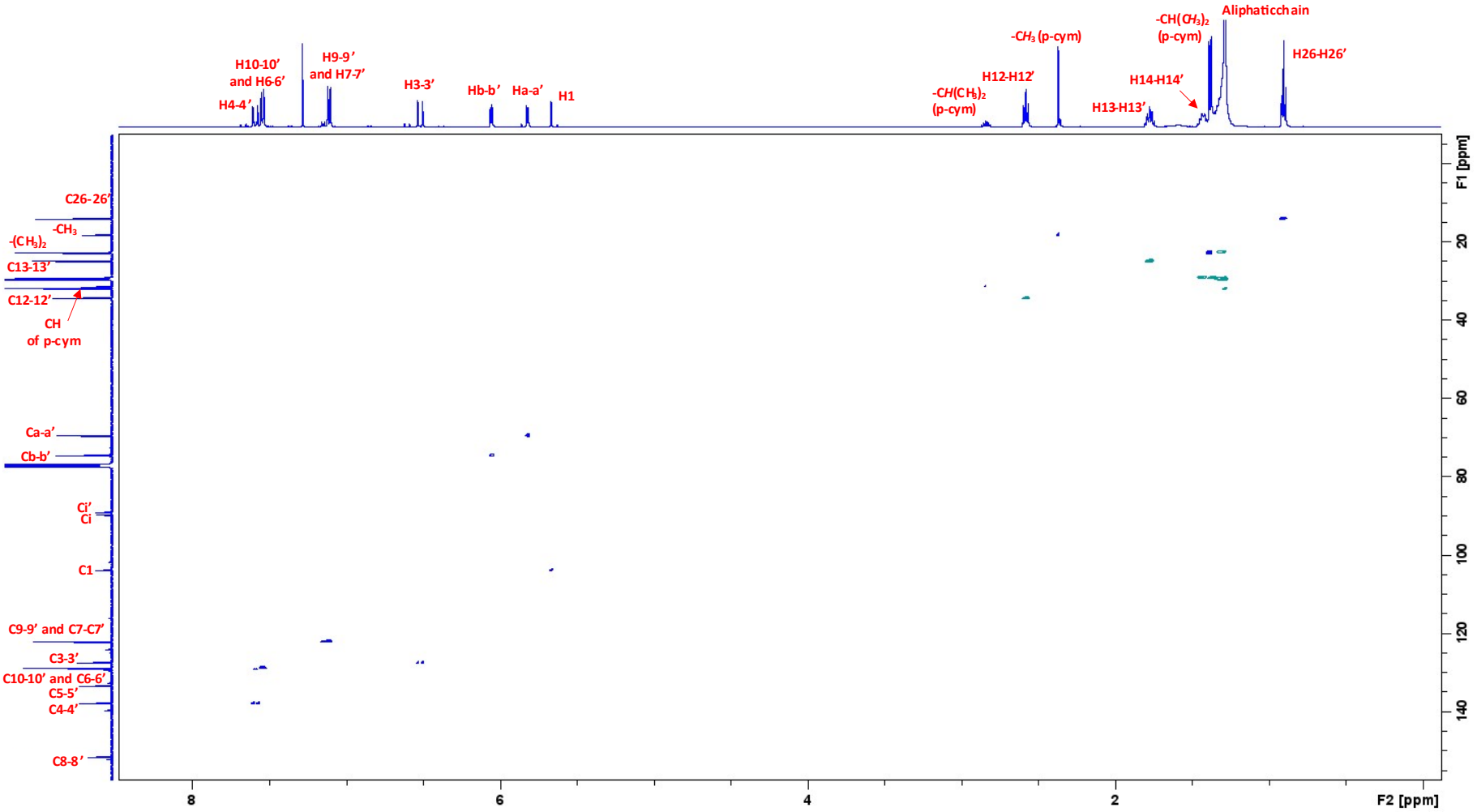

Figure S21. {^{1}H-^{13}C}-HSQC NMR of **4** in $CDCl_3$ at 293 K

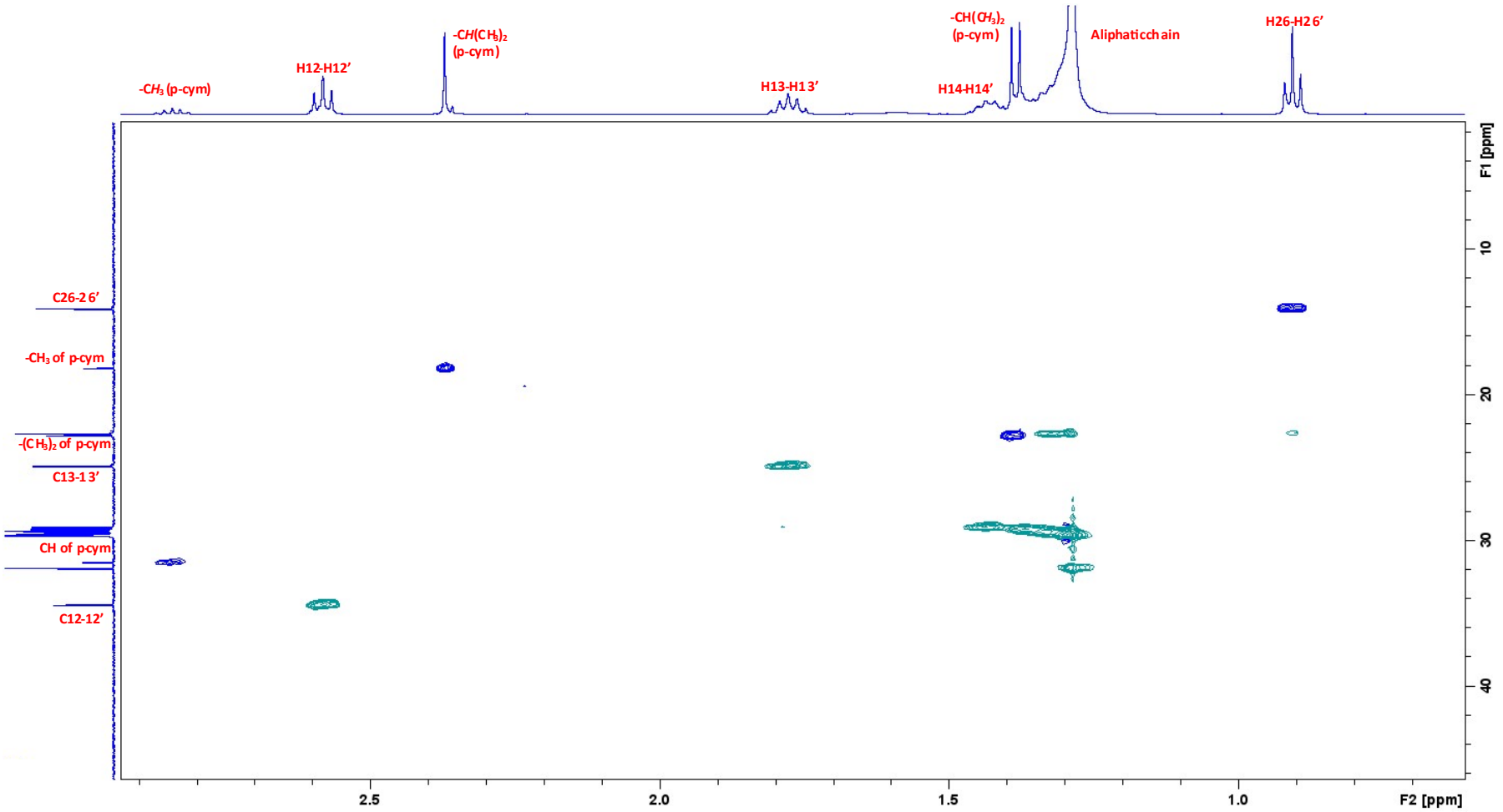

Figure S21 (a). Magnification of {^{1}H-^{13}C}-HSQC NMR

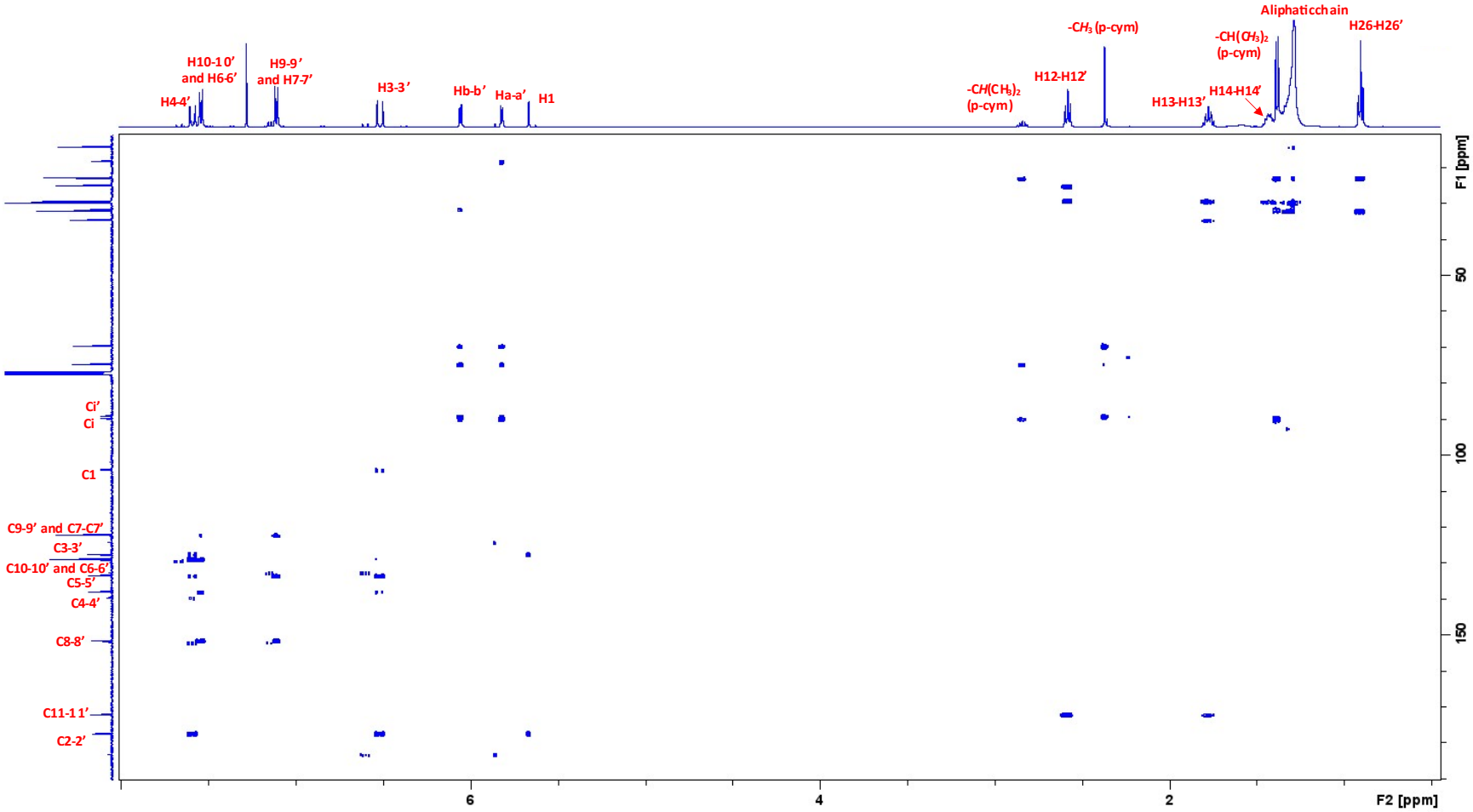

Figure S22. {^{1}H-^{13}C}-HMBC NMR of **4** in $CDCl_3$ at 293 K

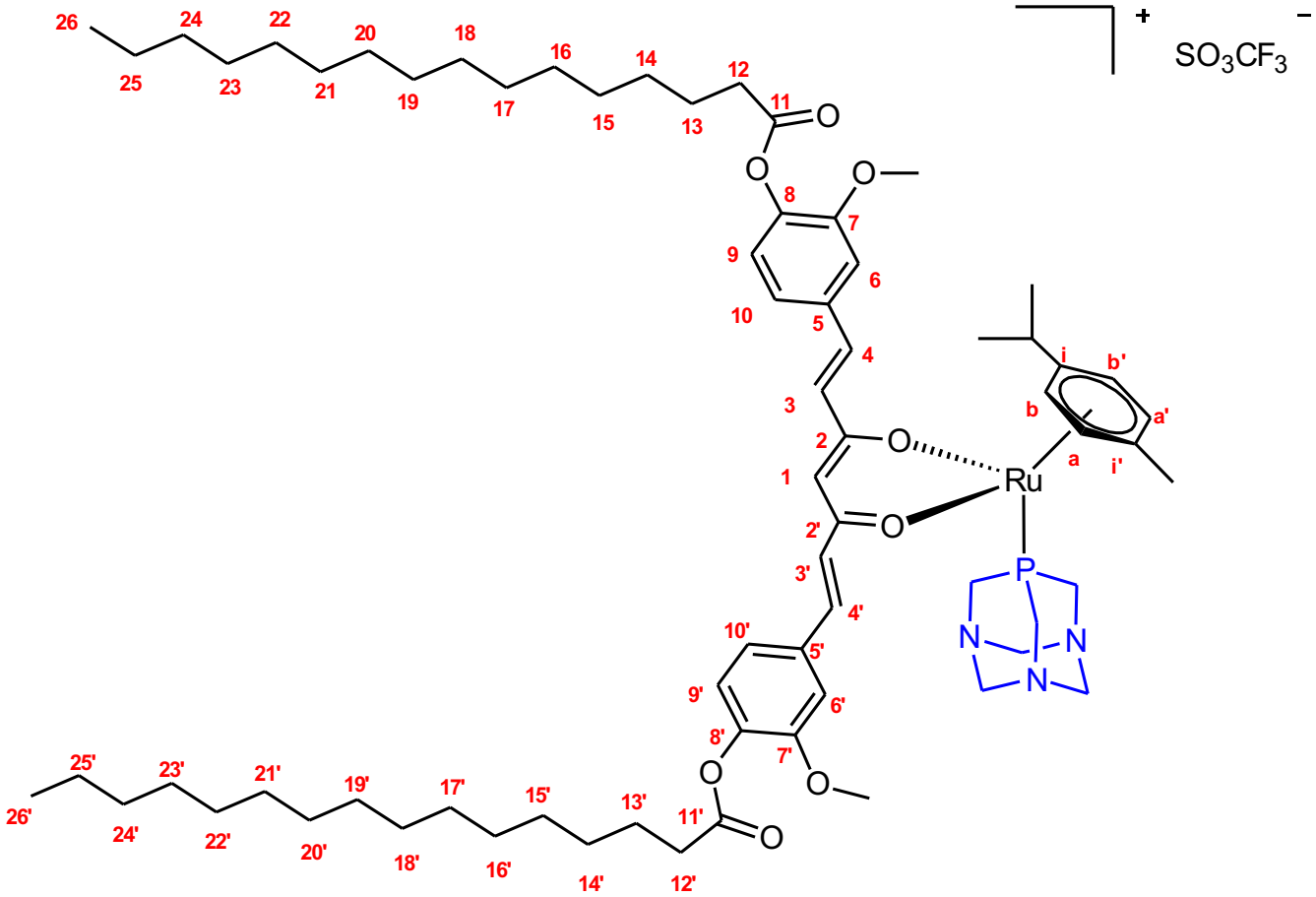
SO3CF3
Ru
O
P
N

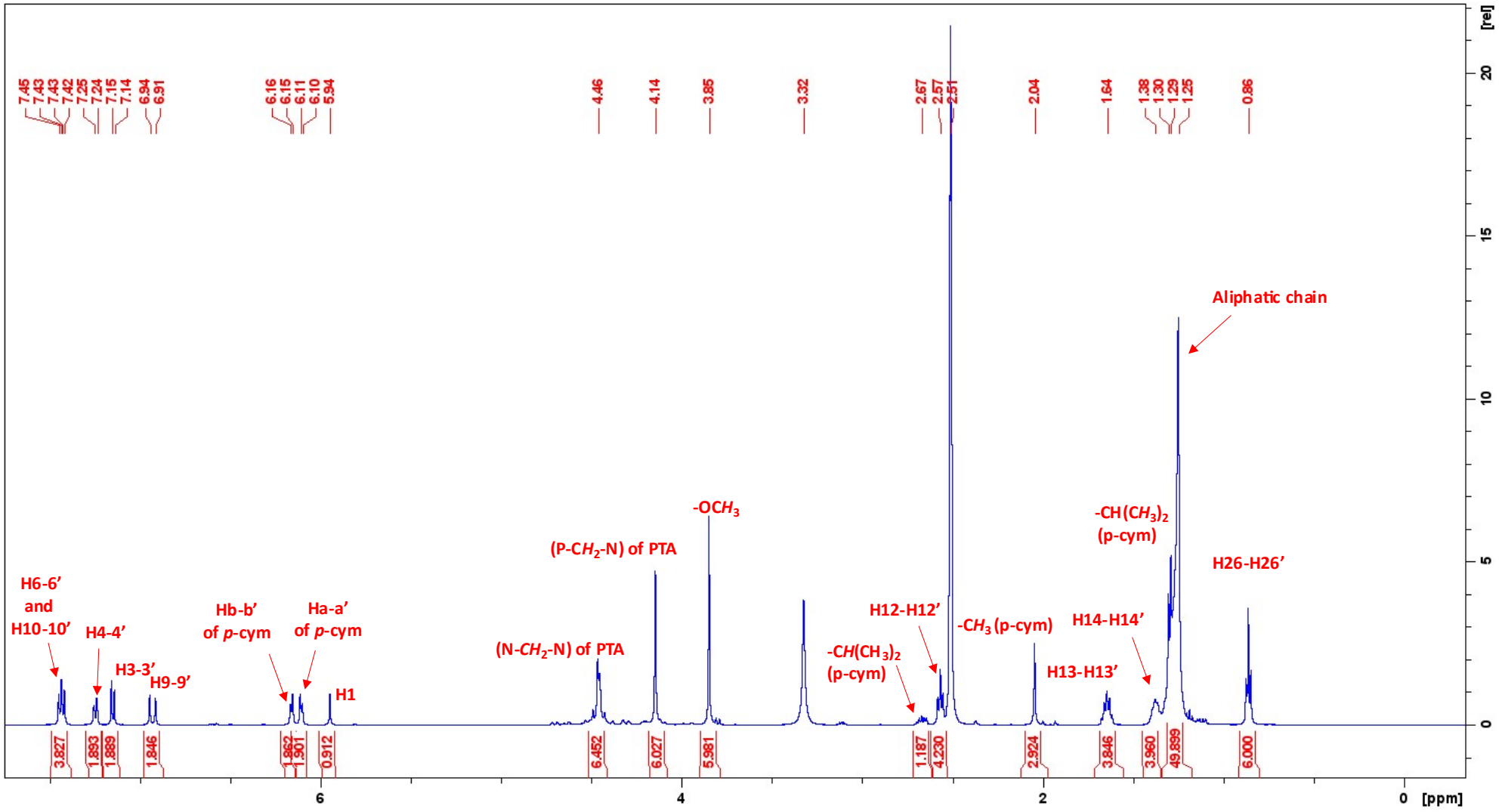

Figure S23. ^{1}H-NMR of **5** in DMSO at 293 K

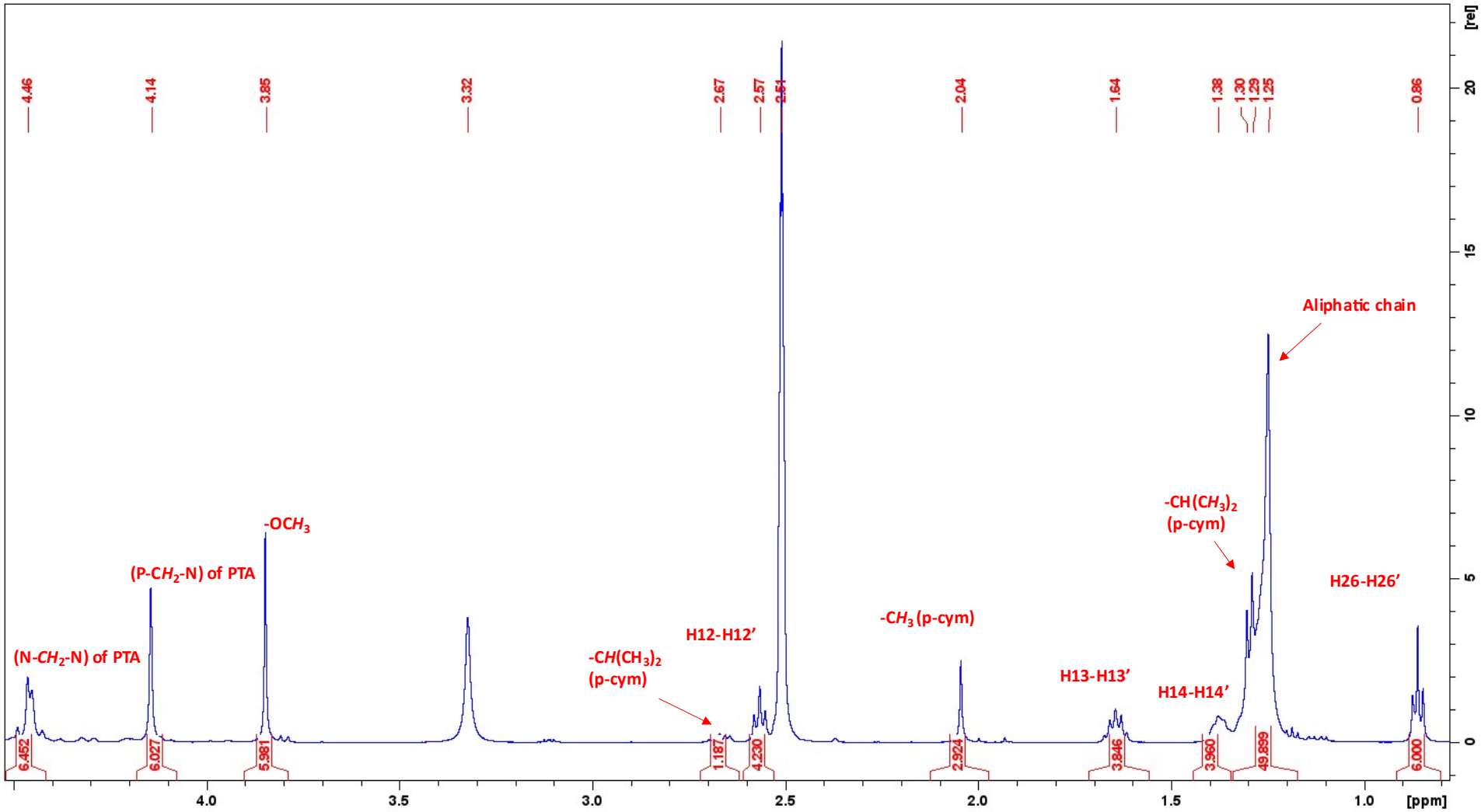

Figure S23 (a). Magnification of ^{1}H-NMR (1-5 ppm)

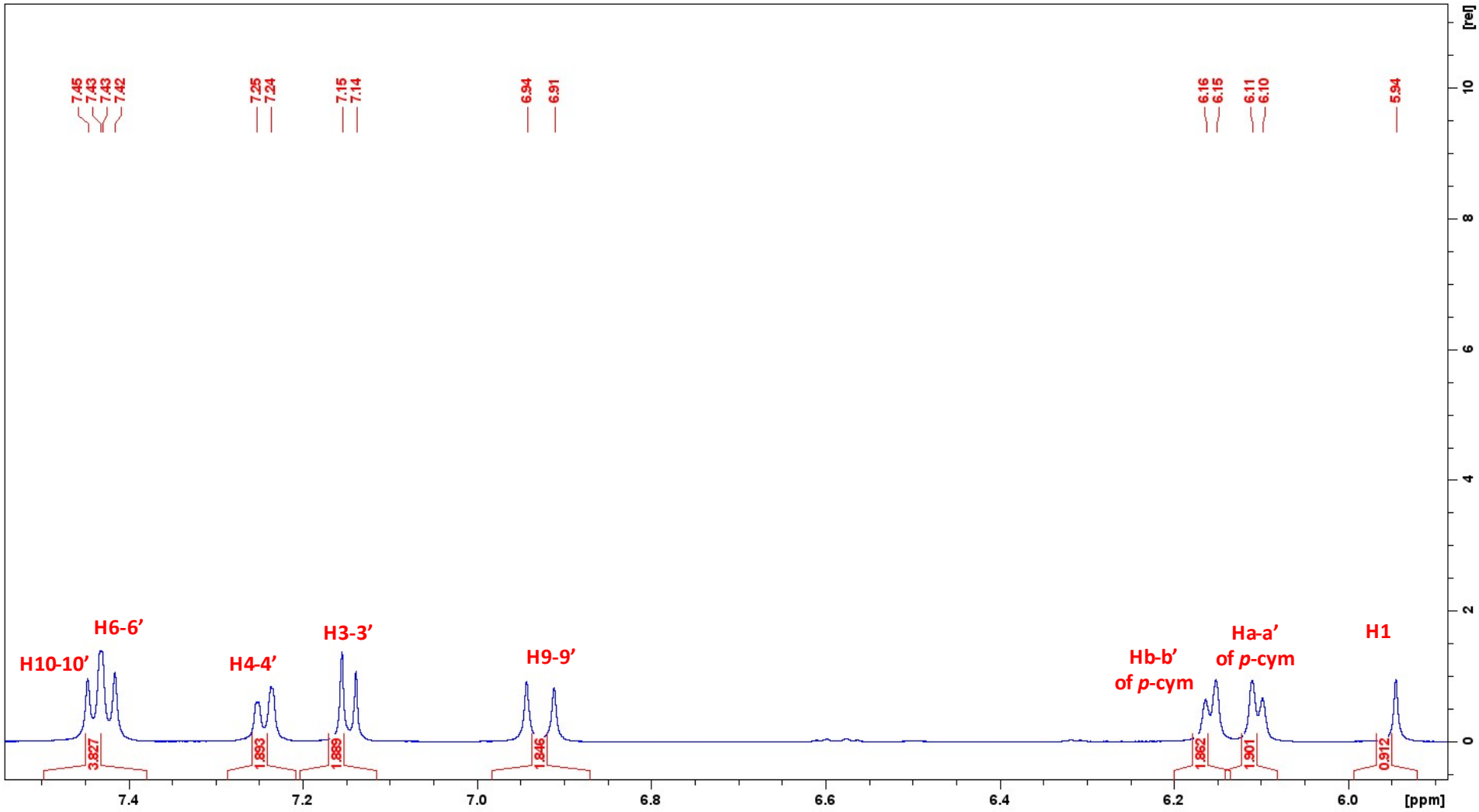

Figure S23 (b). Magnification of ^{1}H-NMR (6-8 ppm)

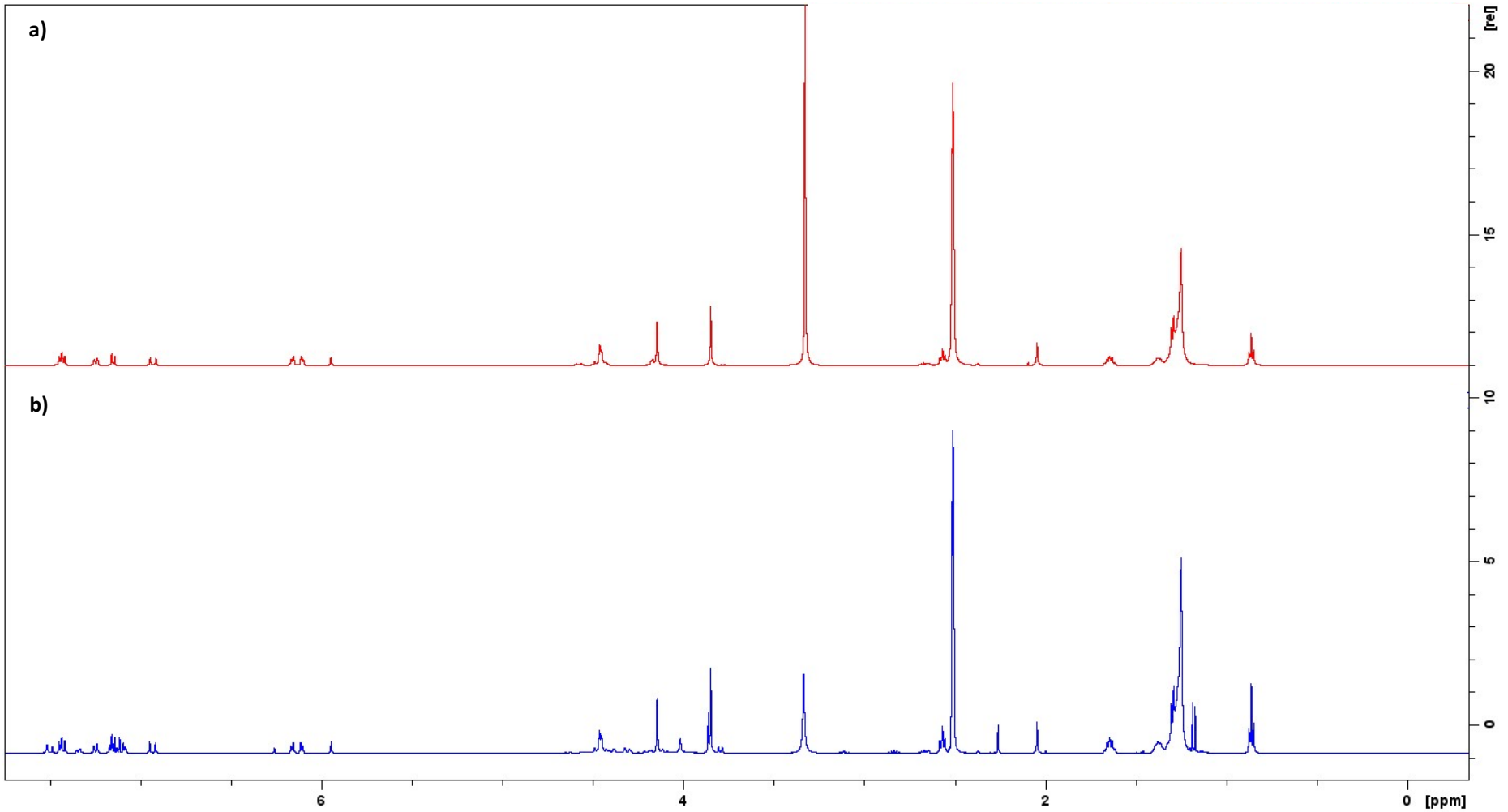

Figure S23 (c). Comparison of ^{1}H-NMR spectra of complex **5** at t=0 (a) and after 5 days (b)

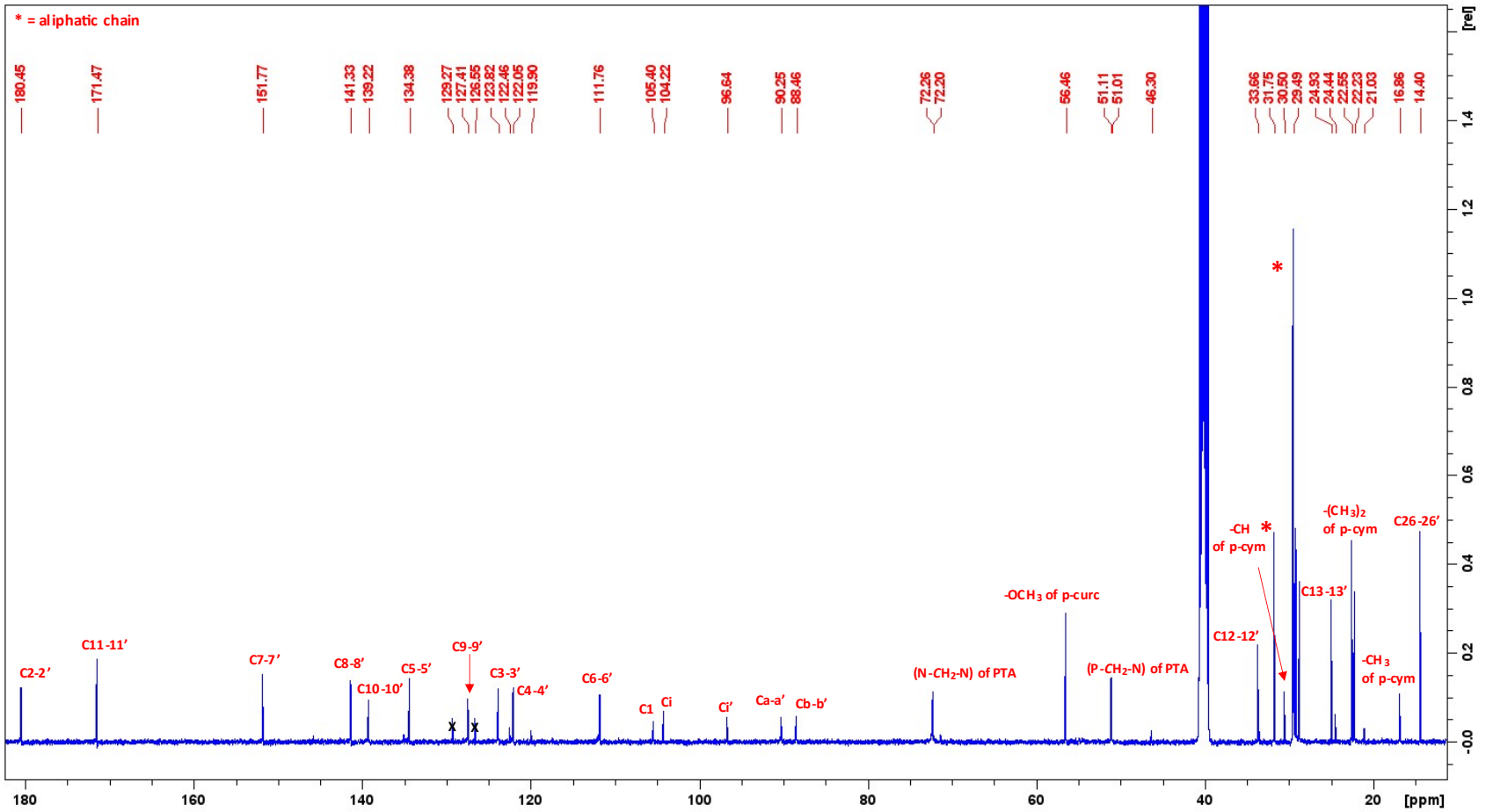

Figure S24. ^{13}C-NMR of **5** in DMSO at 293 K

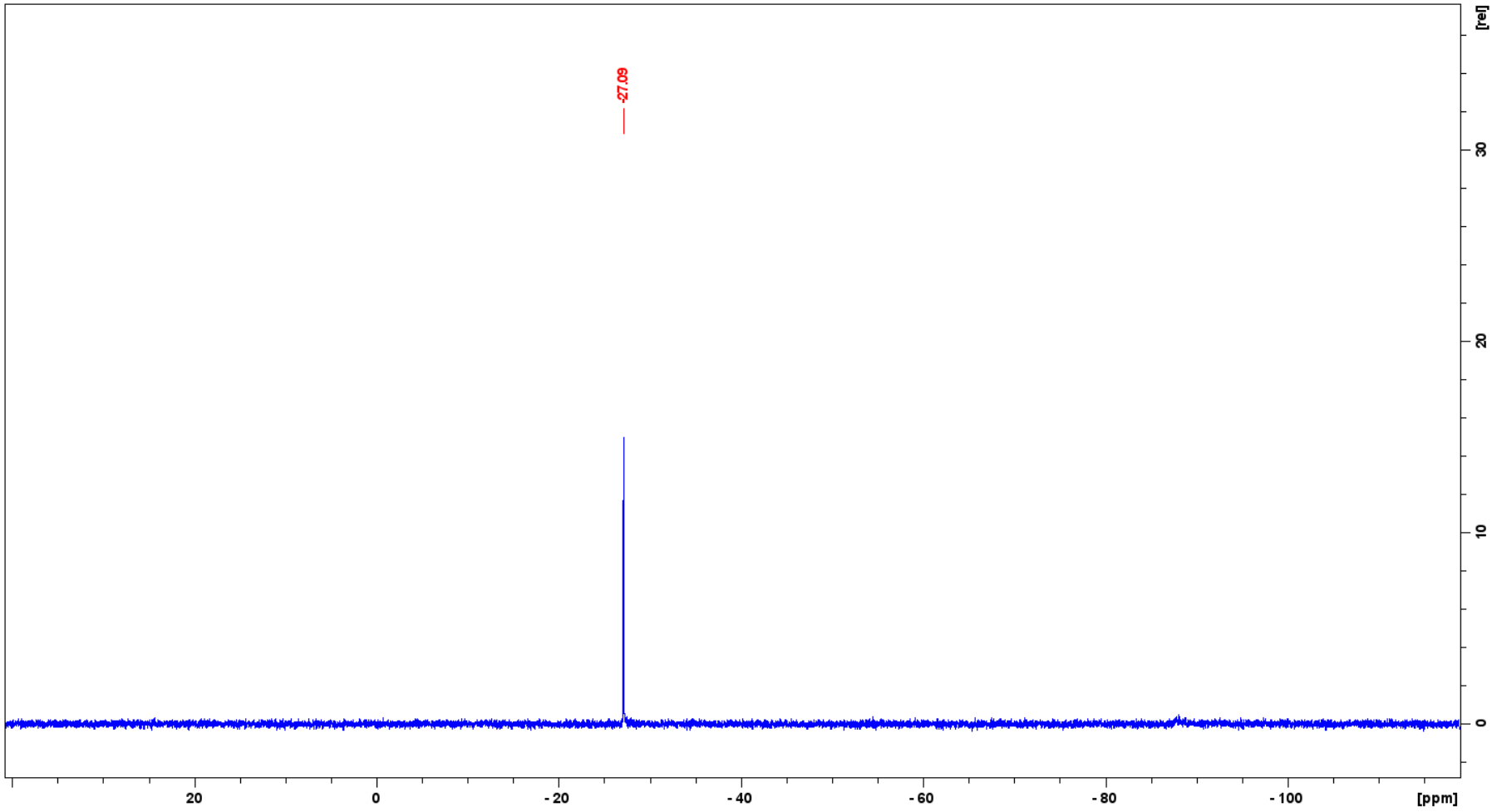

Figure S25. ^{31}P-NMR of **5** in DMSO at 293 K

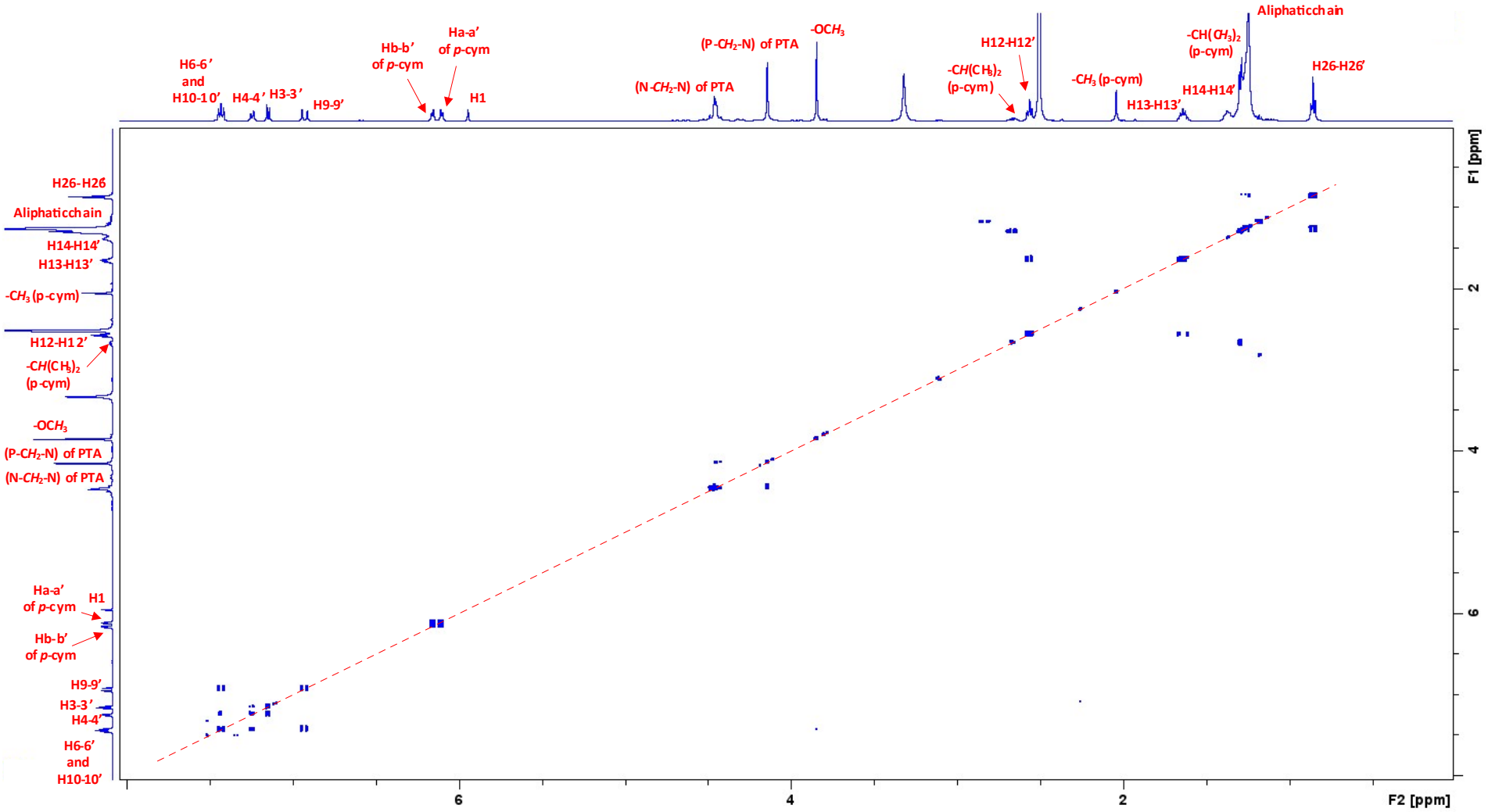

Figure S26.{^{1}H-^{1}H}- COSY NMR of **5** in DMSO at 293 K.

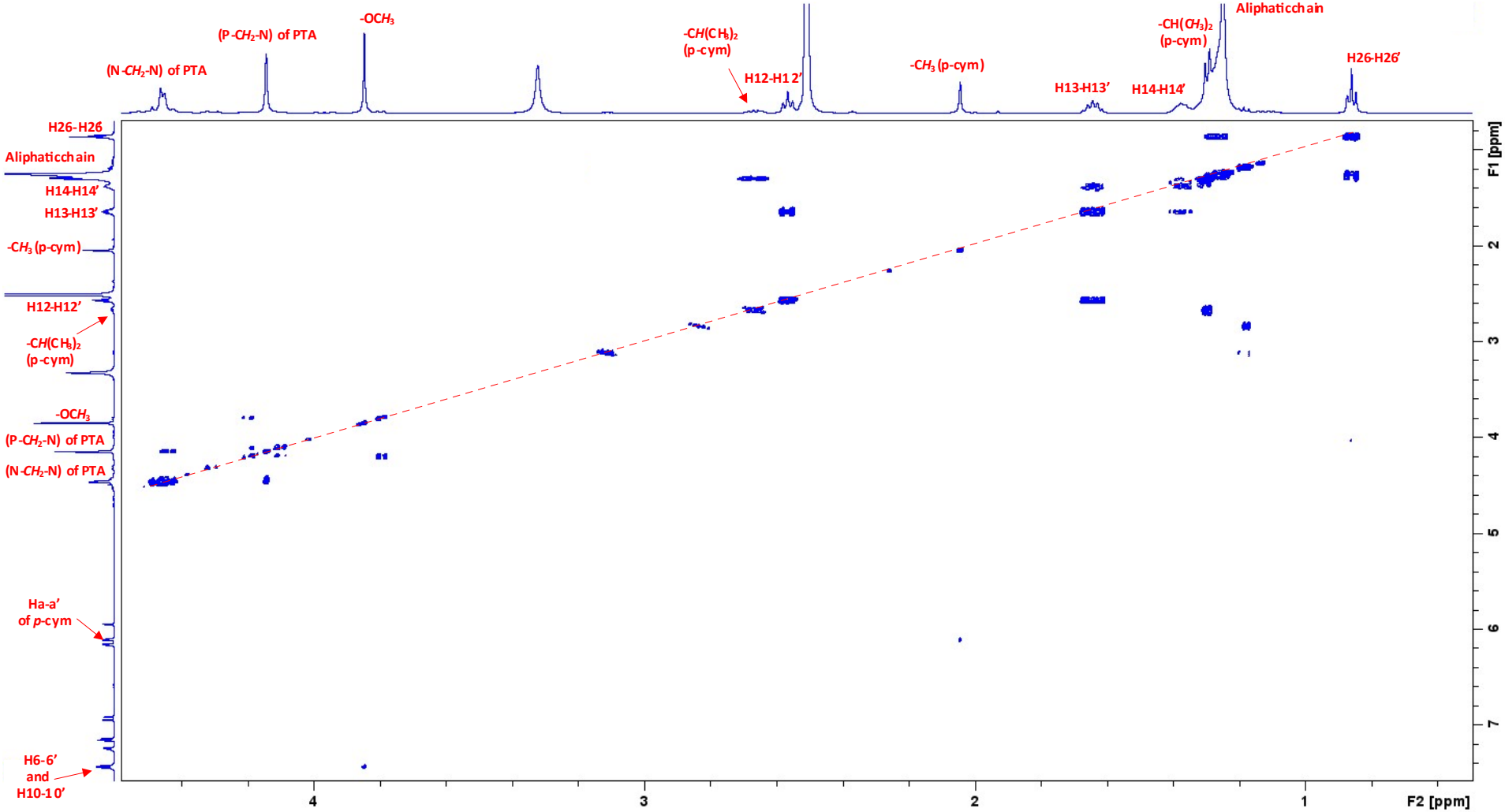

Figure S26 (a). Magnification of {^{1}H-^{1}H}- COSY NMR

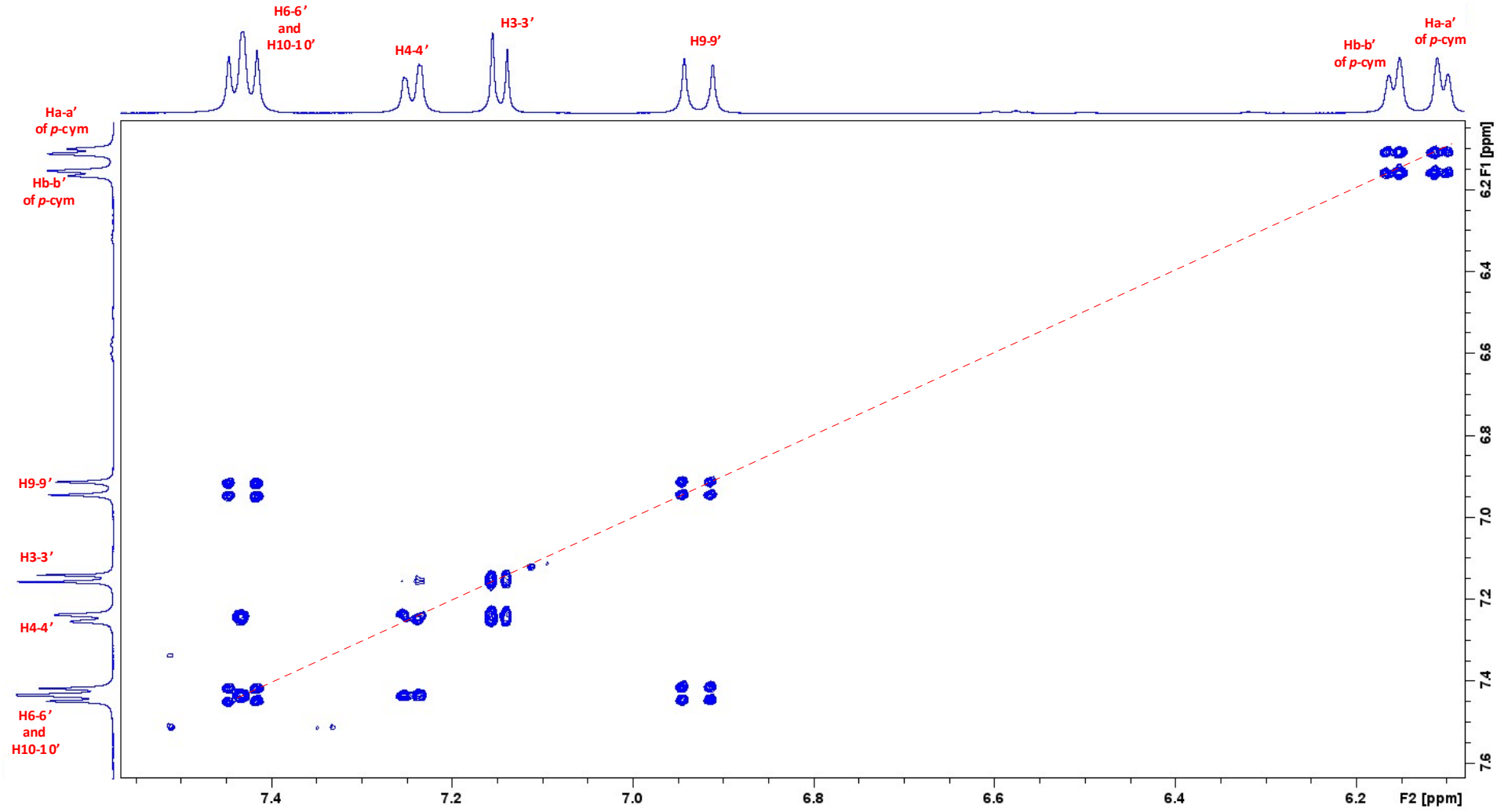

Figure S26 (b). Magnification of {^{1}H-^{1}H}- COSY NMR

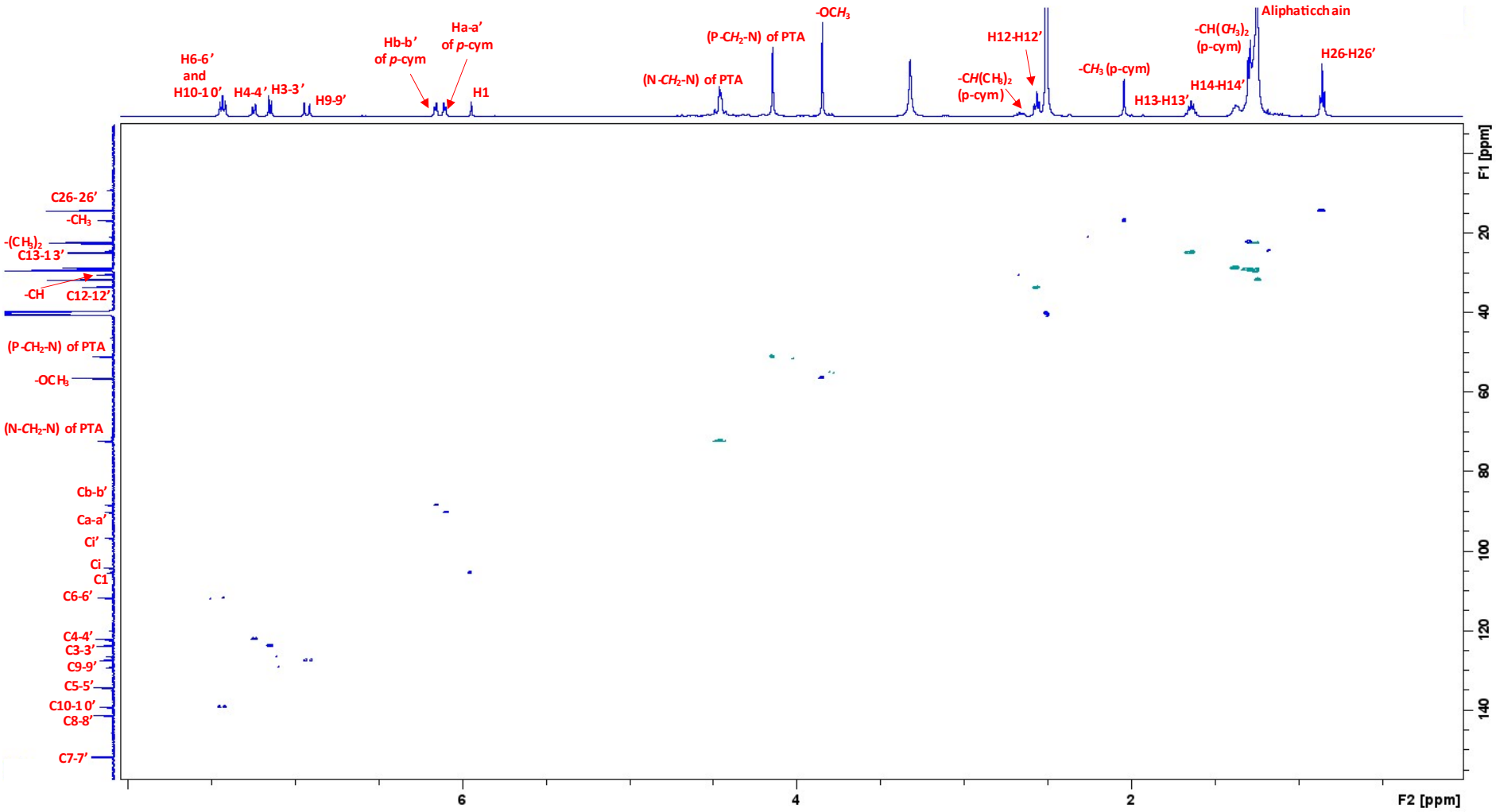

Figure S27. {^{1}H-^{13}C}-HSQC NMR of **5** in DMSO at 293 K

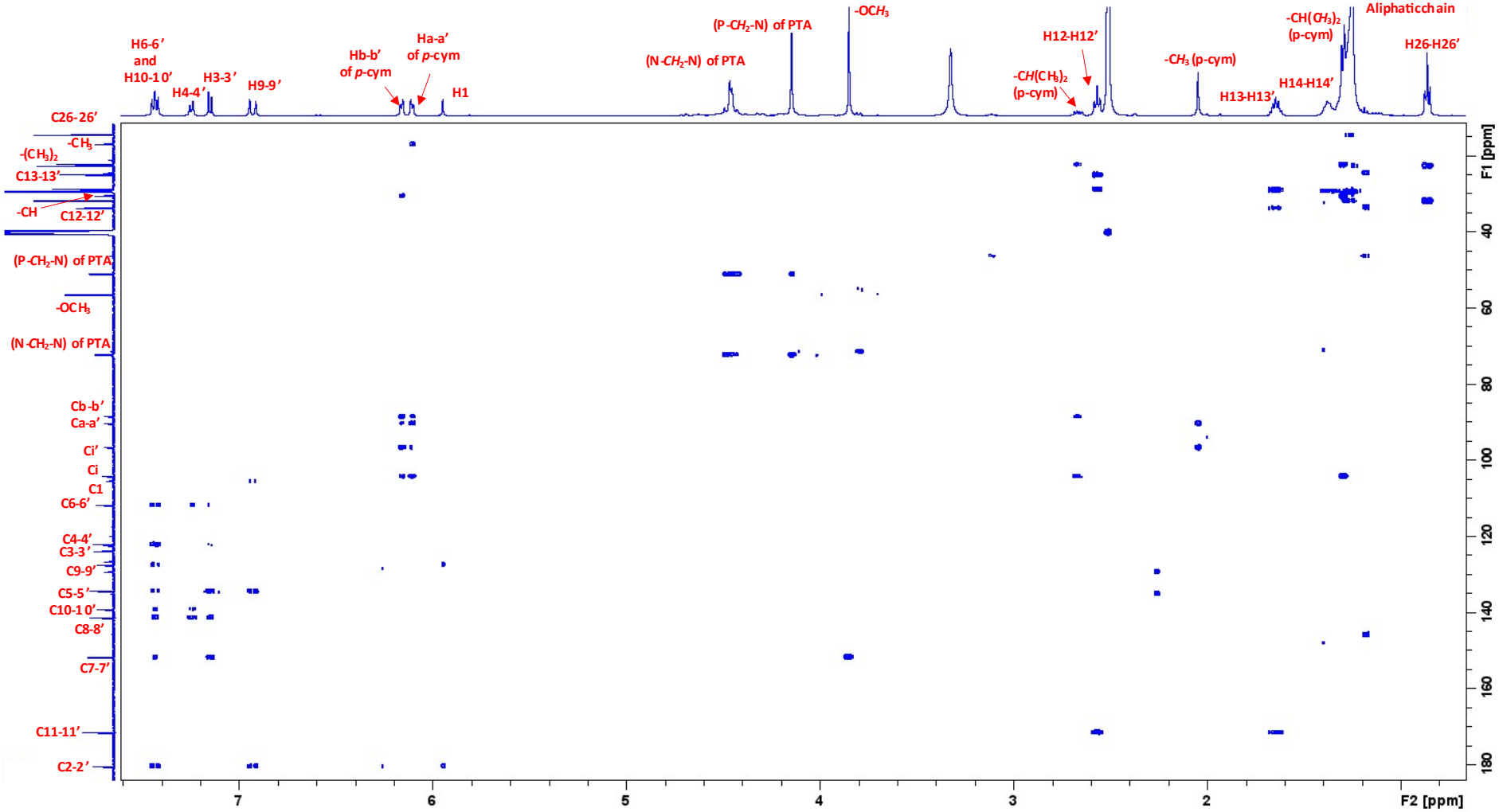

Figure S28. {^{1}H-^{13}C}-HMBC NMR of **5** in DMSO at 293 K

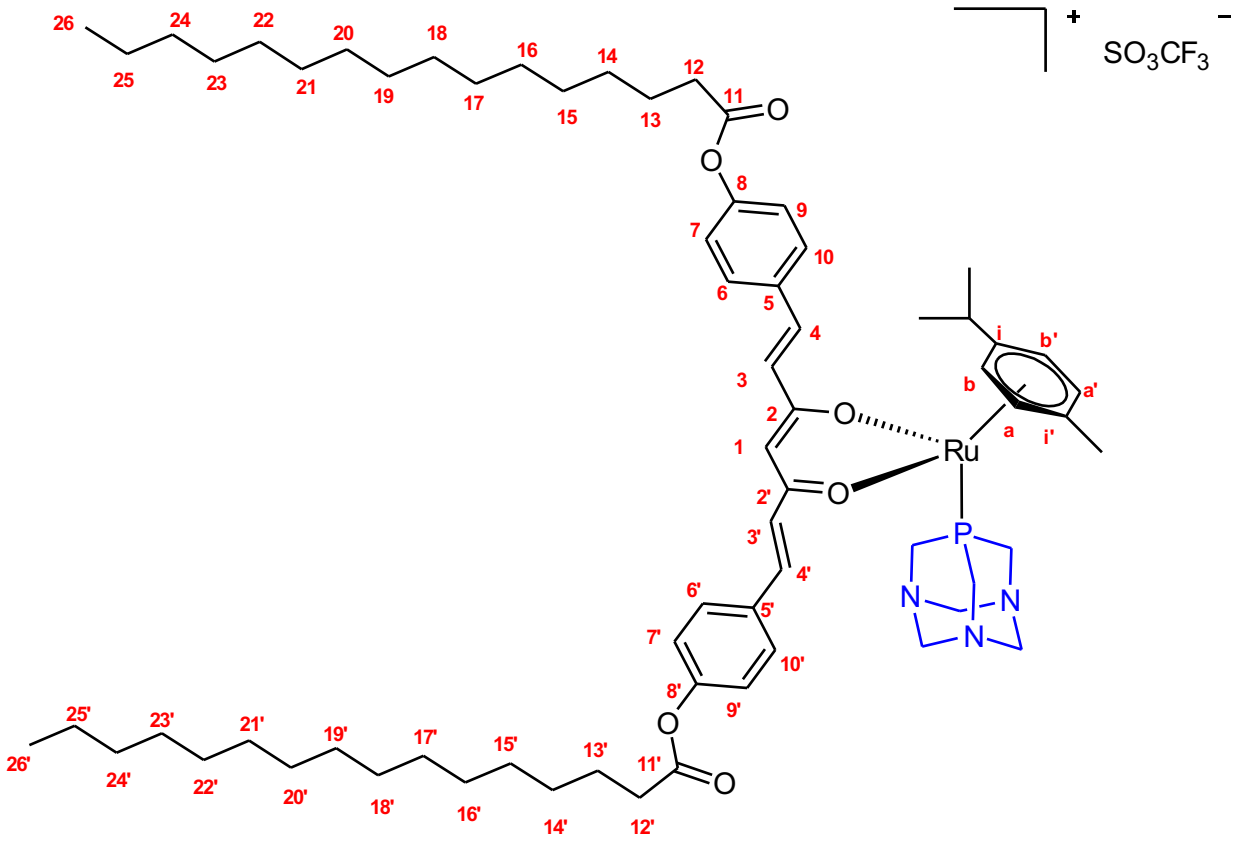
SO3CF3
Ru
P
N
O

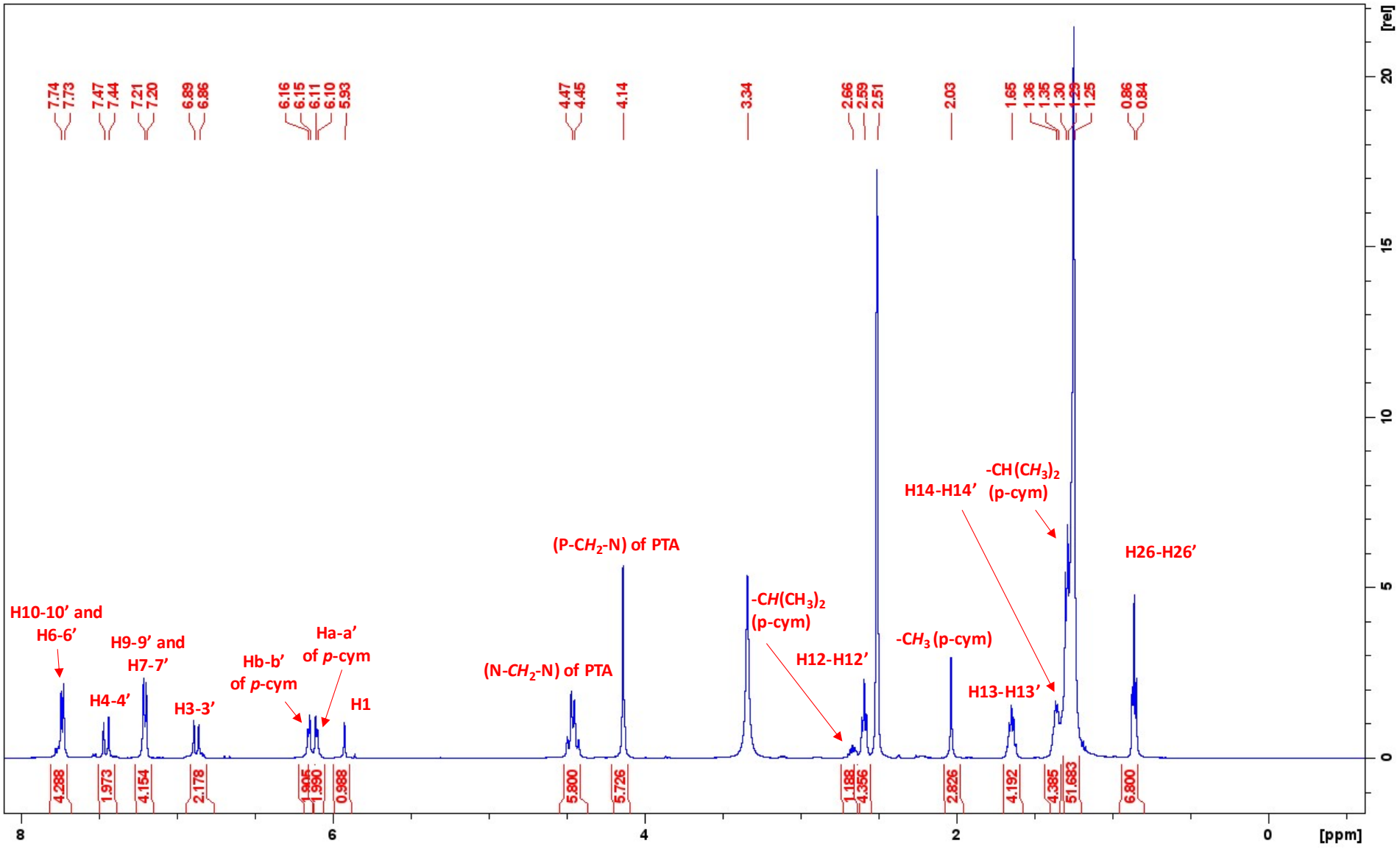

Figure S29. ^{1}H-NMR of **6** in DMSO at 293 K

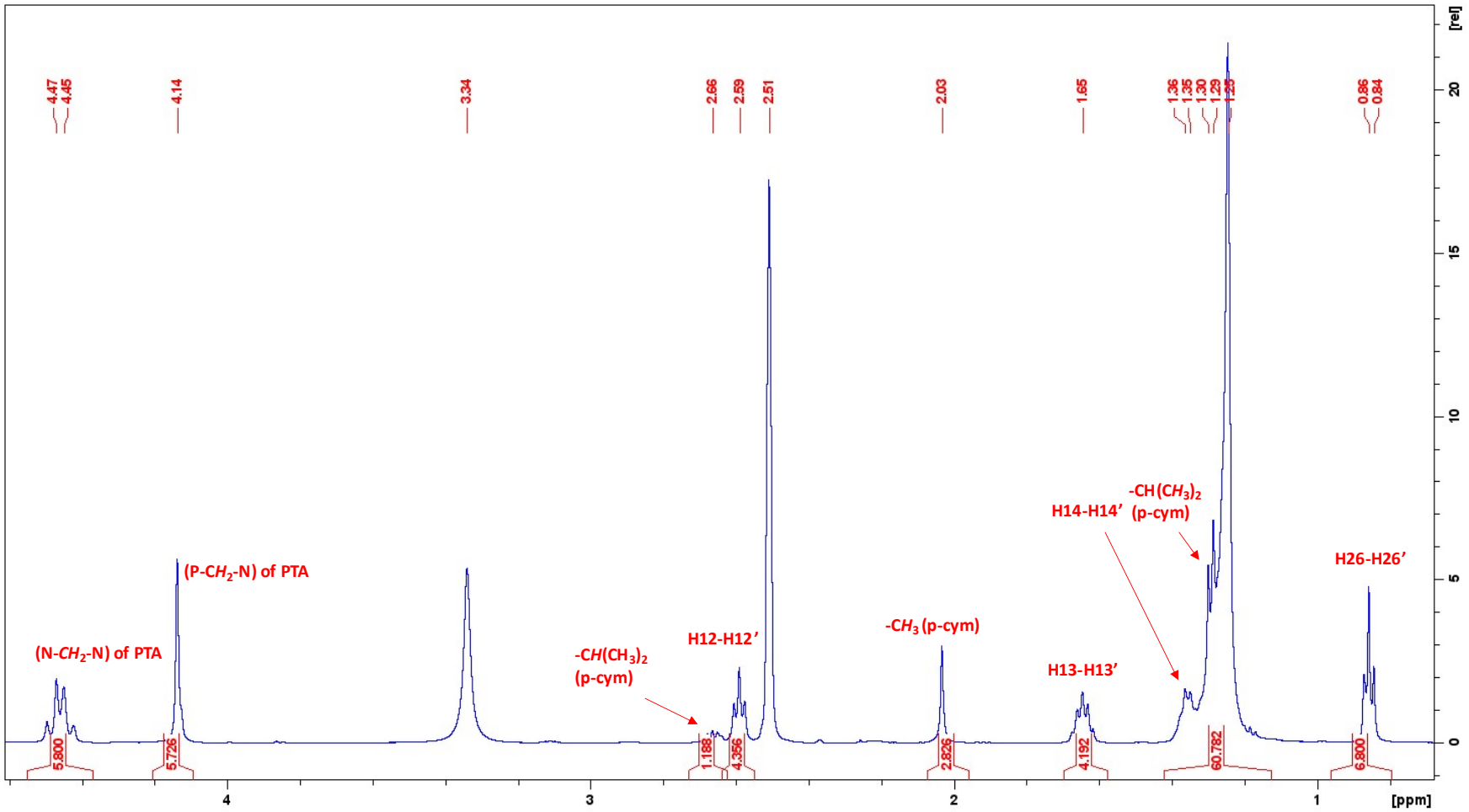

Figure S29 (a). Magnification of ^{1}H-NMR (1-5 ppm)

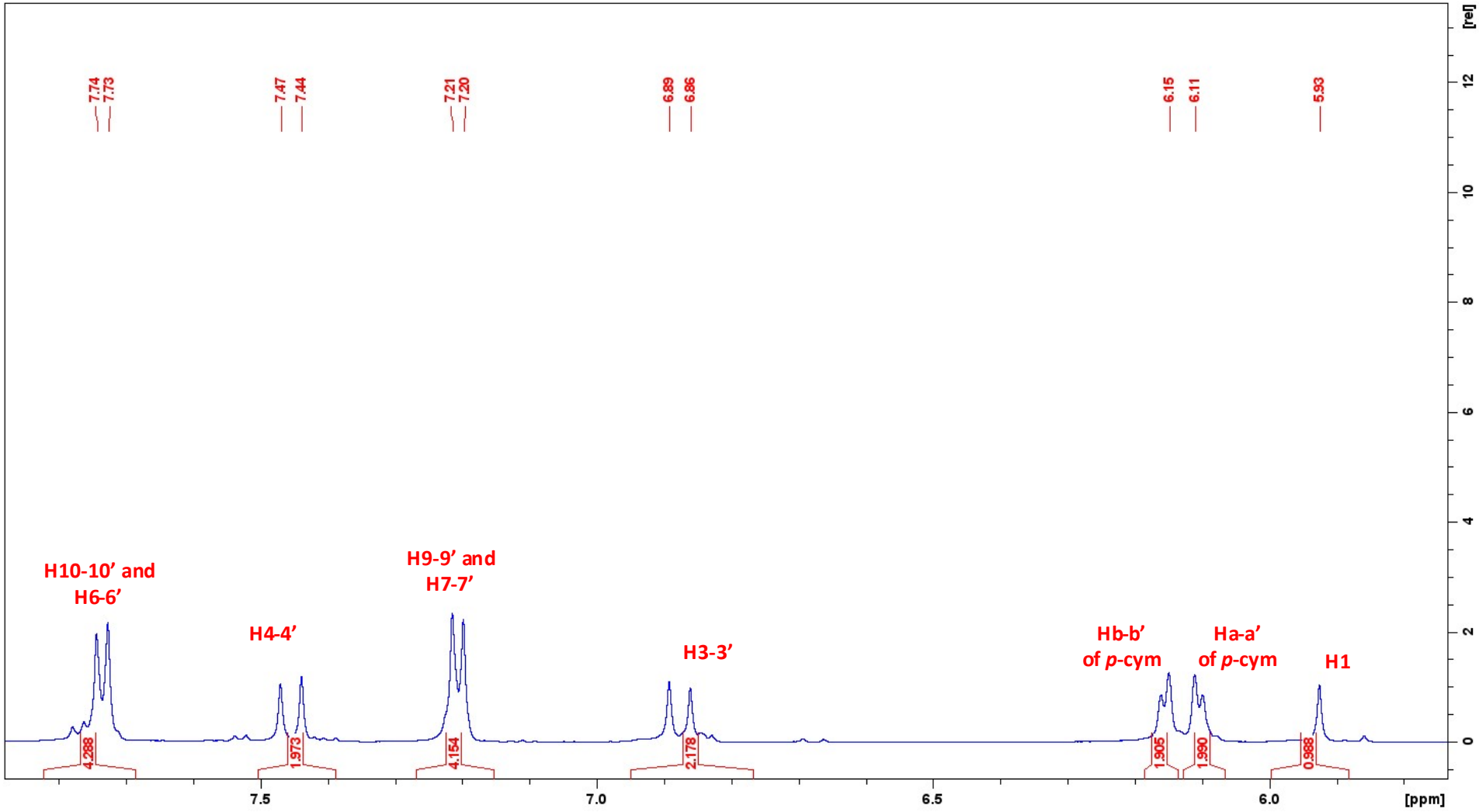

Figure S29 (b). Magnification of ^{1}H-NMR (5-8 ppm)

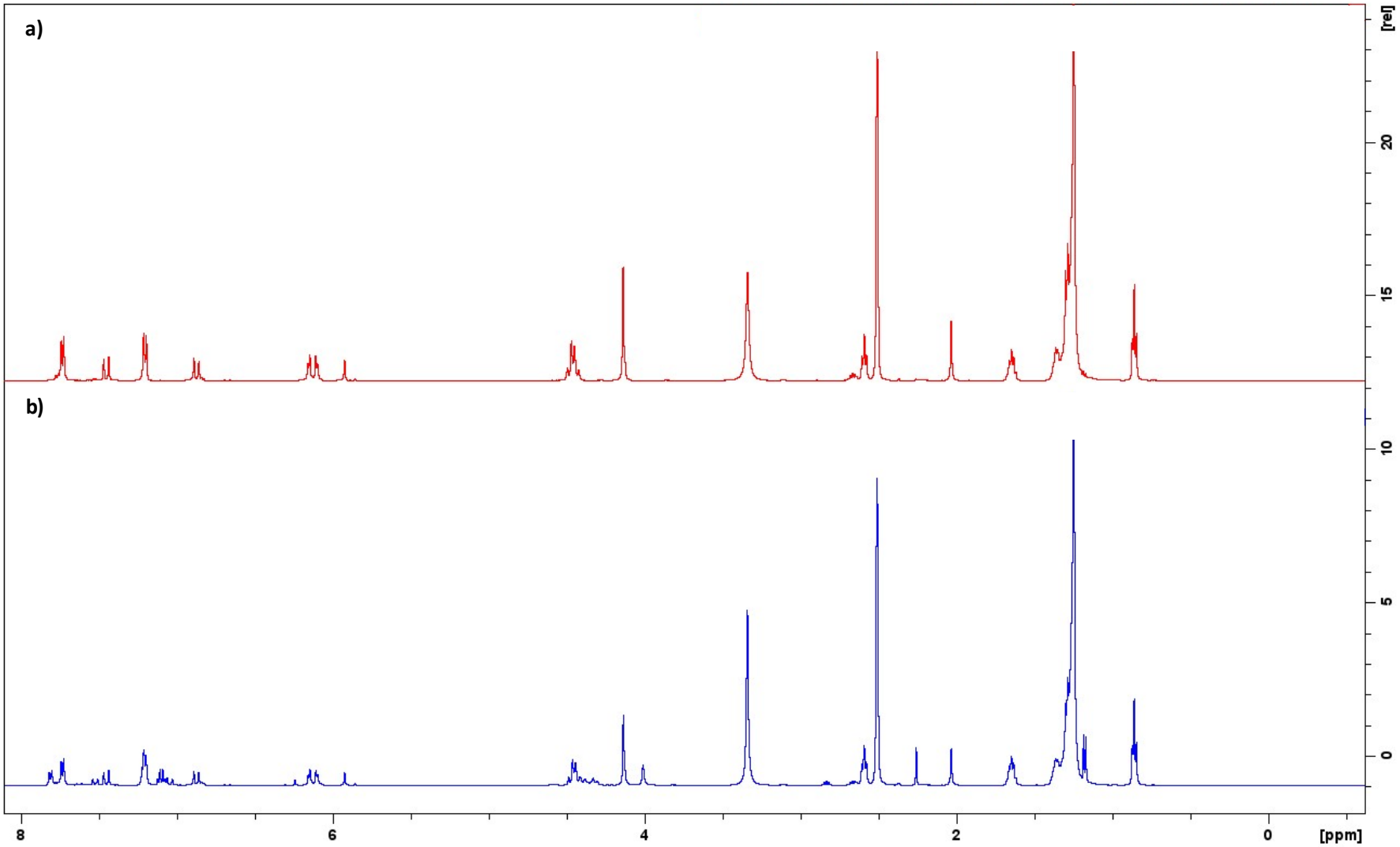

Figure S29 (c). Comparison of ^{1}H-NMR spectra of complex **6** at t=0 (a) and after 5 days (b)

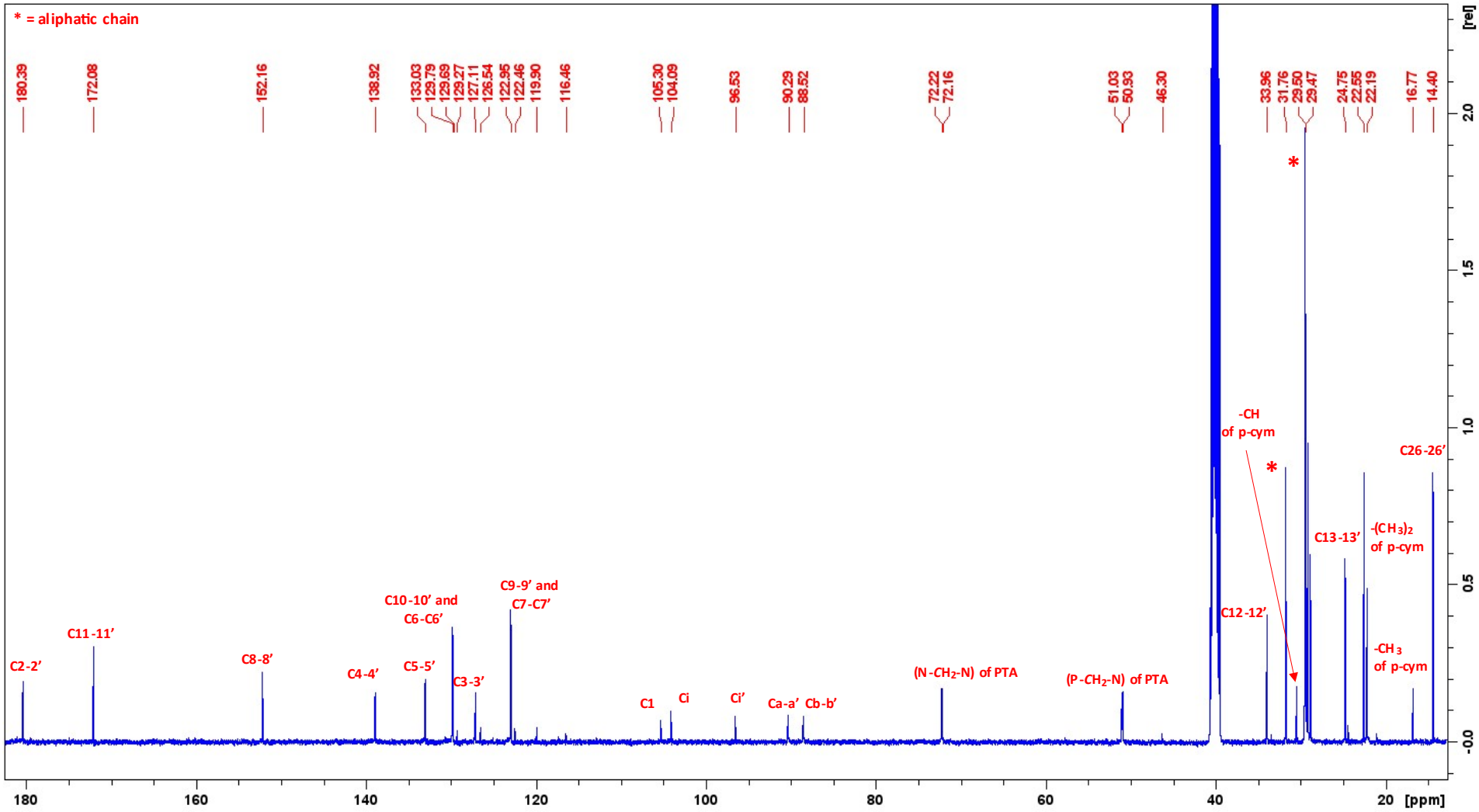

Figure S30. ^{13}C-NMR of **6** in DMSO at 293 K

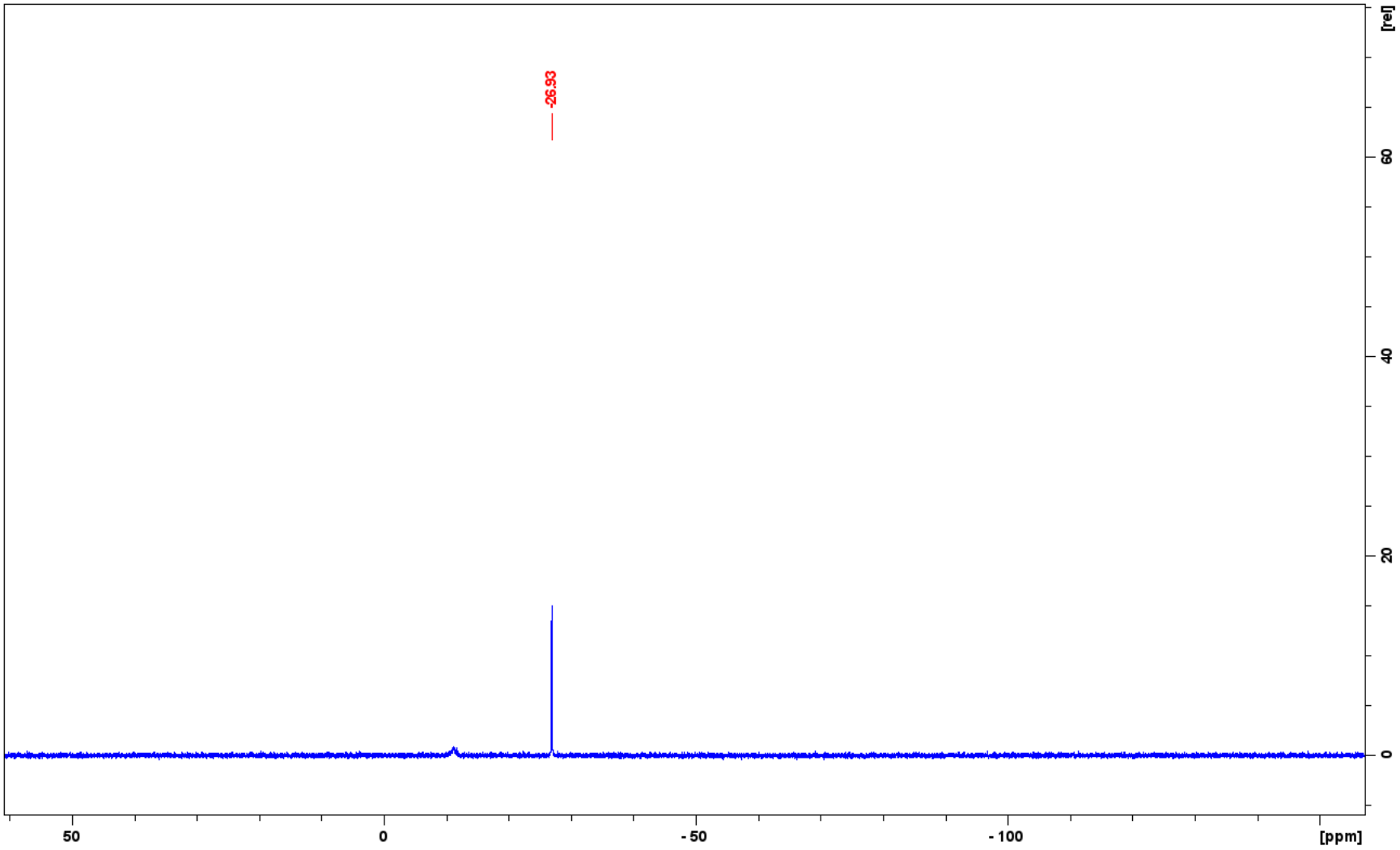

Figure S31. ^{31}P-NMR of **6** in DMSO at 293 K

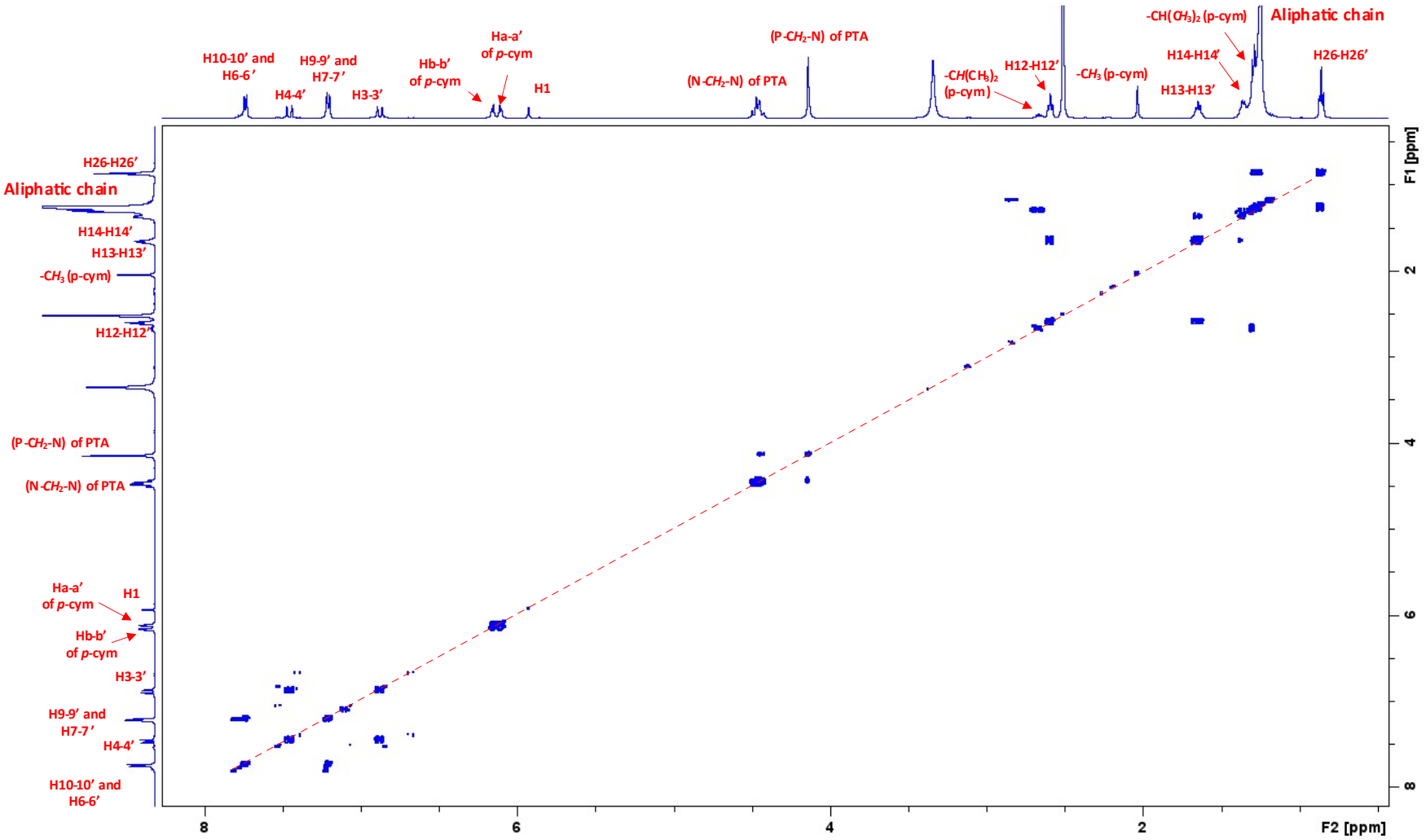

Figure S32.{^{1}H-^{1}H}- COSY NMR of **6** in DMSO at 293 K

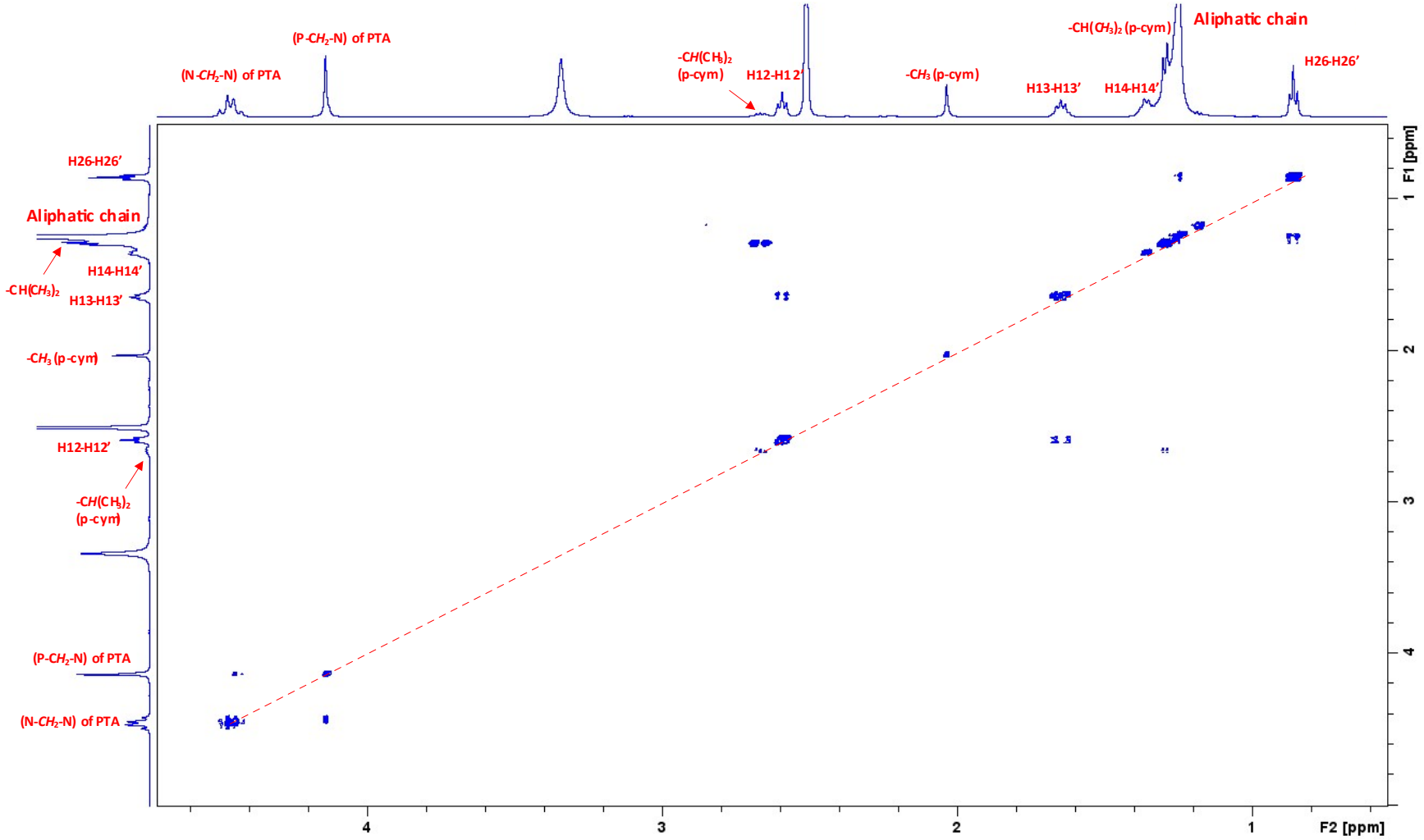

Figure S32 (a). Magnification of {^{1}H-^{1}H}- COSY NMR

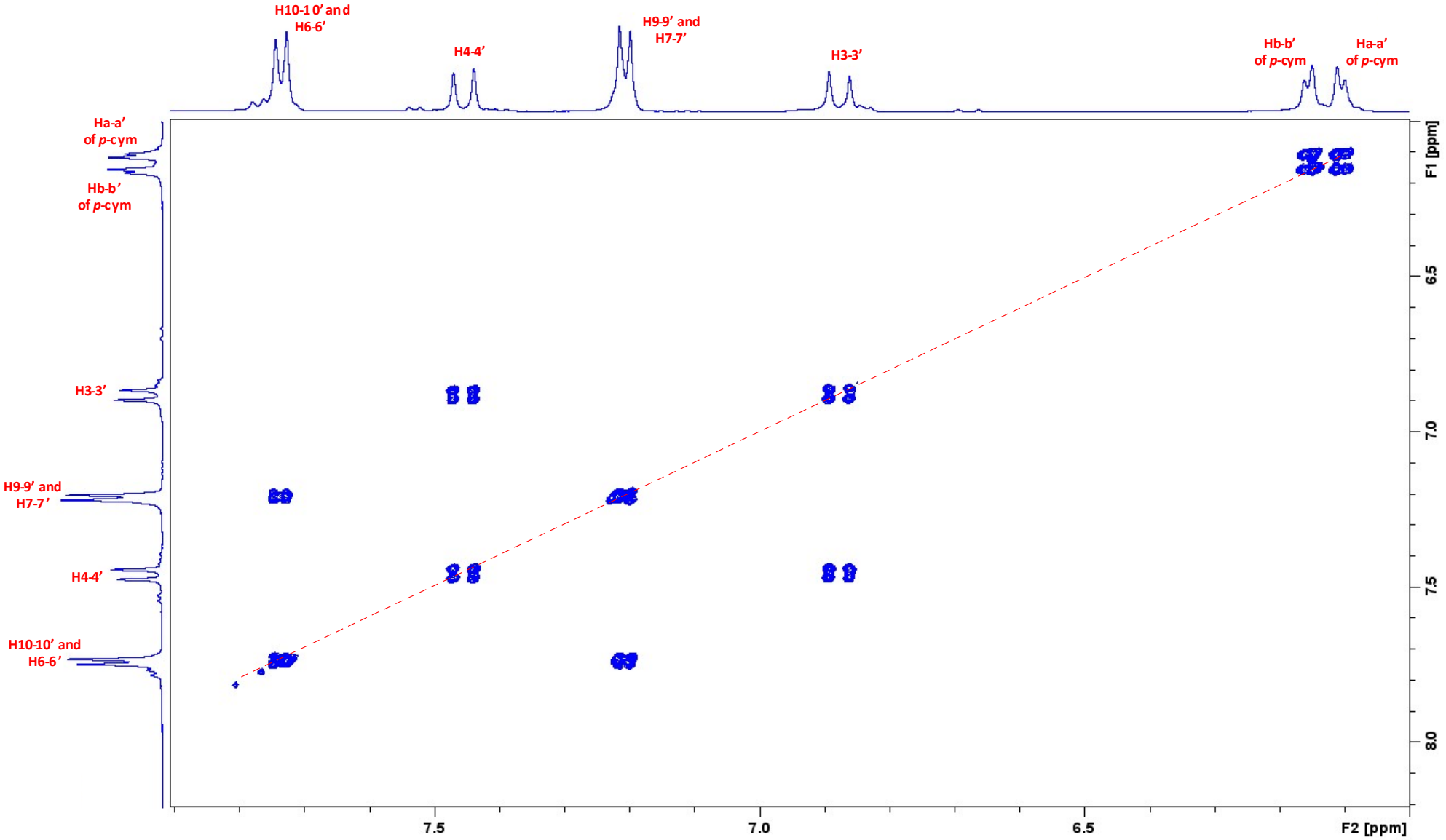

Figure S32 (b). Magnification of {^{1}H-^{1}H}- COSY NMR

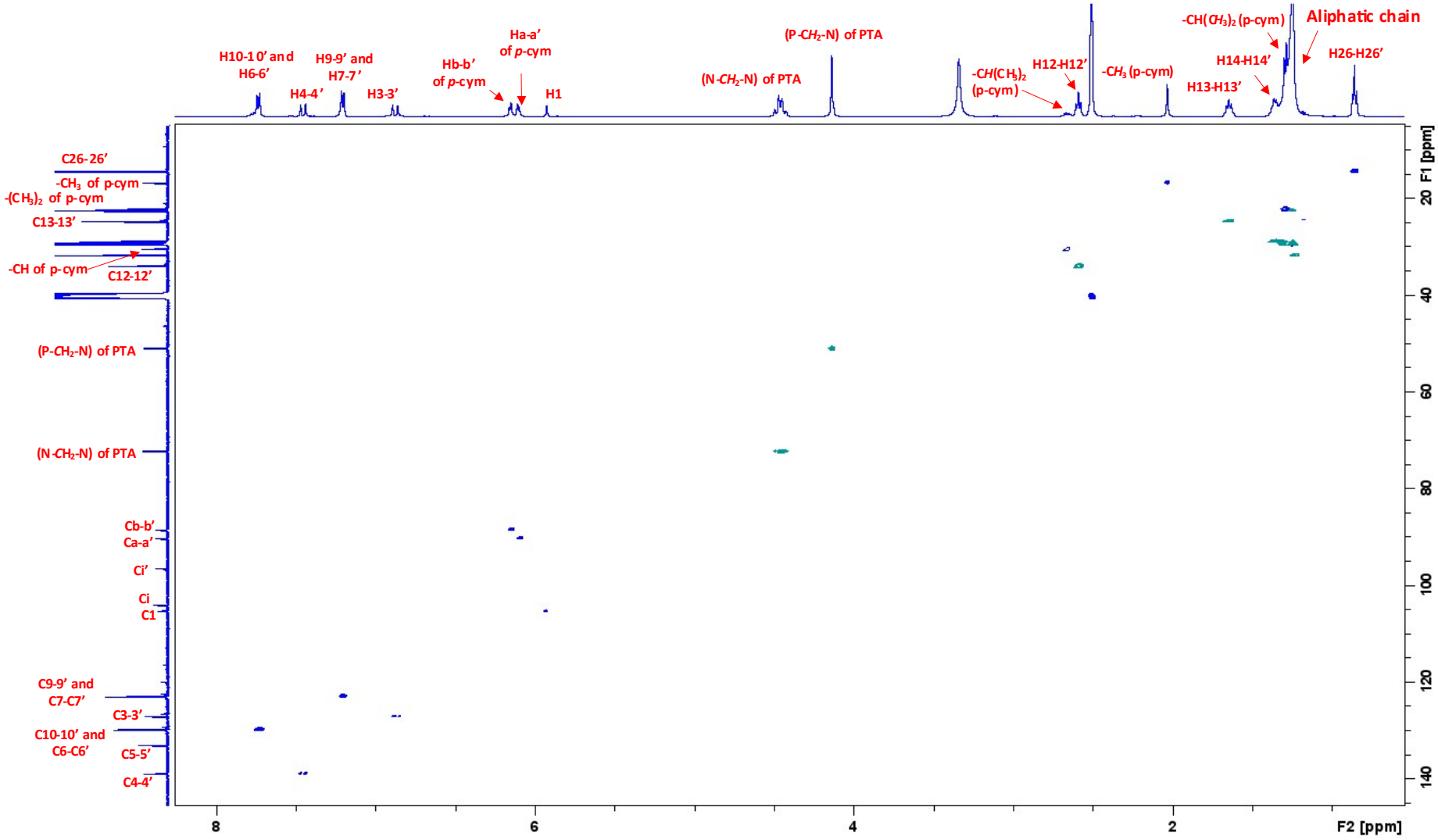

Figure S33. {^{1}H-^{13}C}-HSQC NMR of **6** in DMSO at 293 K

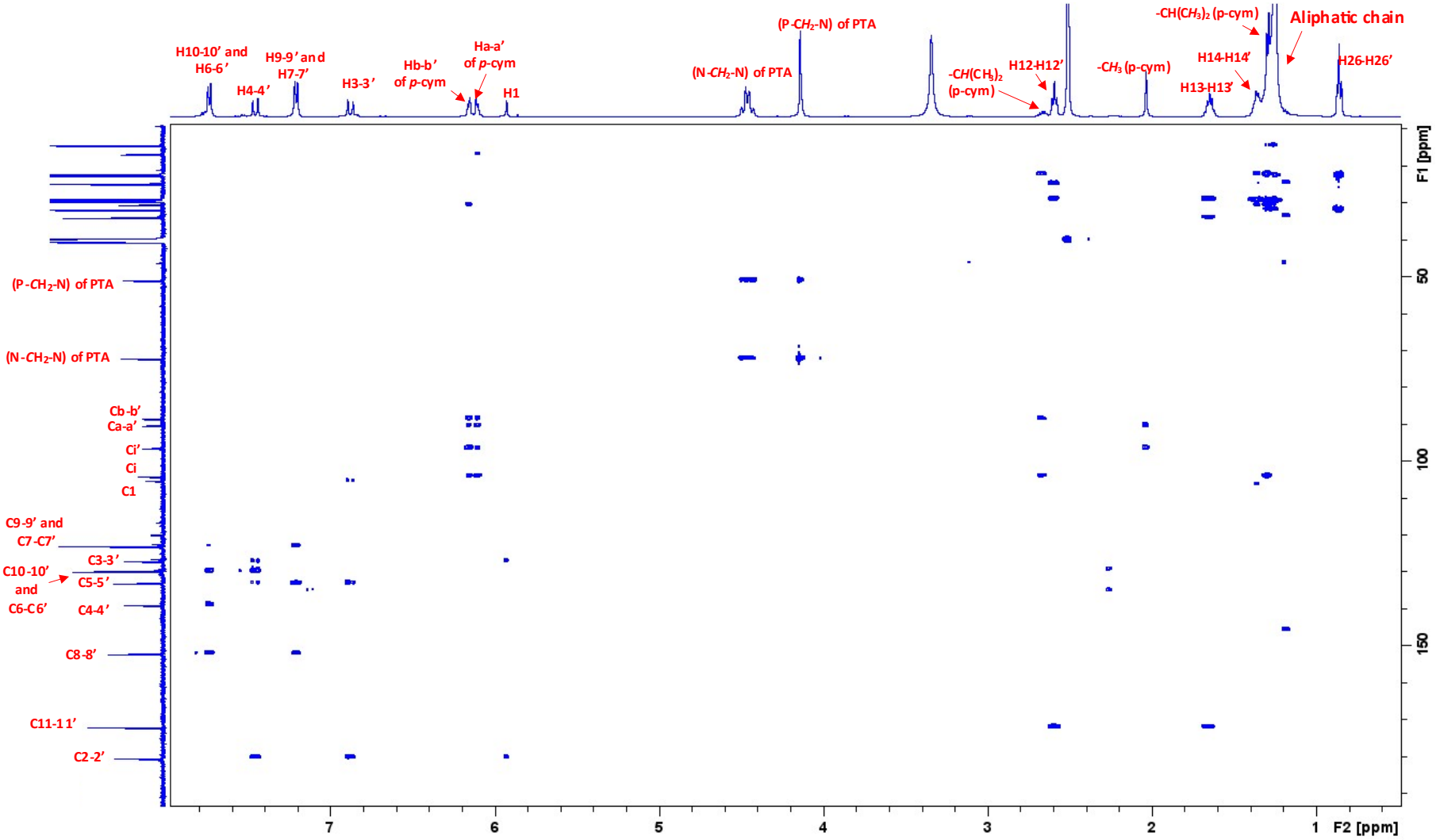

Figure S34. {^{1}H-^{13}C}-HMBC NMR of **6** in DMSO at 293 K

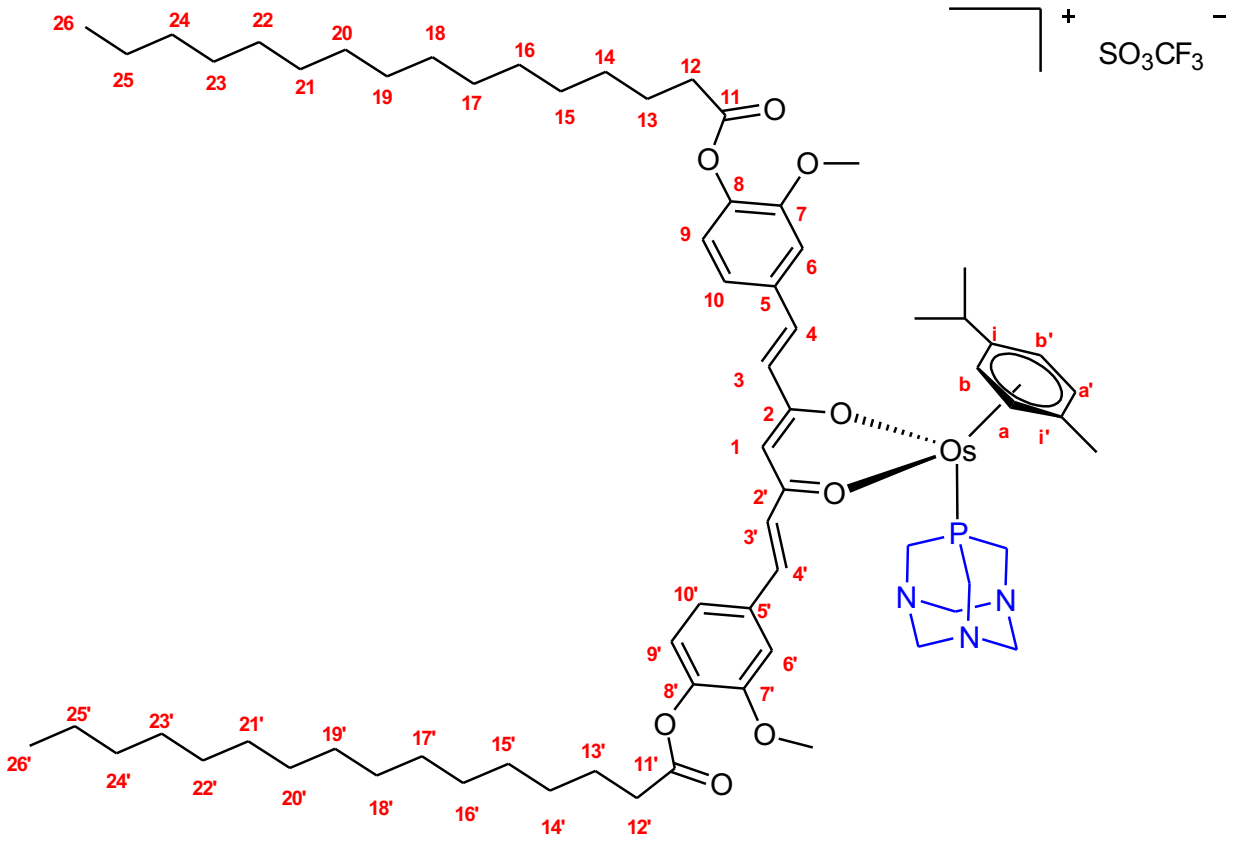
SO3CF3
Os
O
P
N

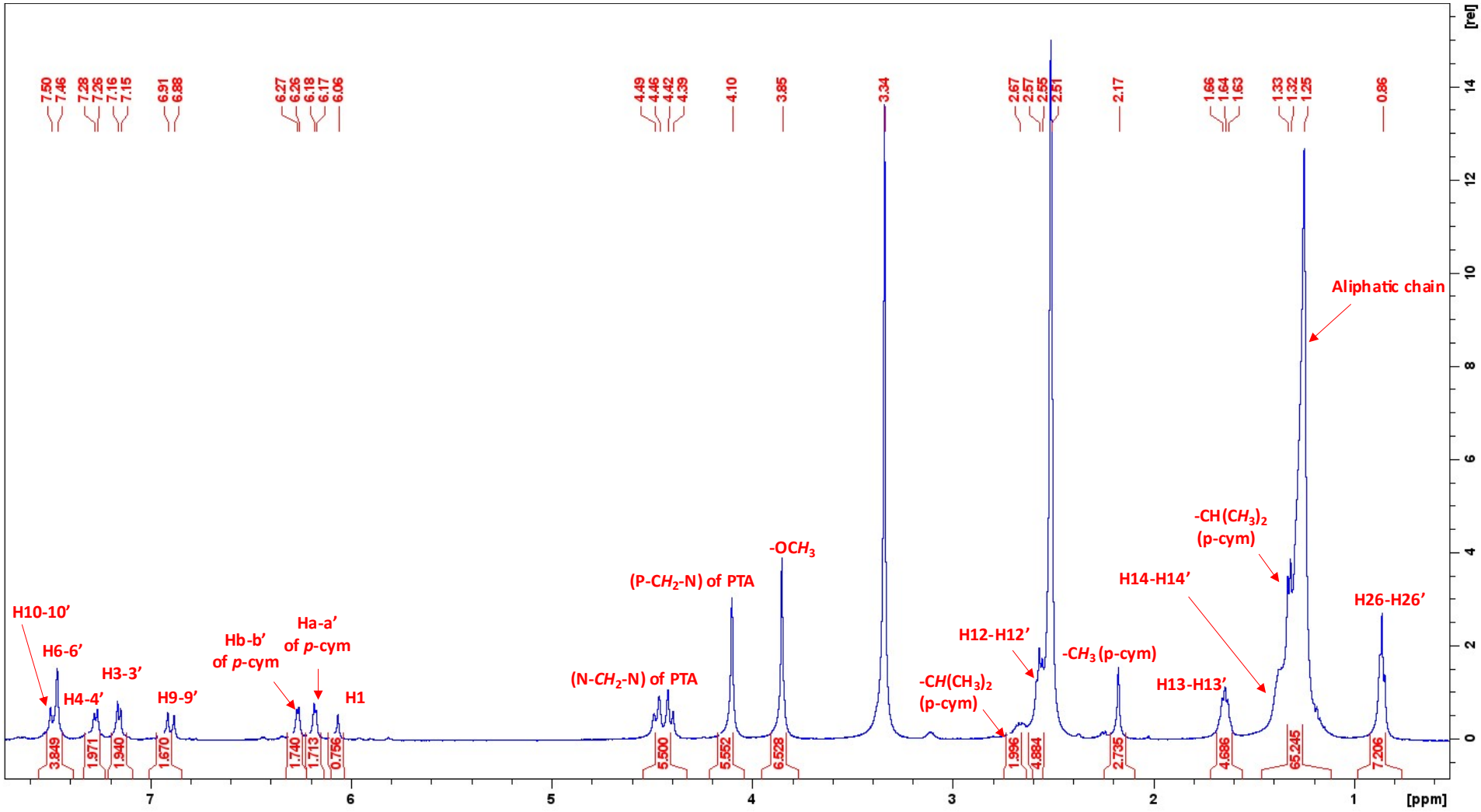

Figure S35. ^{1}H-NMR of **7** in DMSO at 293 K

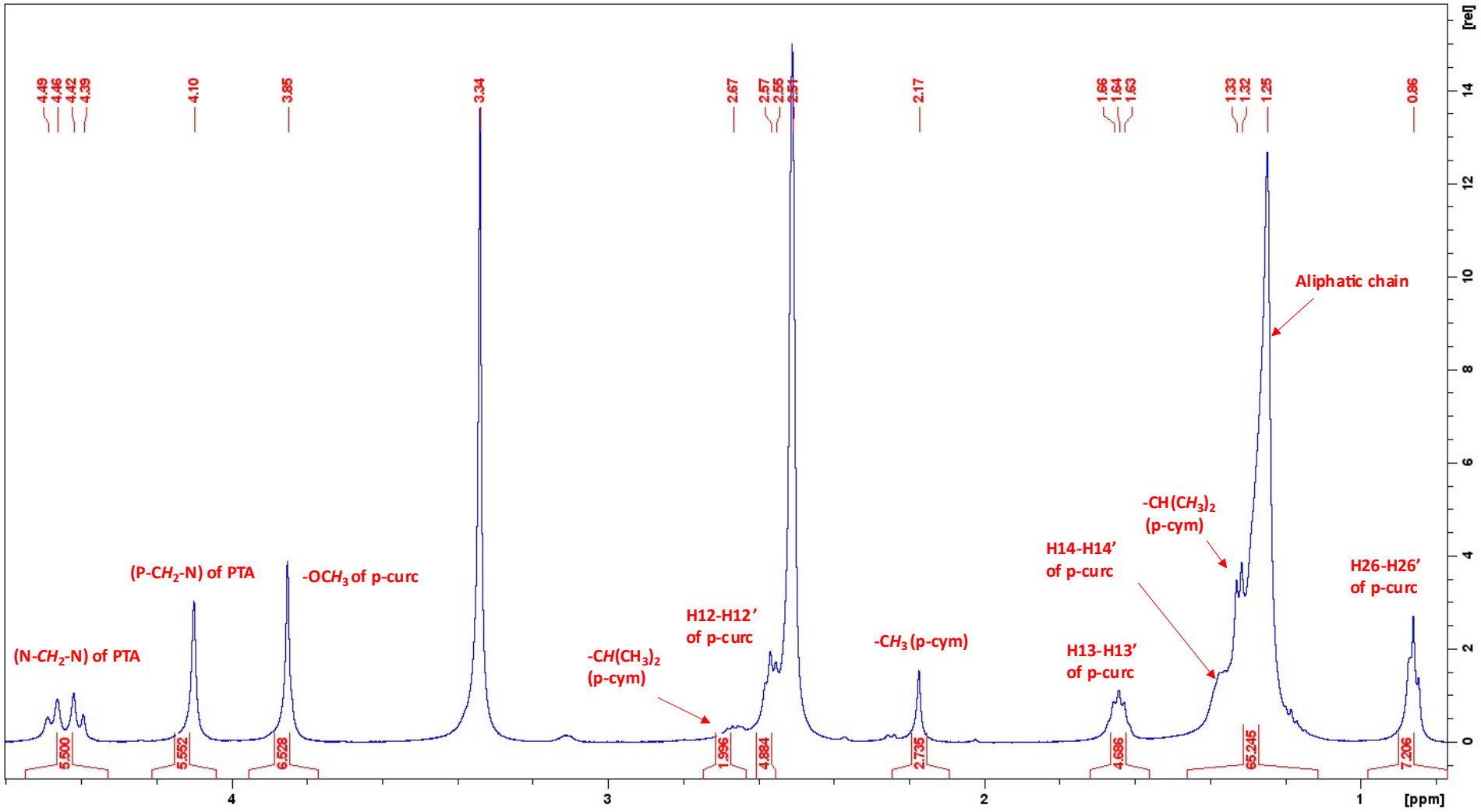

Figure S35 (a). Magnification of ^{1}H-NMR (1-5 ppm)

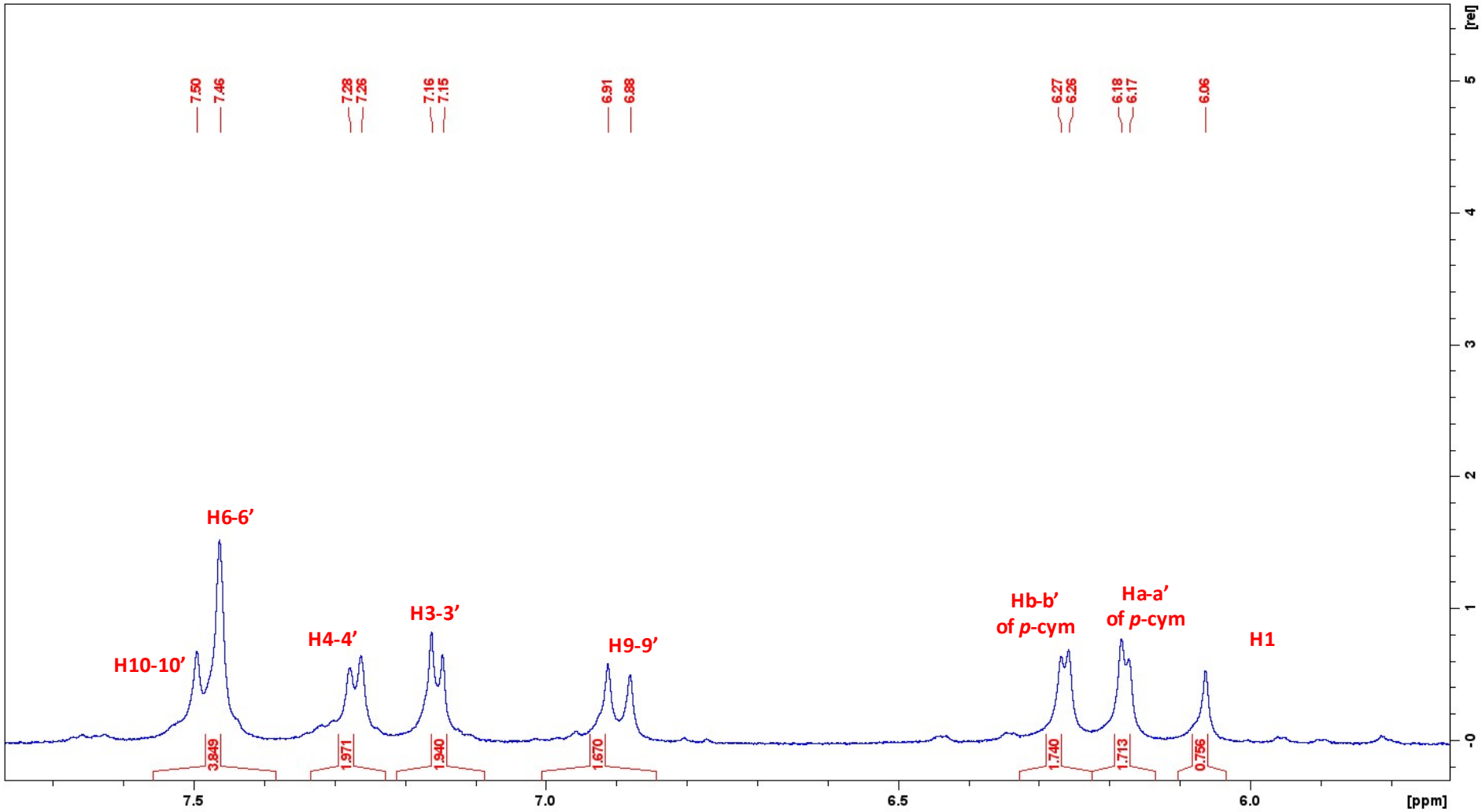

Figure S35 (b). Magnification of ^{1}H-NMR (5-8 ppm)

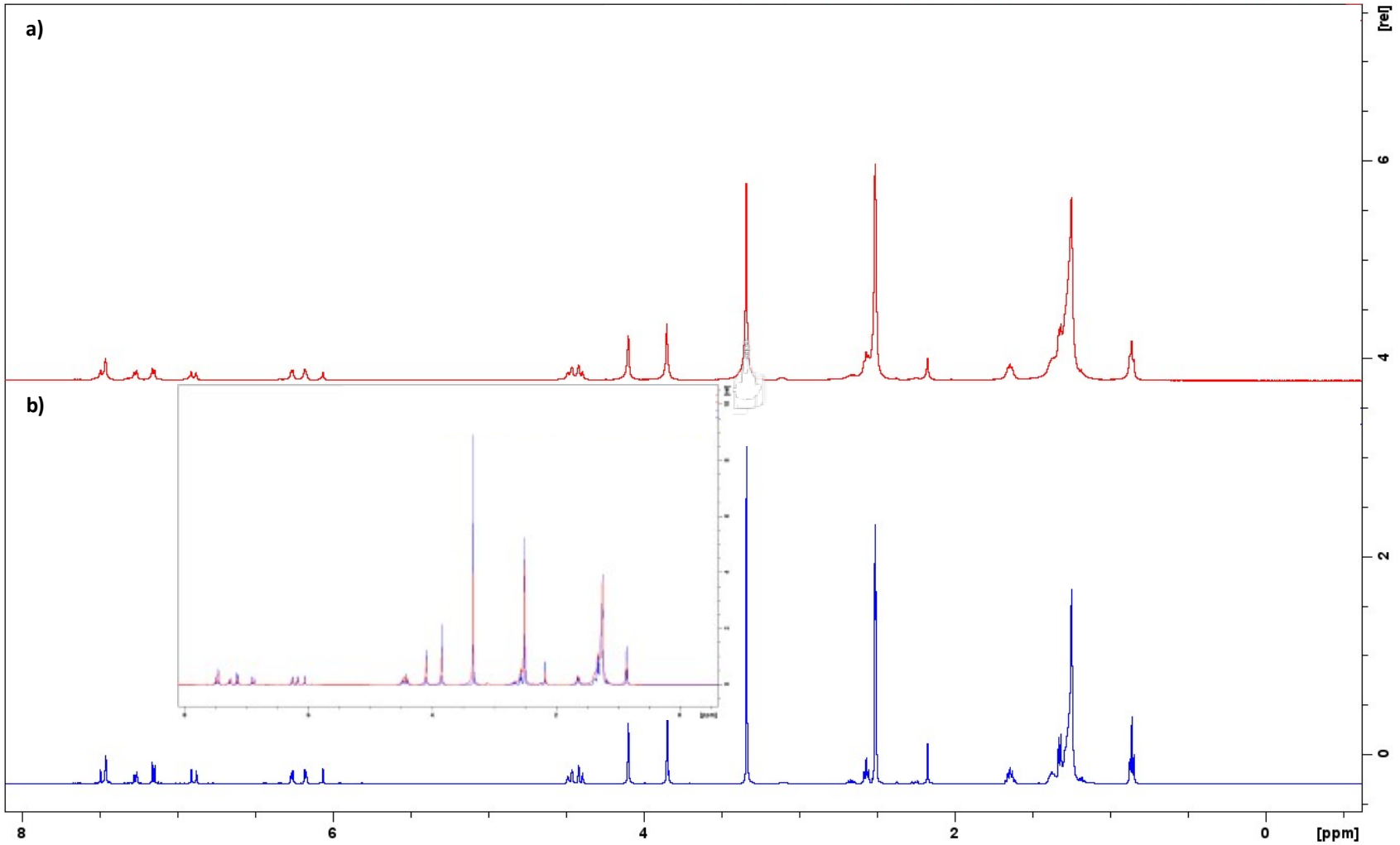

Figure S35 (c). Comparison of ^{1}H-NMR spectra of complex **7** at t=0 (a) and after 5 days (b)

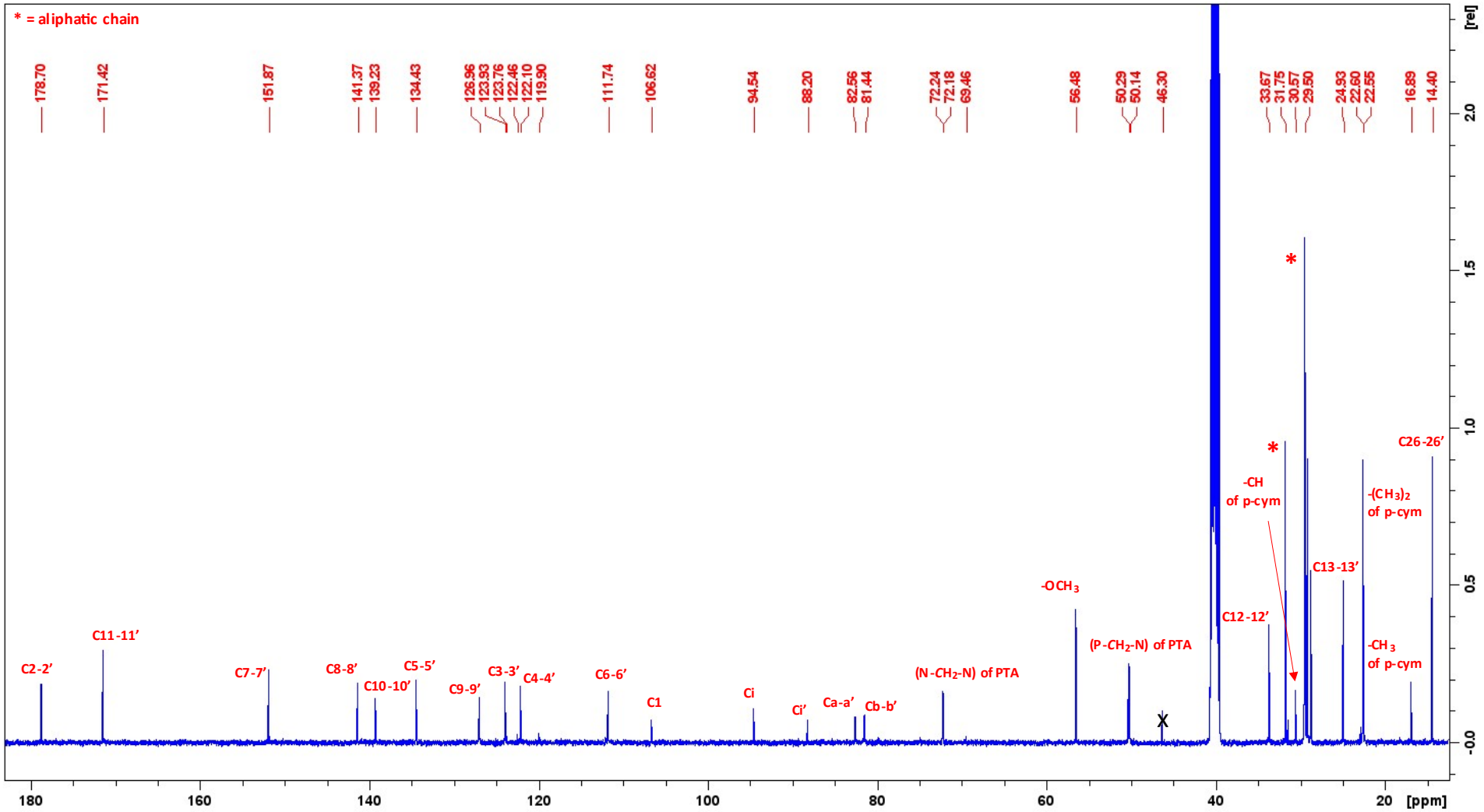

Figure S36. ^{13}C-NMR of **7** in DMSO at 293 K

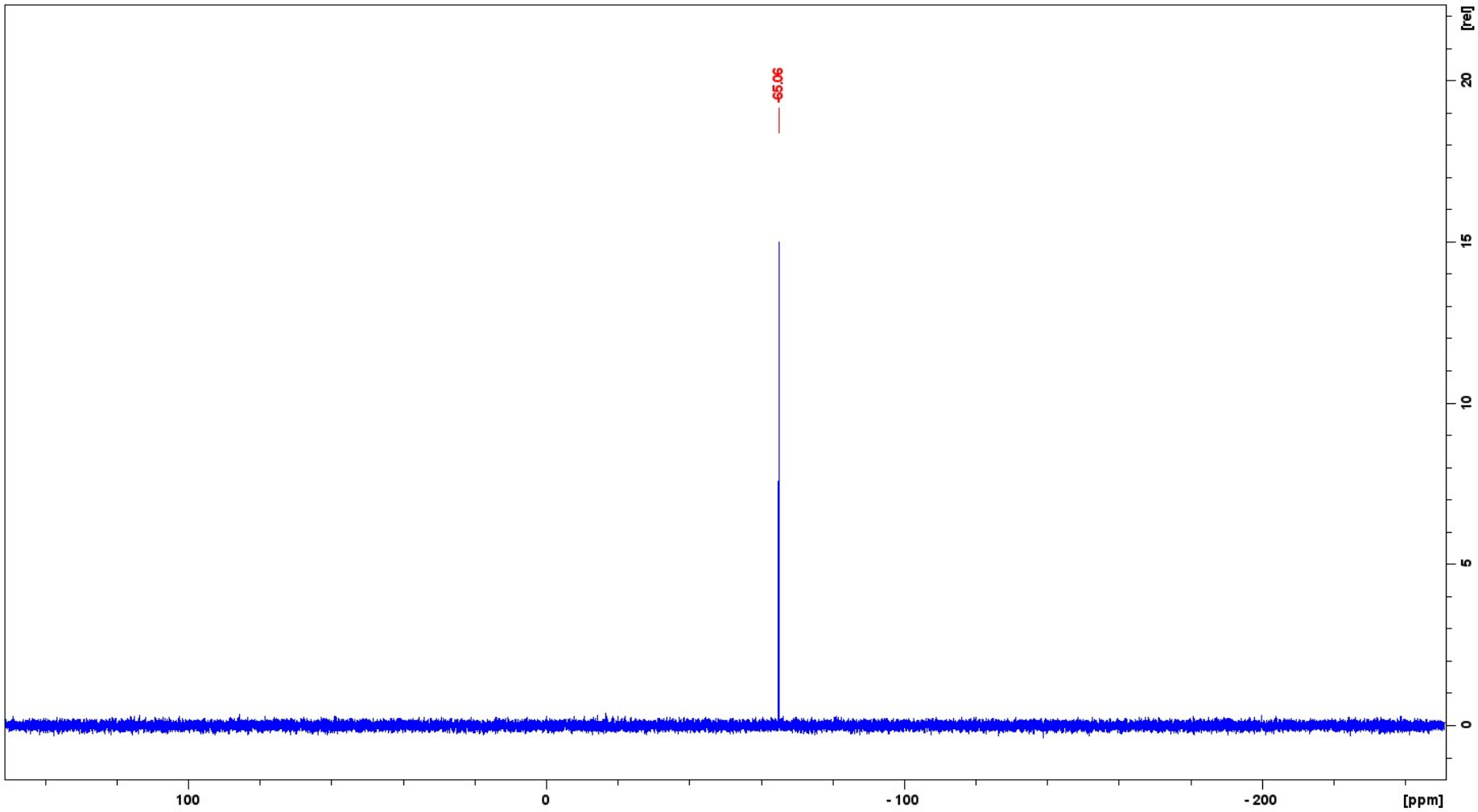

Figure S37. ^{31}P-NMR of **7** in DMSO at 293 K

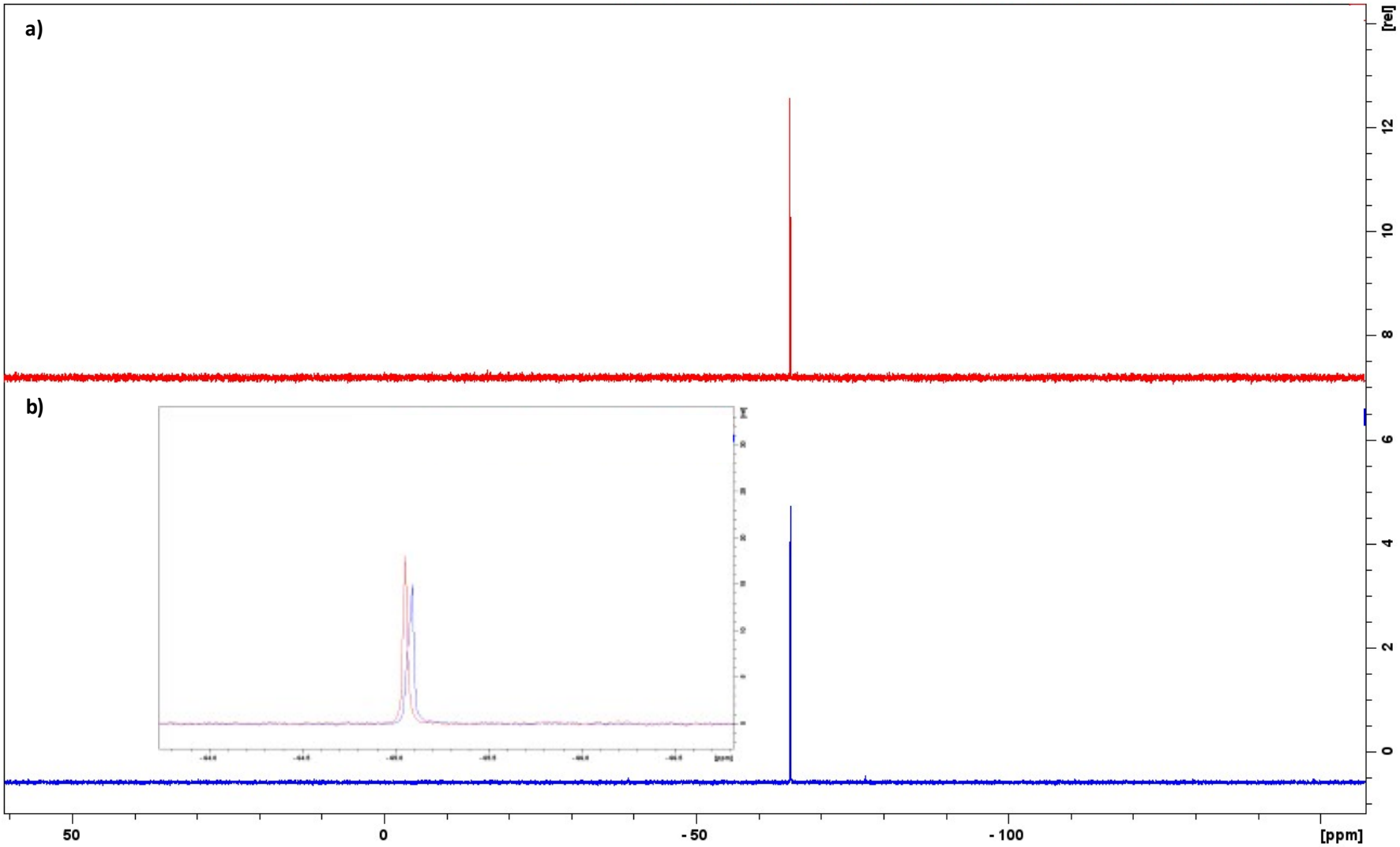

Figure S37 (a). Comparison of ^{31}P-NMR spectra of complex **7** at t=0 (a) and after 5 days (b)

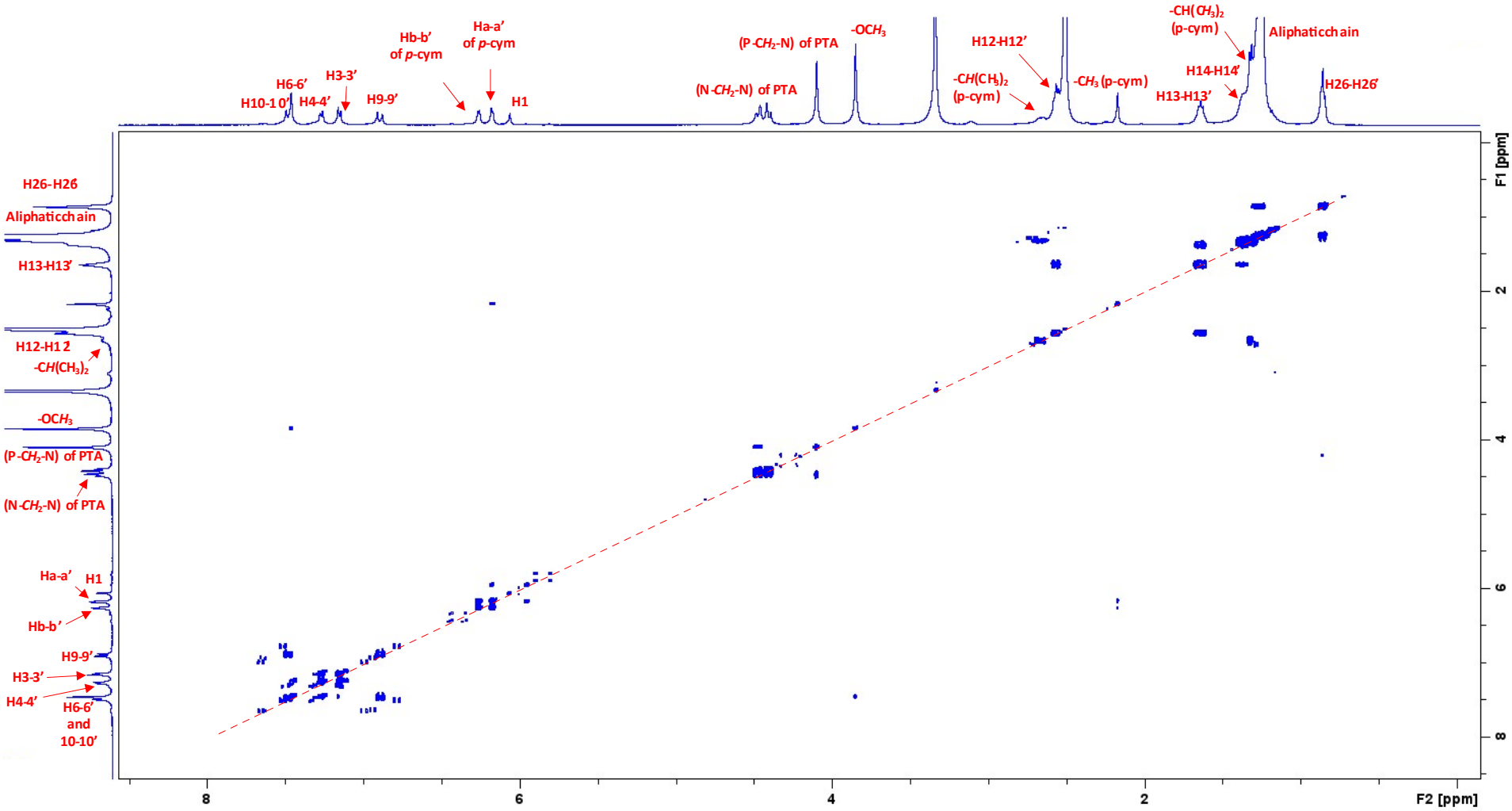

Figure S38.{^{1}H-^{1}H}- COSY NMR of **7** in DMSO at 293 K

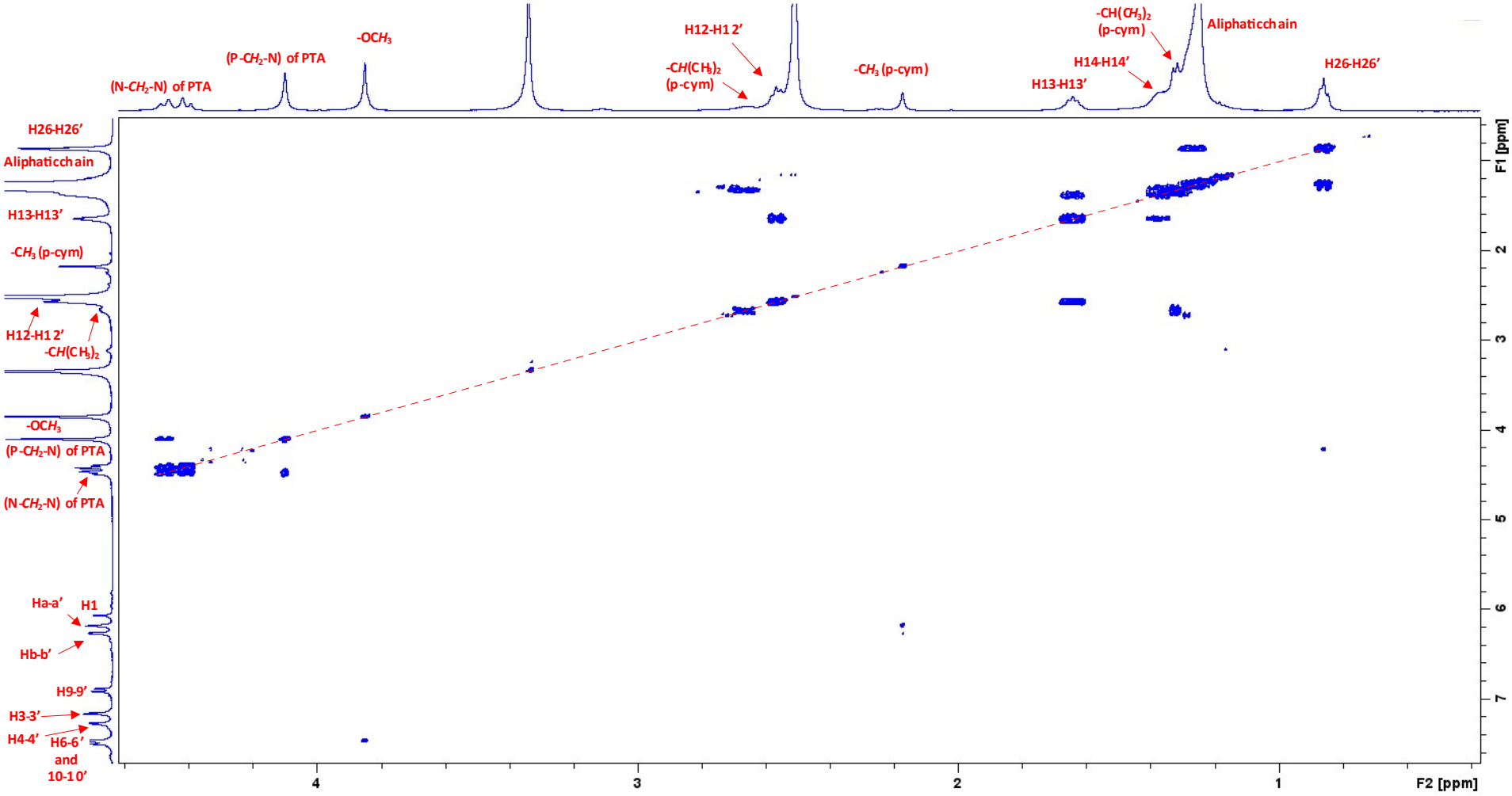

Figure S38 (a). Magnification of {^{1}H-^{1}H}- COSY NMR

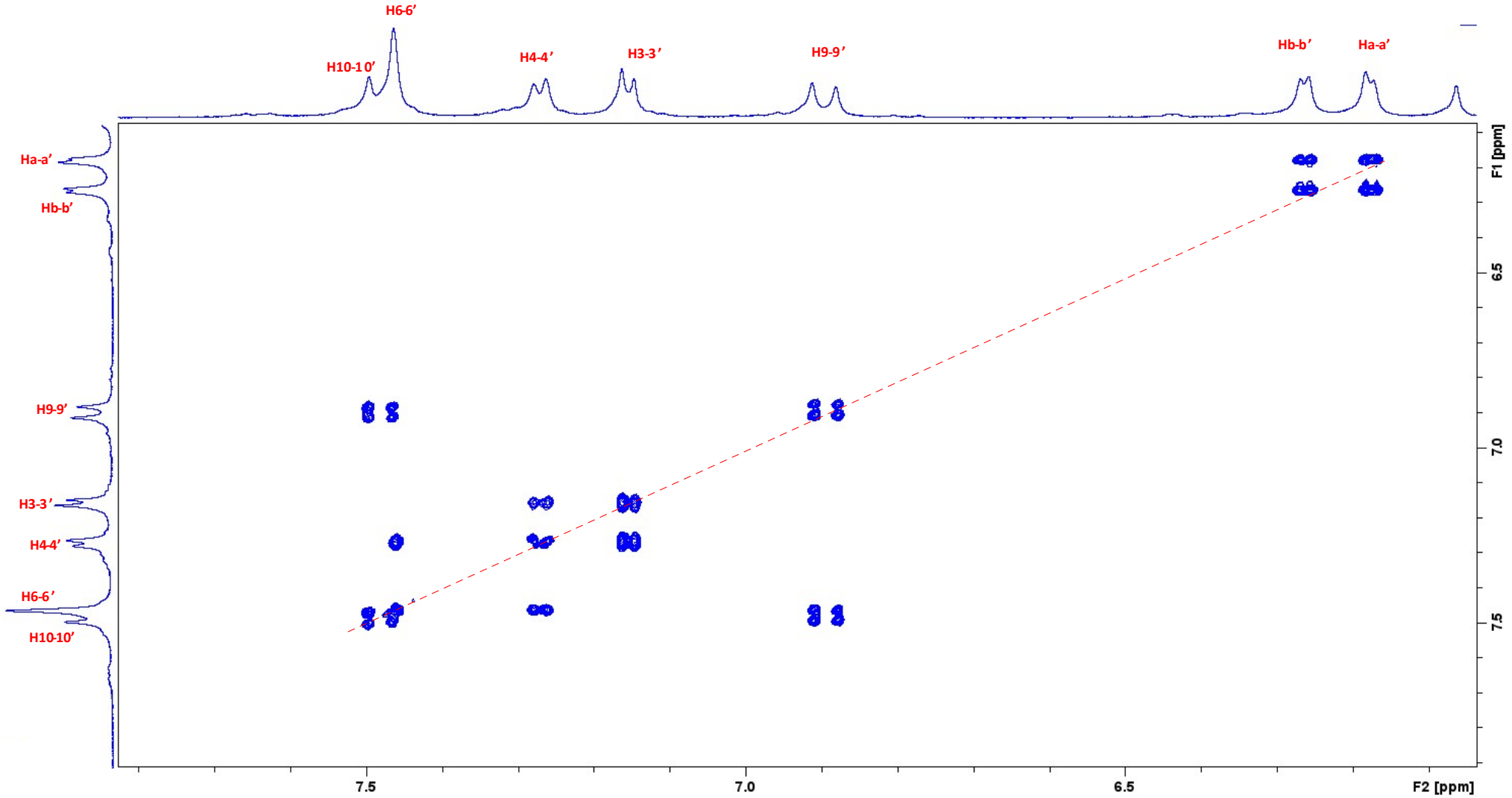

Figure S38 (b). Magnification of {^{1}H-^{1}H}- COSY NMR

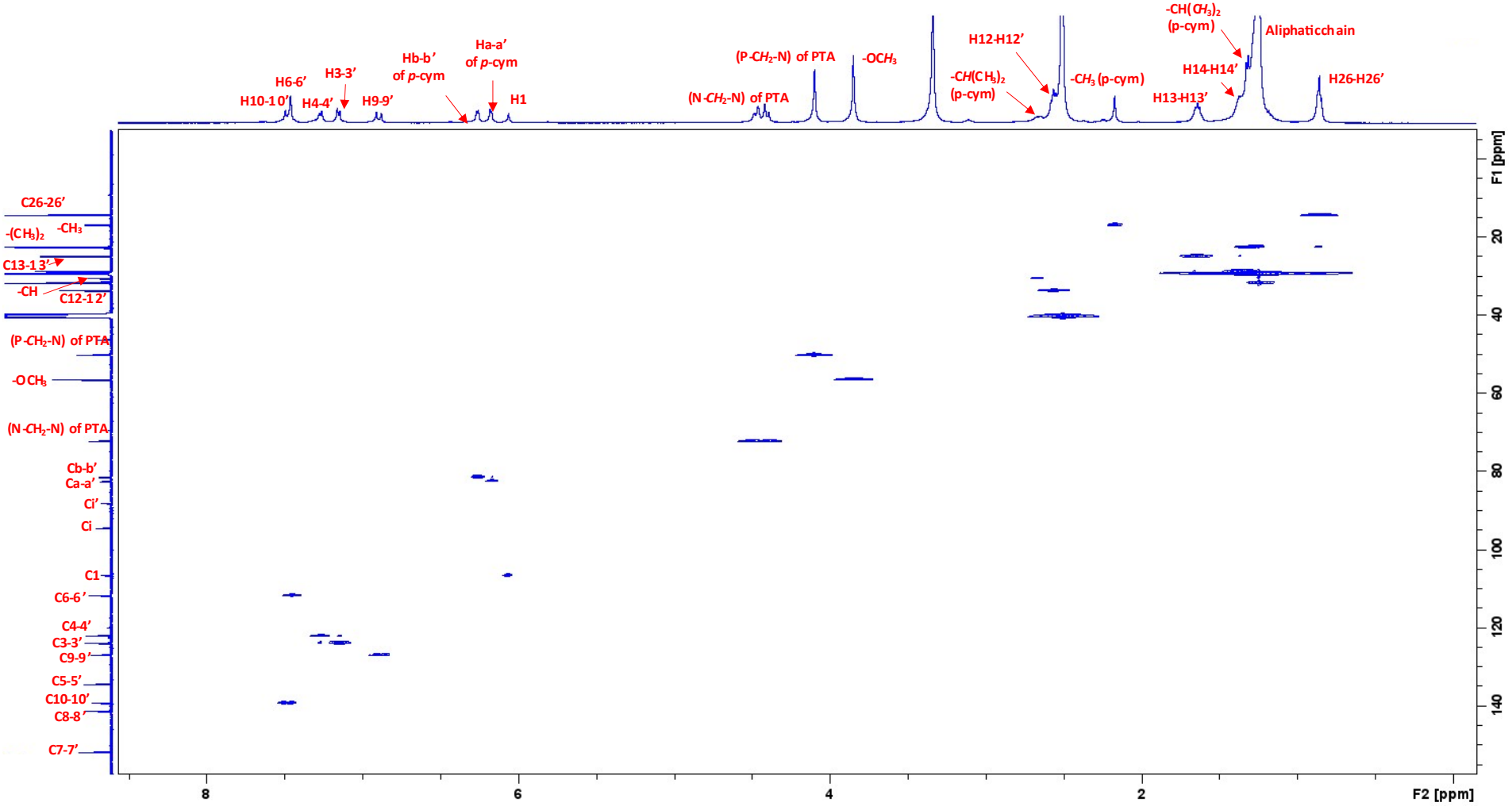

Figure S39. {^{1}H-^{13}C}-HSQC NMR of **7** in DMSO at 293 K

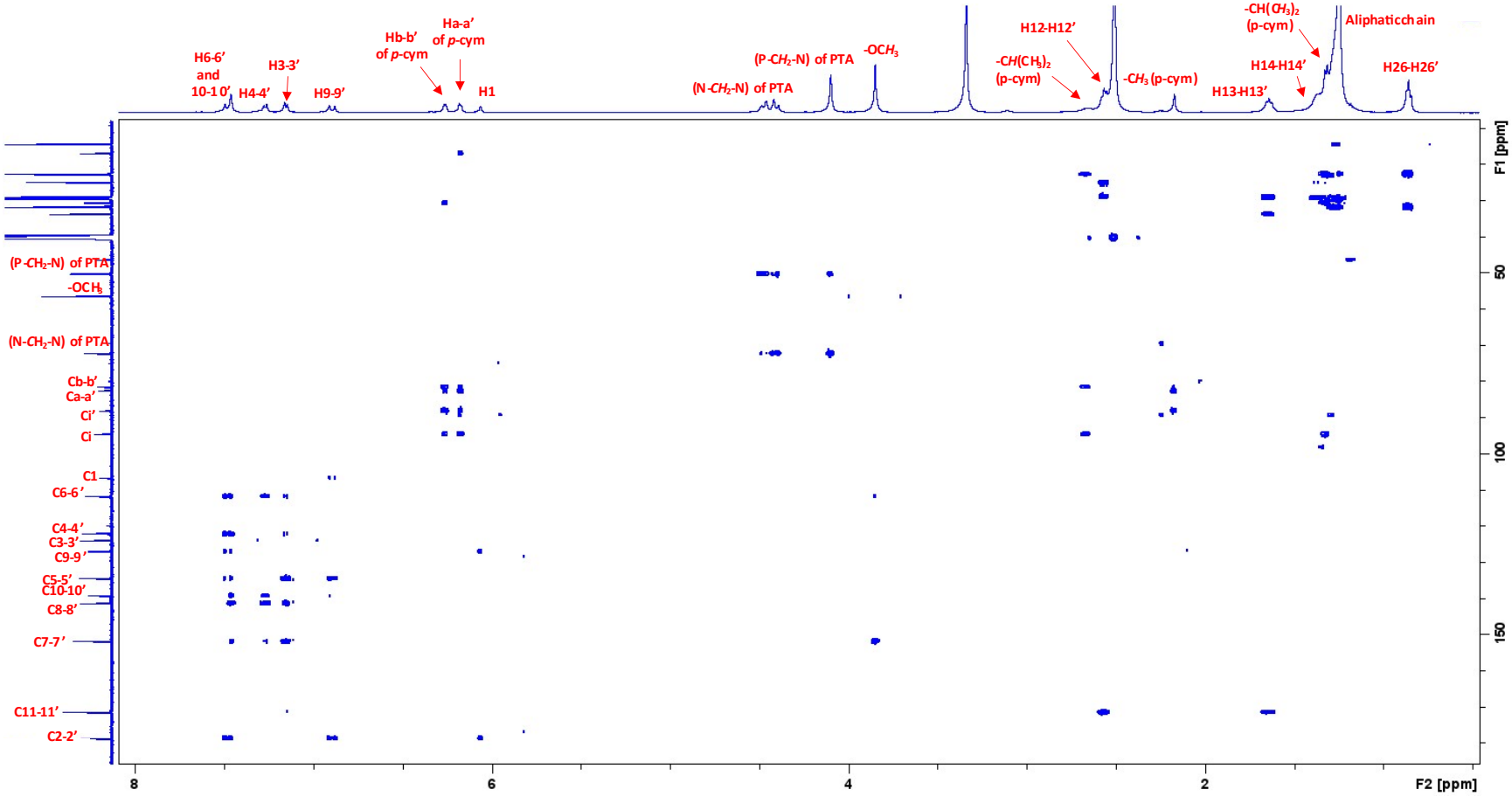

Figure S40. {^{1}H-^{13}C}-HMBC NMR of **7** in DMSO at 293 K

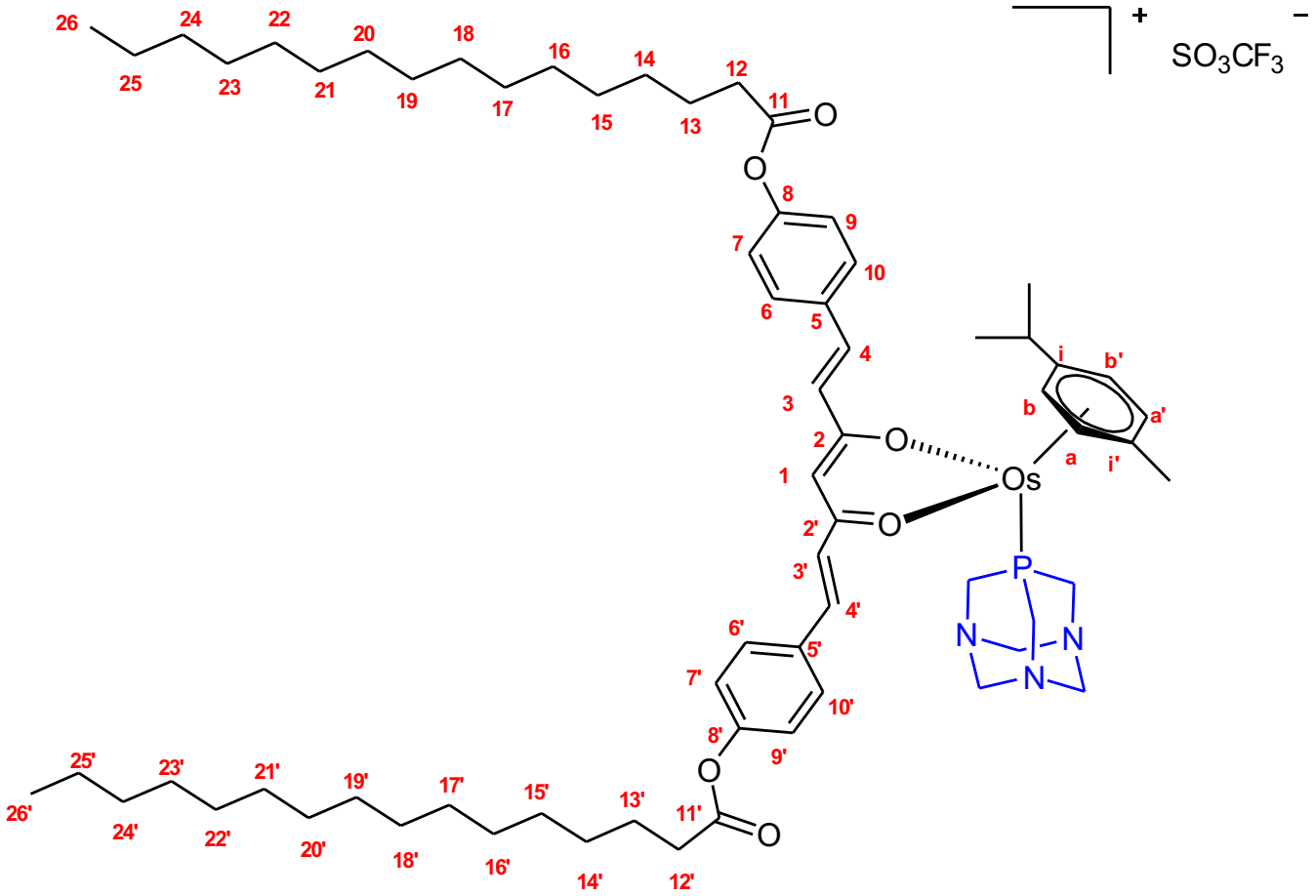
SO3CF3
Os
O
P
N

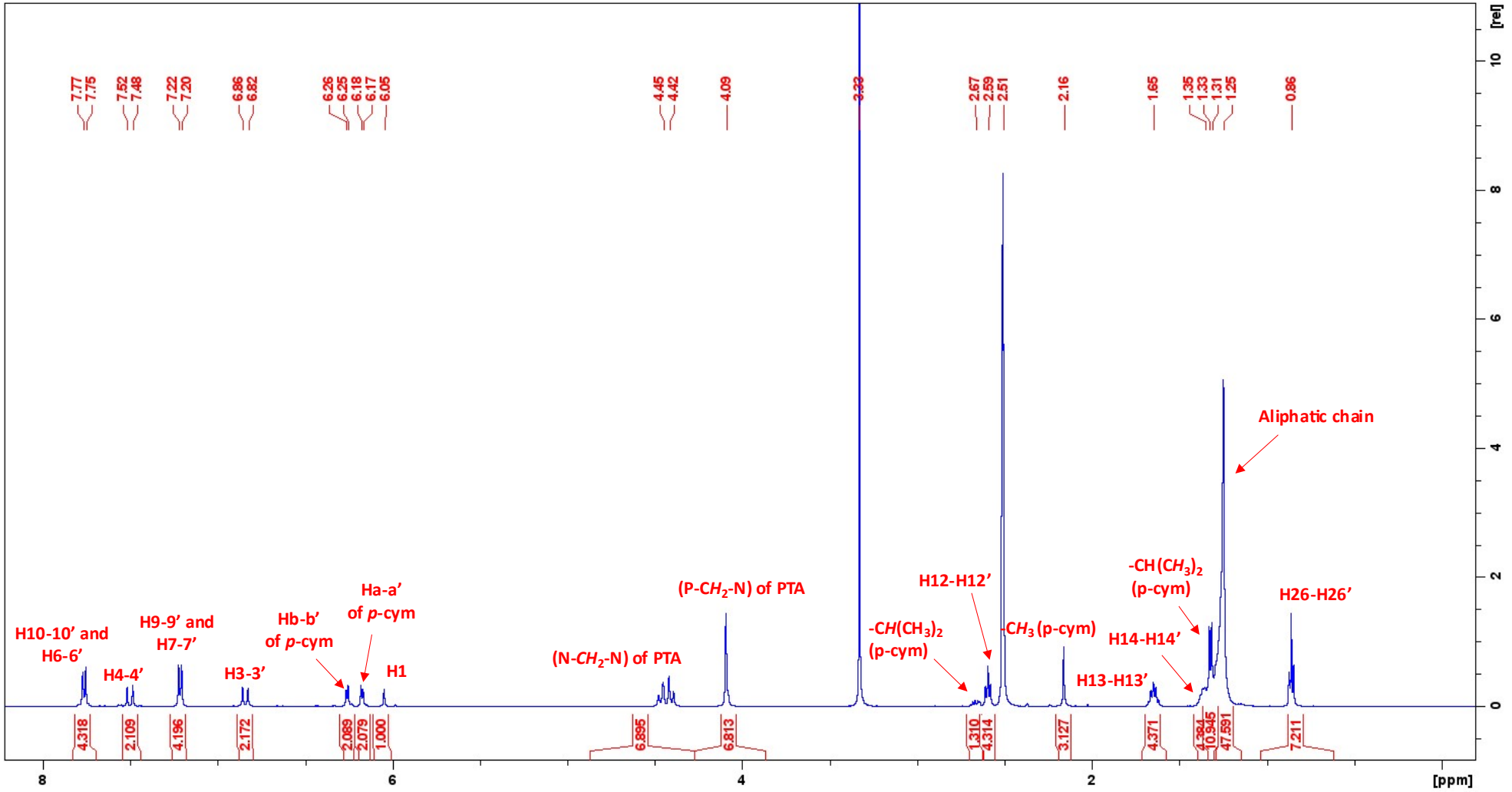

Figure S41. ^{1}H-NMR of **8** in DMSO at 293 K

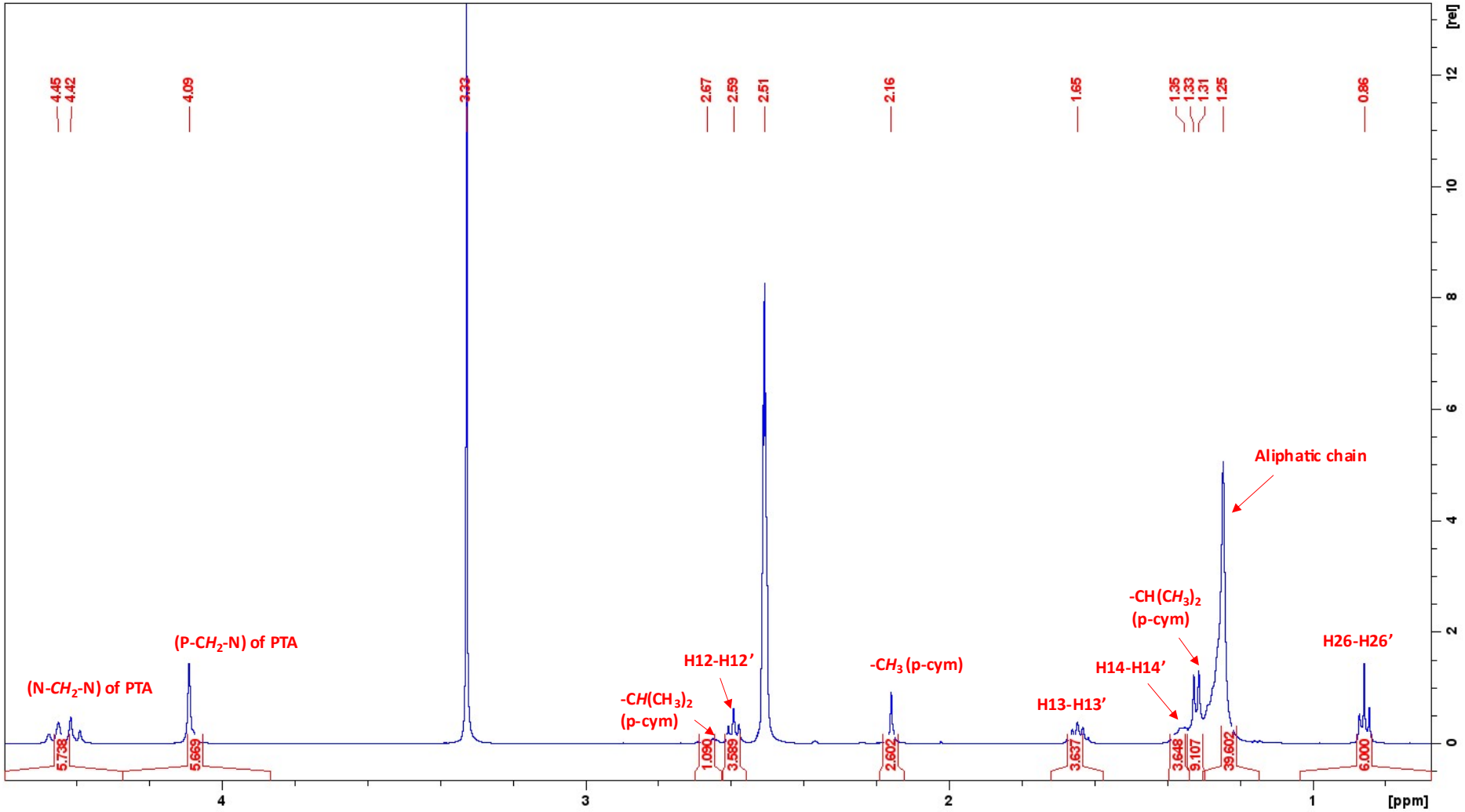

Figure S41 (a). Magnification of ^{1}H-NMR (1-5 ppm)

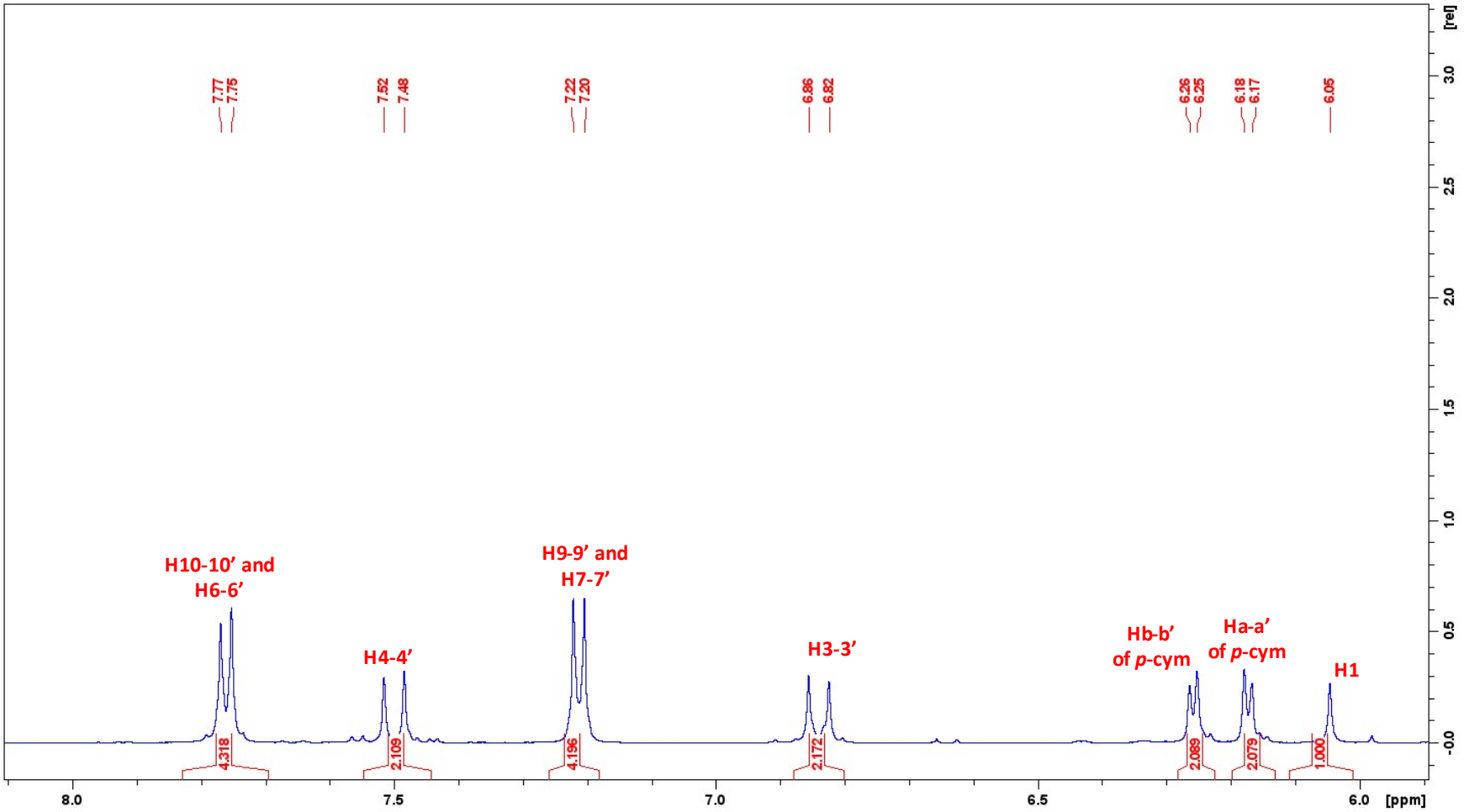

Figure S41 (b). Magnification of ^{1}H-NMR (5-8 ppm)

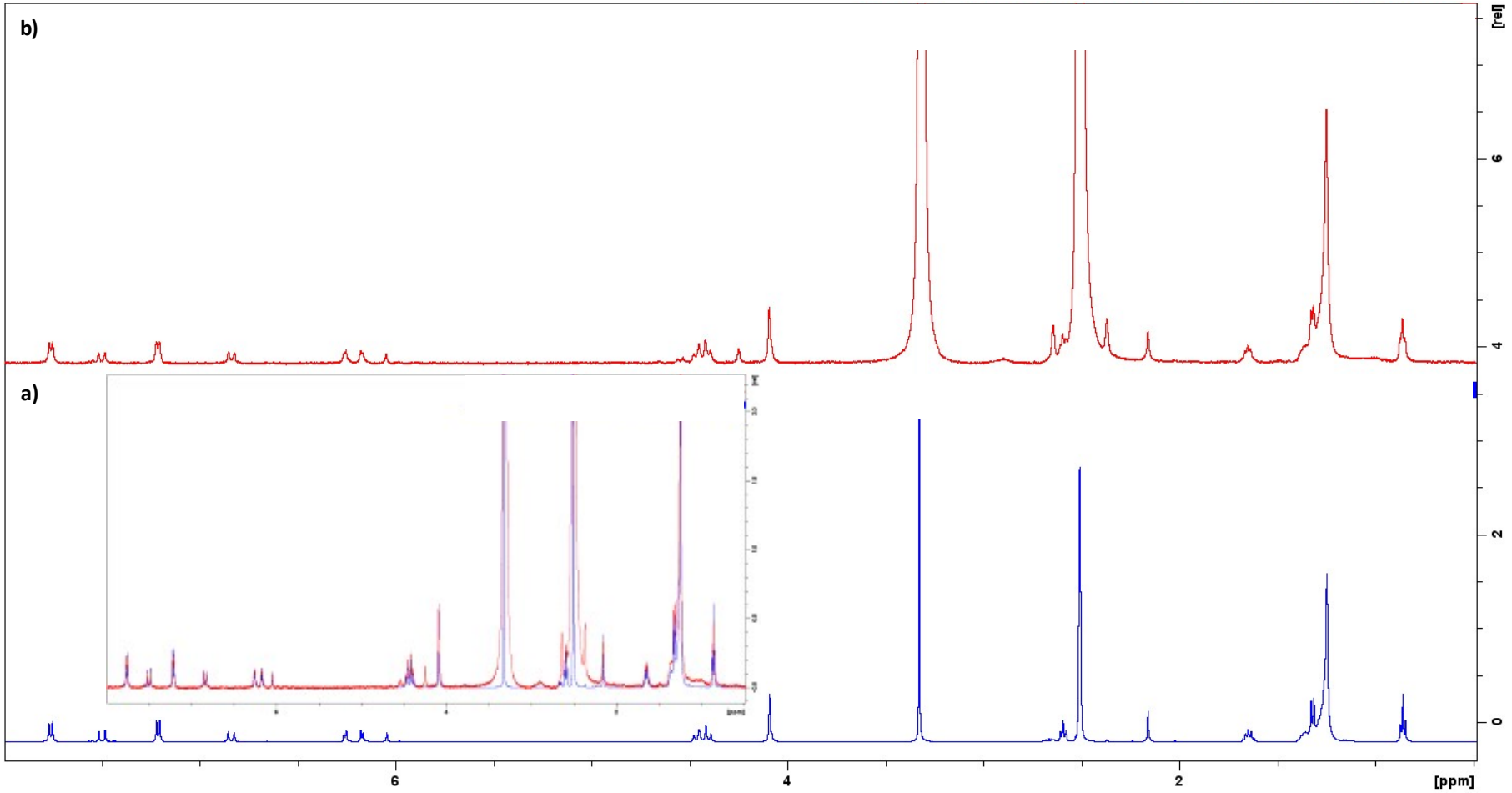

Figure S41 (c). Comparison of ^{1}H-NMR spectra of complex **8** at t=0 (a) and after 5 days (b)

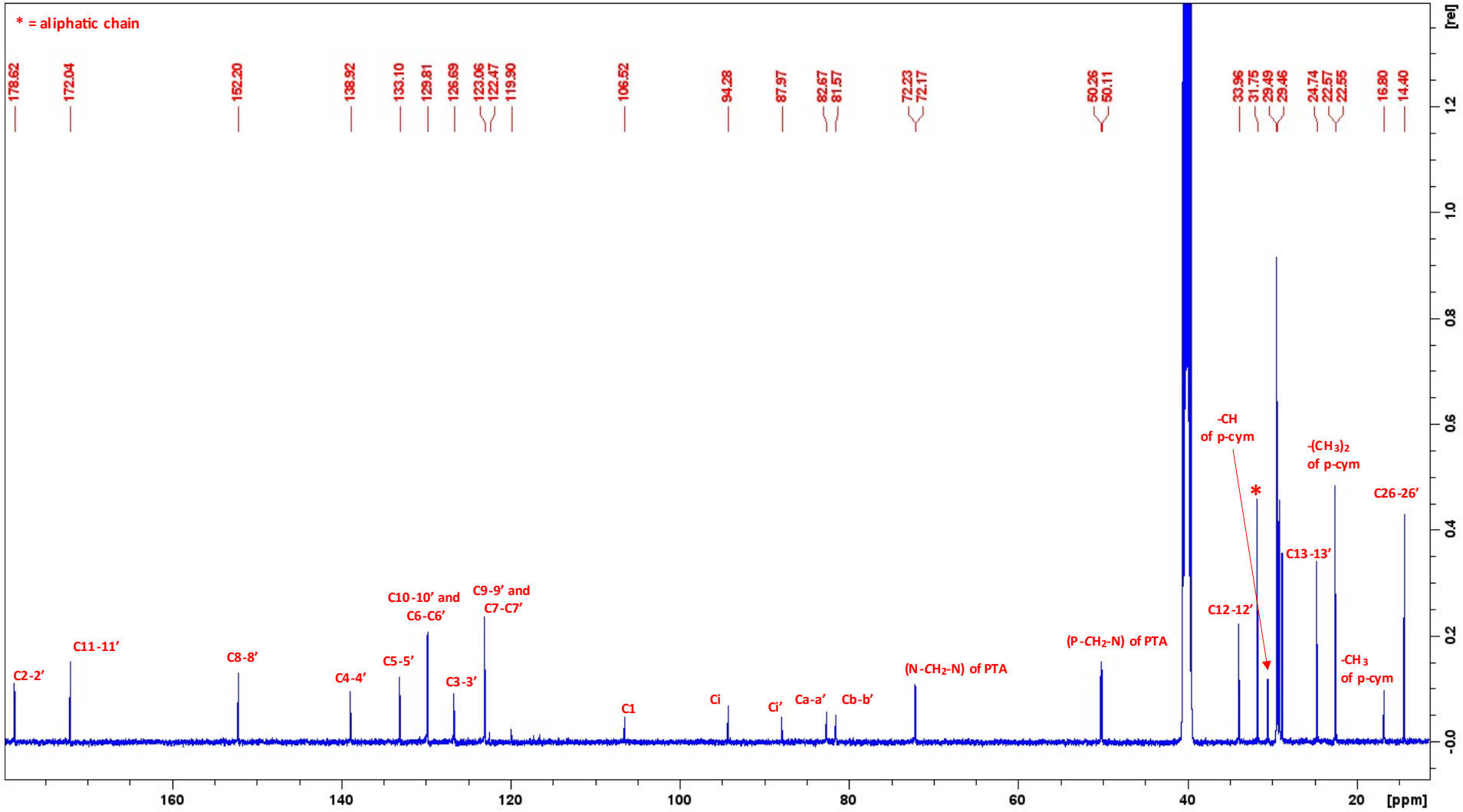

Figure S42. ^{13}C-NMR of **8** in DMSO at 293 K

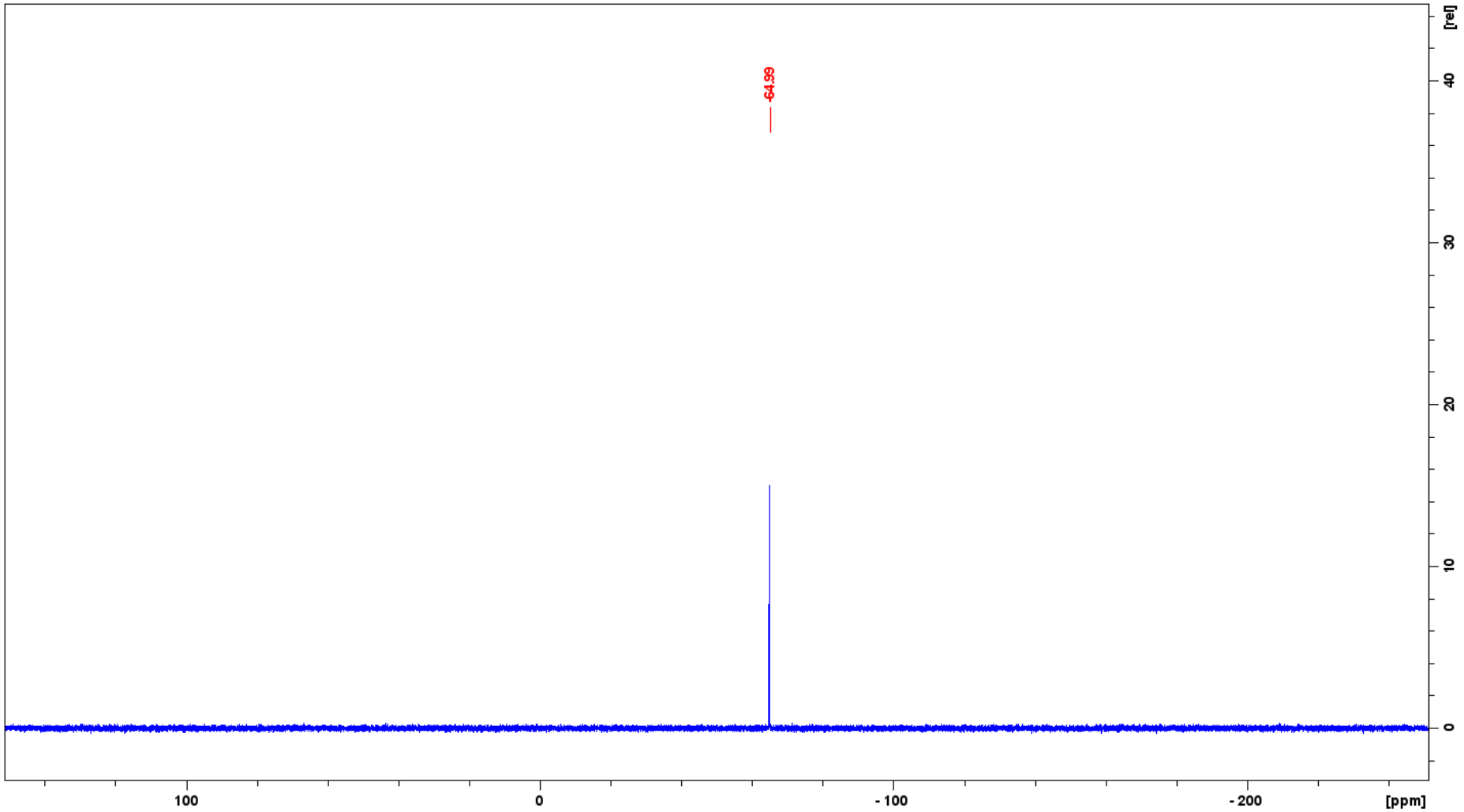

Figure S43. ^{31}P-NMR of **8** in DMSO at 293 K

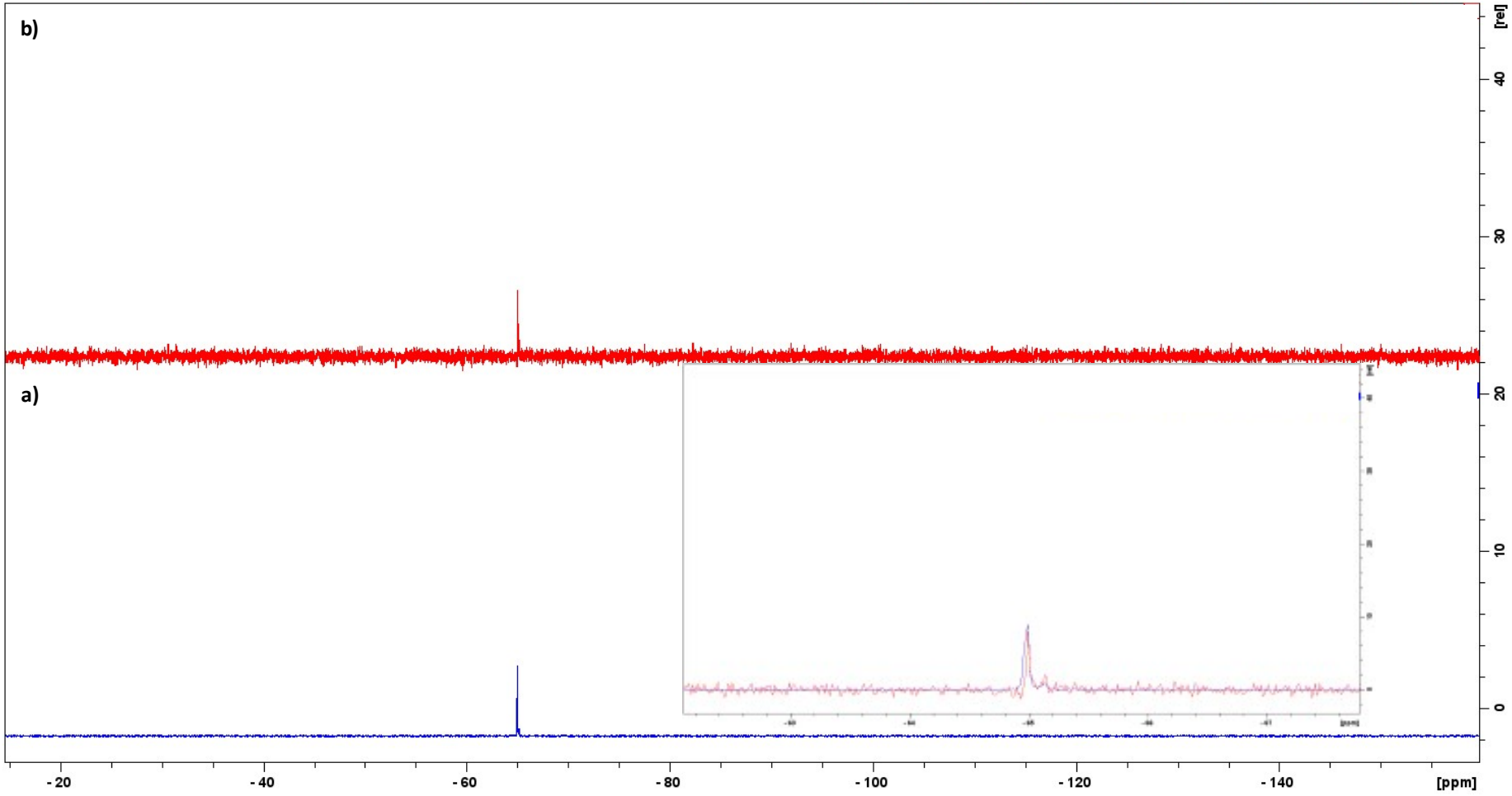

Figure S43 (a). Comparison of ^{31}P-NMR spectra of complex **8** at t=0 (a) and after 5 days (b)

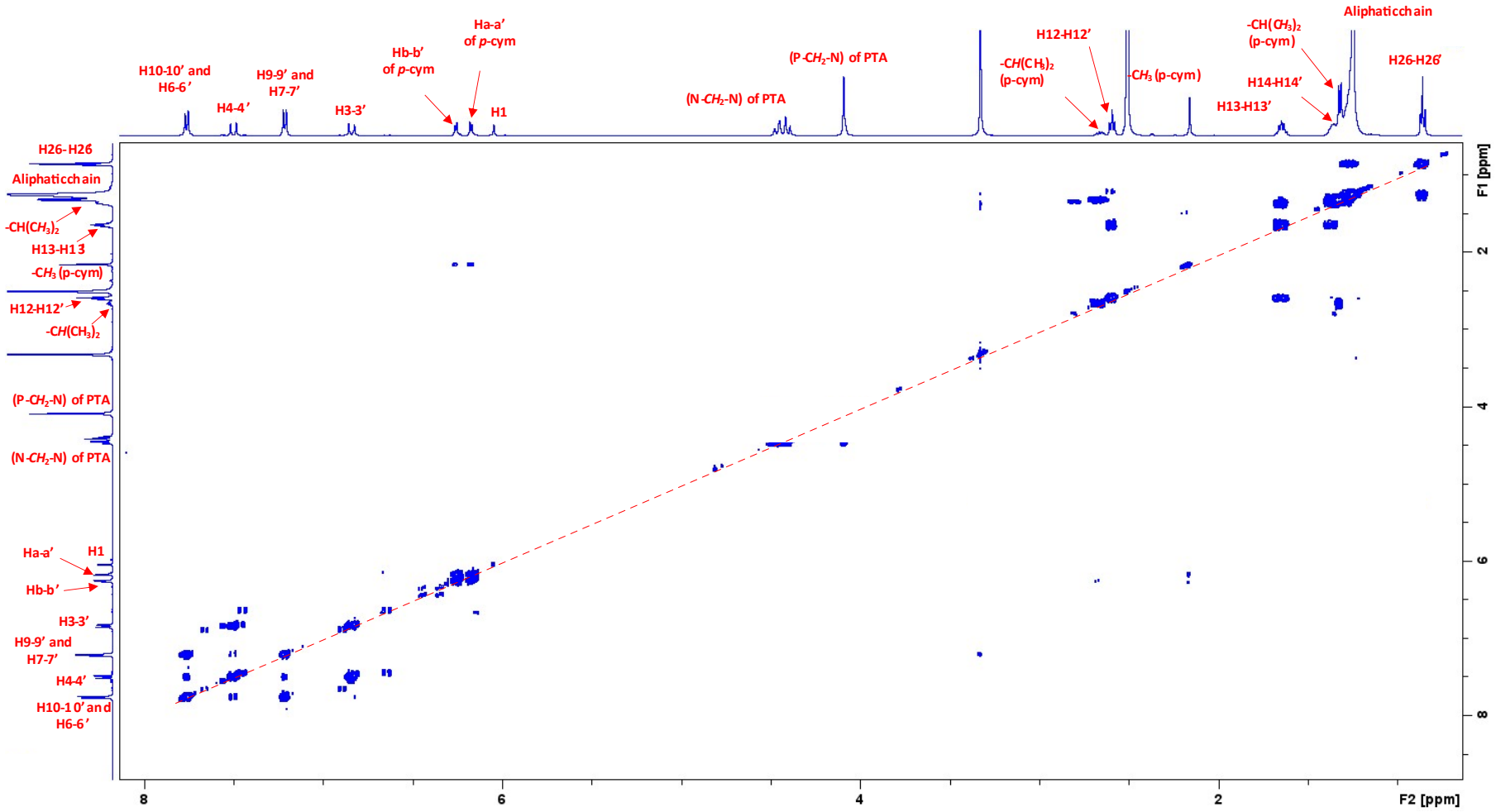

Figure S44.{^{1}H-^{1}H}- COSY NMR of **8** in DMSO at 293 K

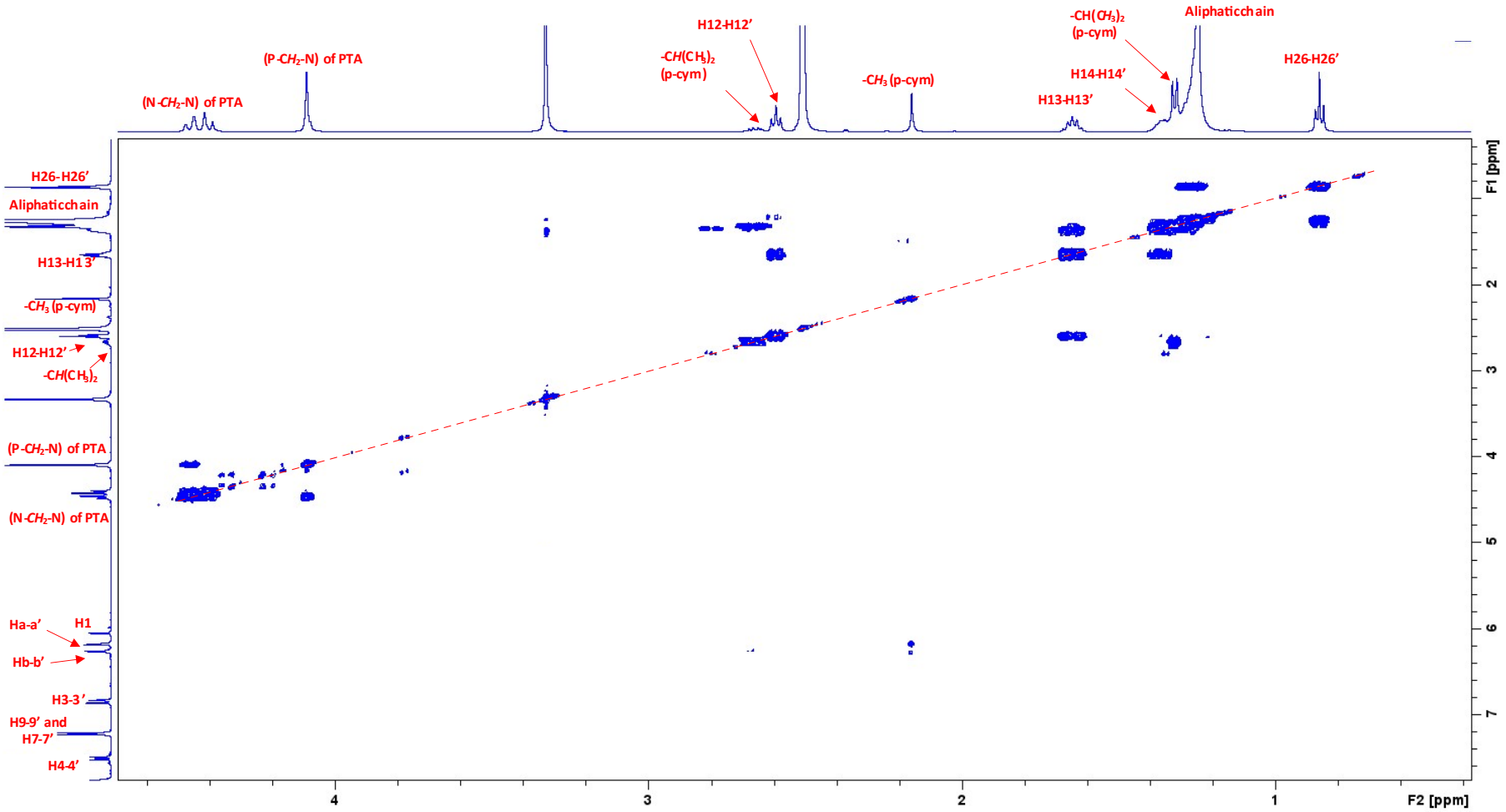

Figure S44 (a). Magnification of {^{1}H-^{1}H}- COSY NMR

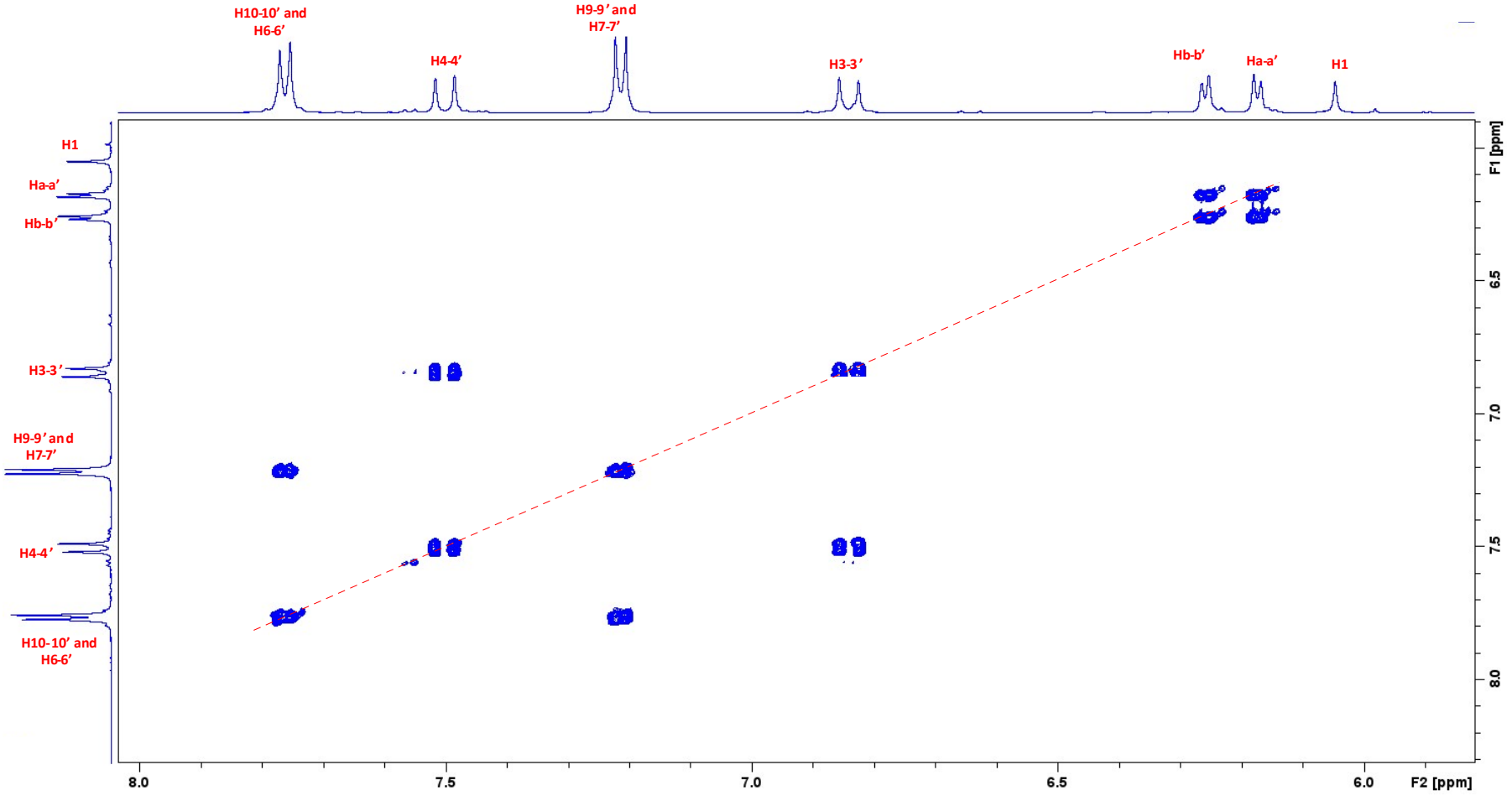

Figure S44 (b). Magnification of {^{1}H-^{1}H}- COSY NMR

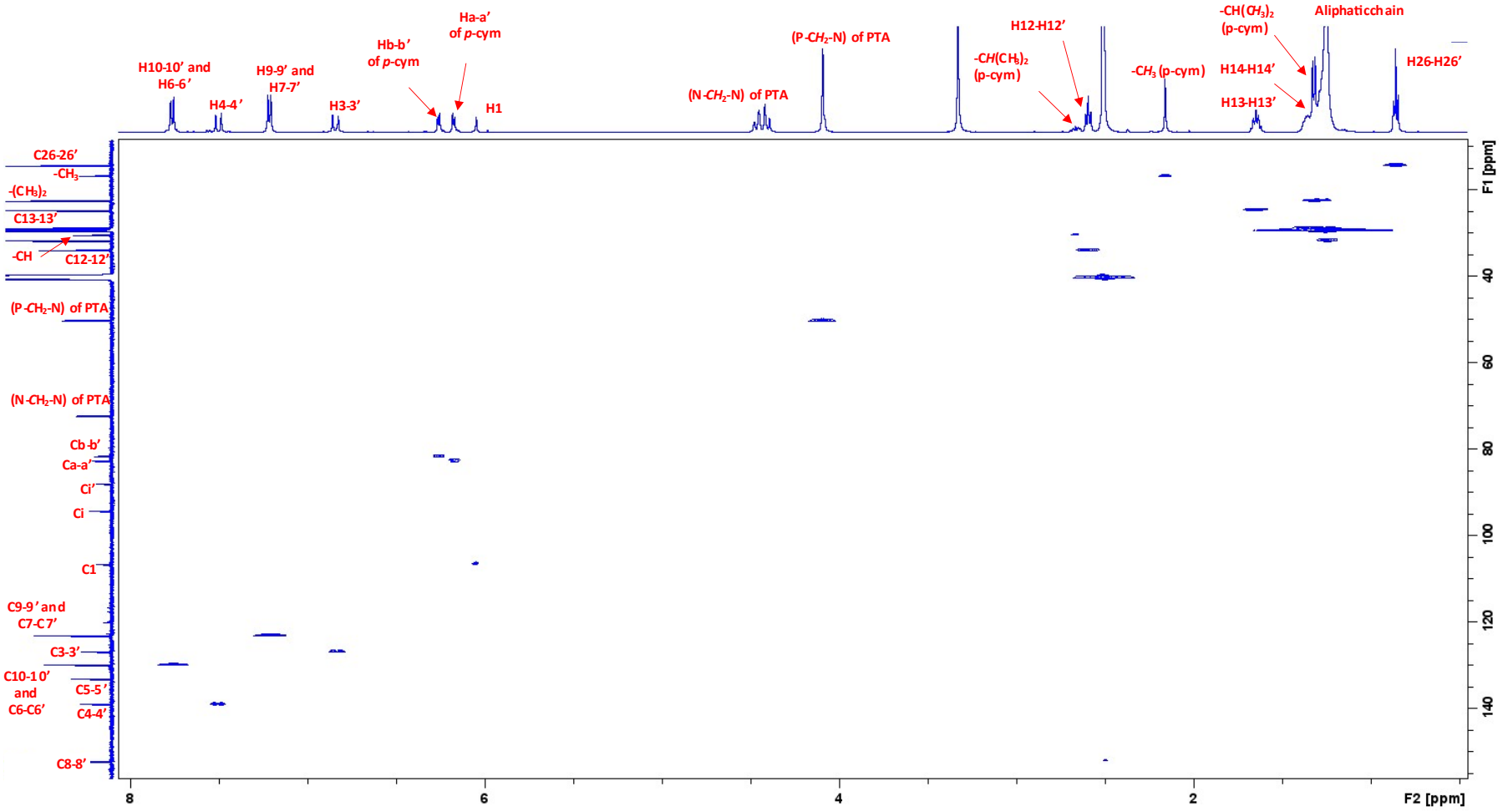

Figure S45. {^{1}H-^{13}C}- HSQC NMR of **8** in DMSO at 293 K

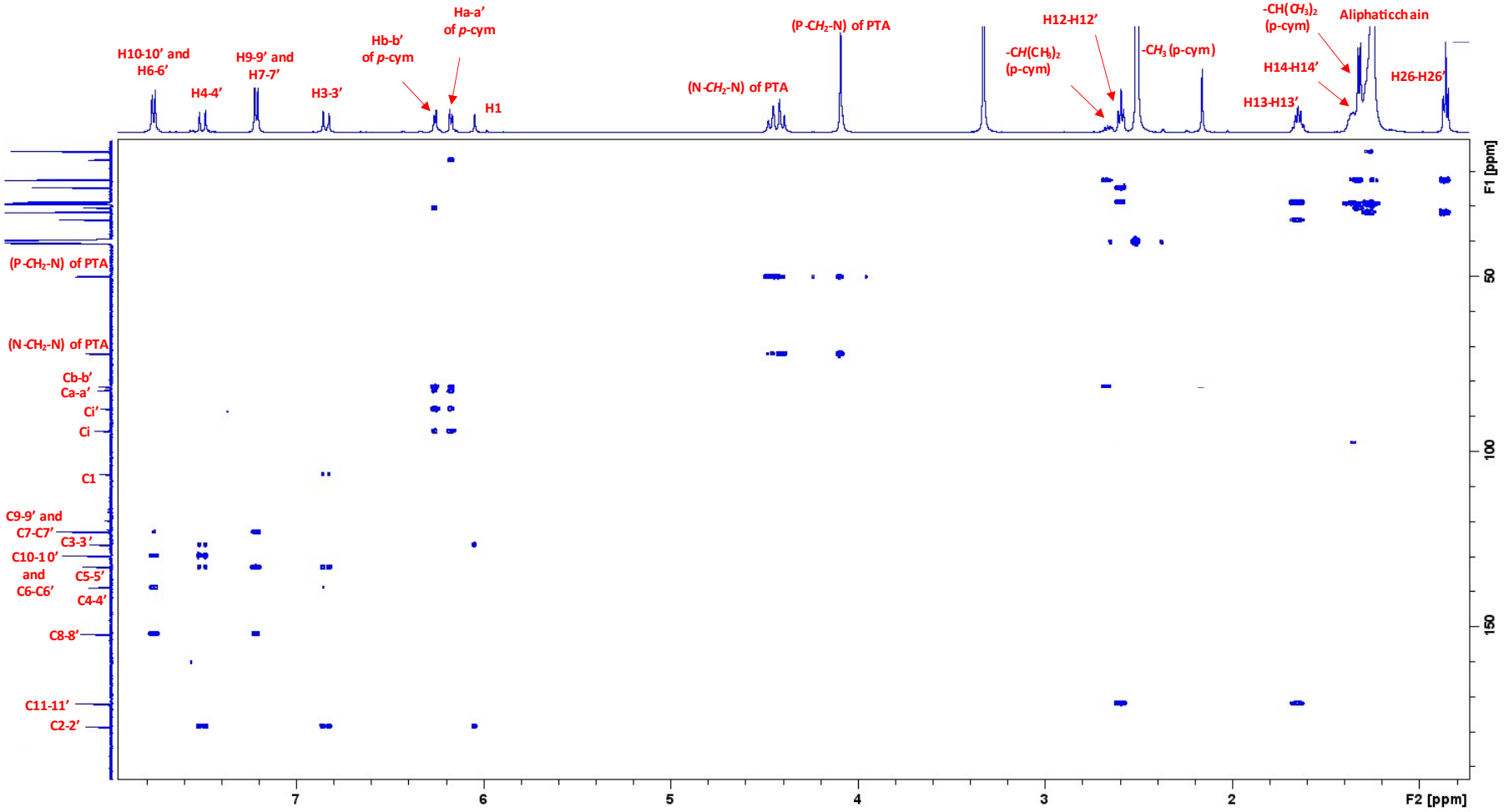

Figure S46. {^{1}H-^{13}C}- HMBC NMR of **8** in DMSO at 293 K

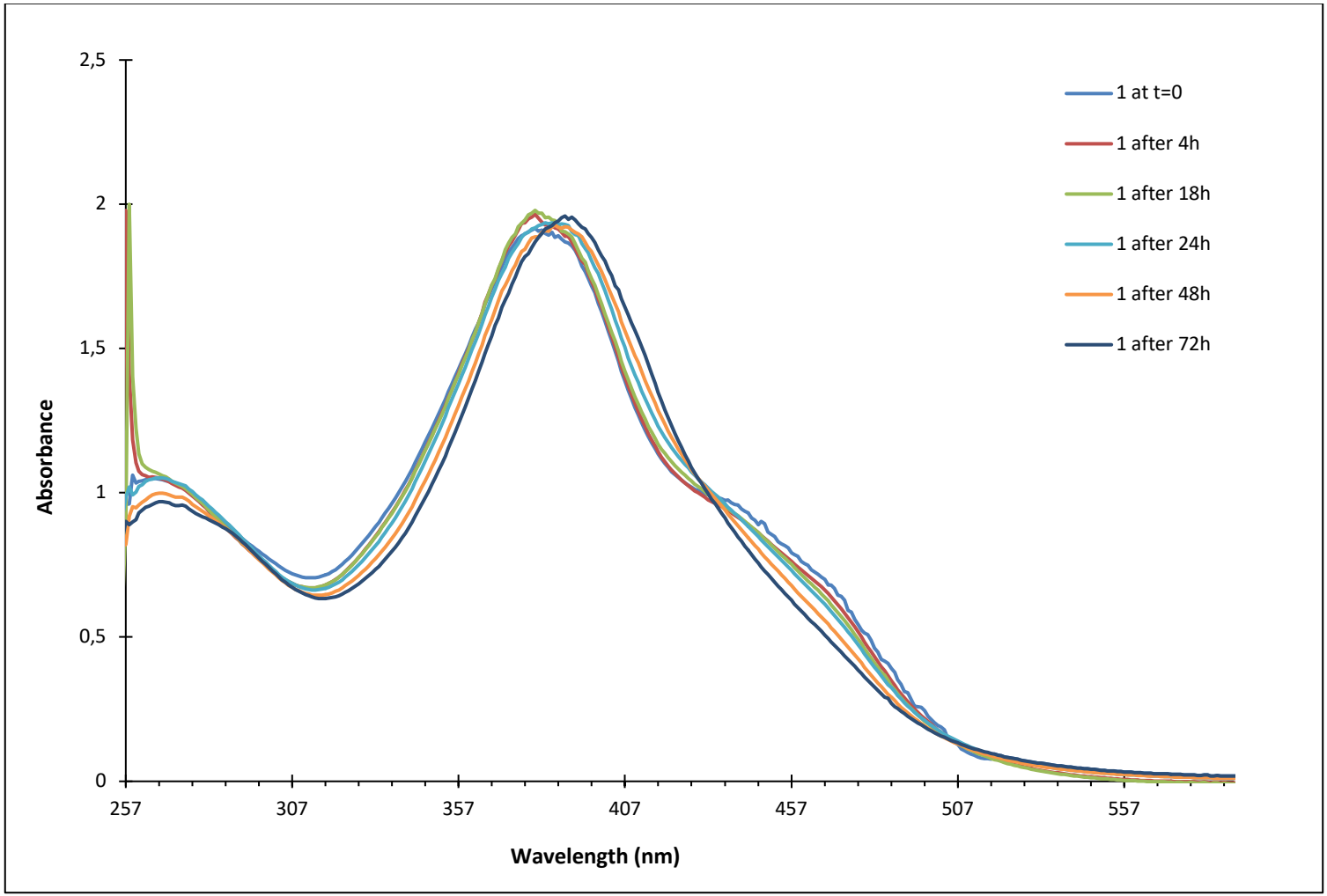

Figure S47. UV-vis spectrum of **1** in DMSO at 293 K

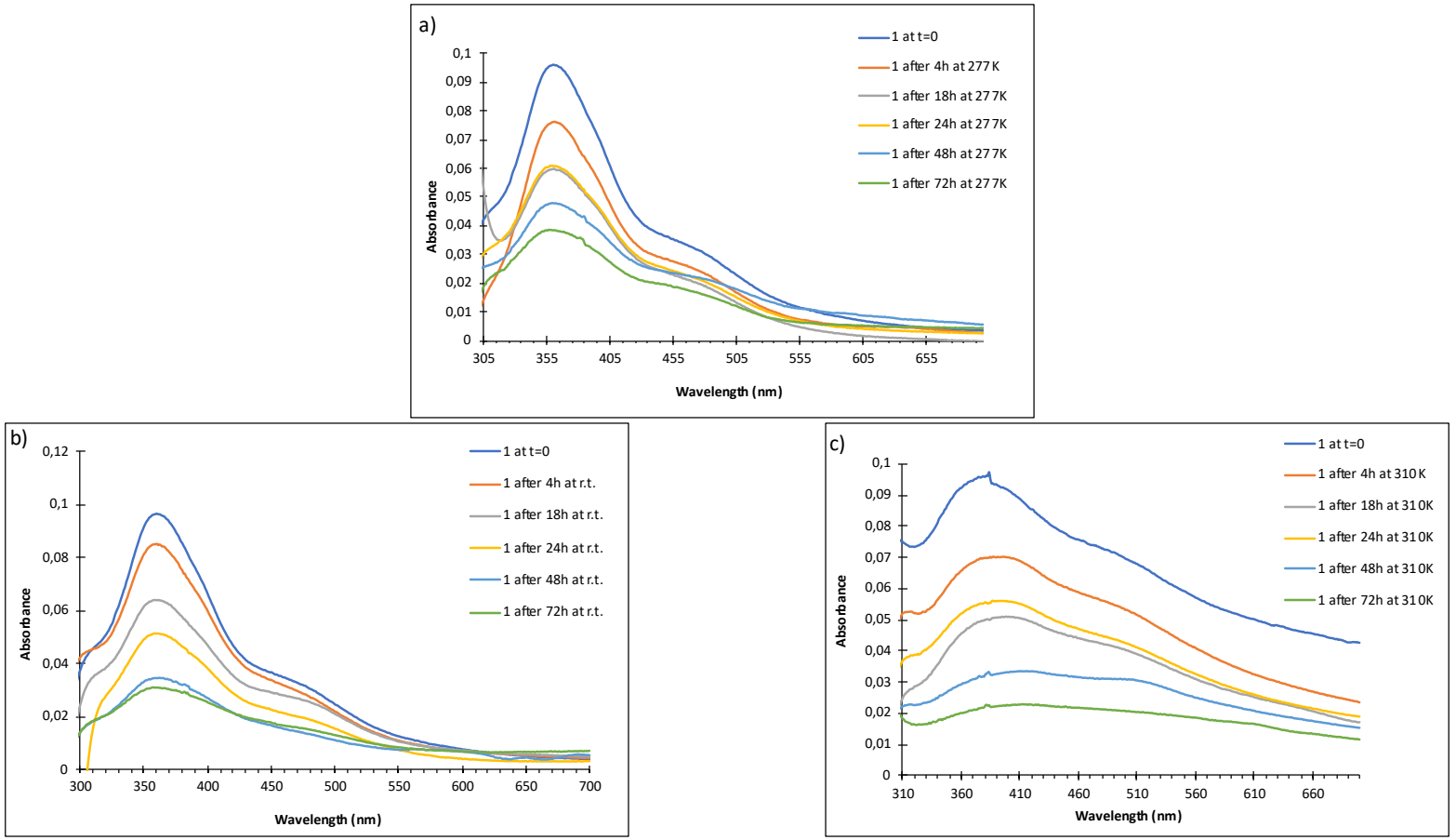

Figure S48. UV-vis spectrum of **1** in DMSO-PBS (5%) at : 277 K (**a**), room temperature (**b**) and 310 K(**c**).

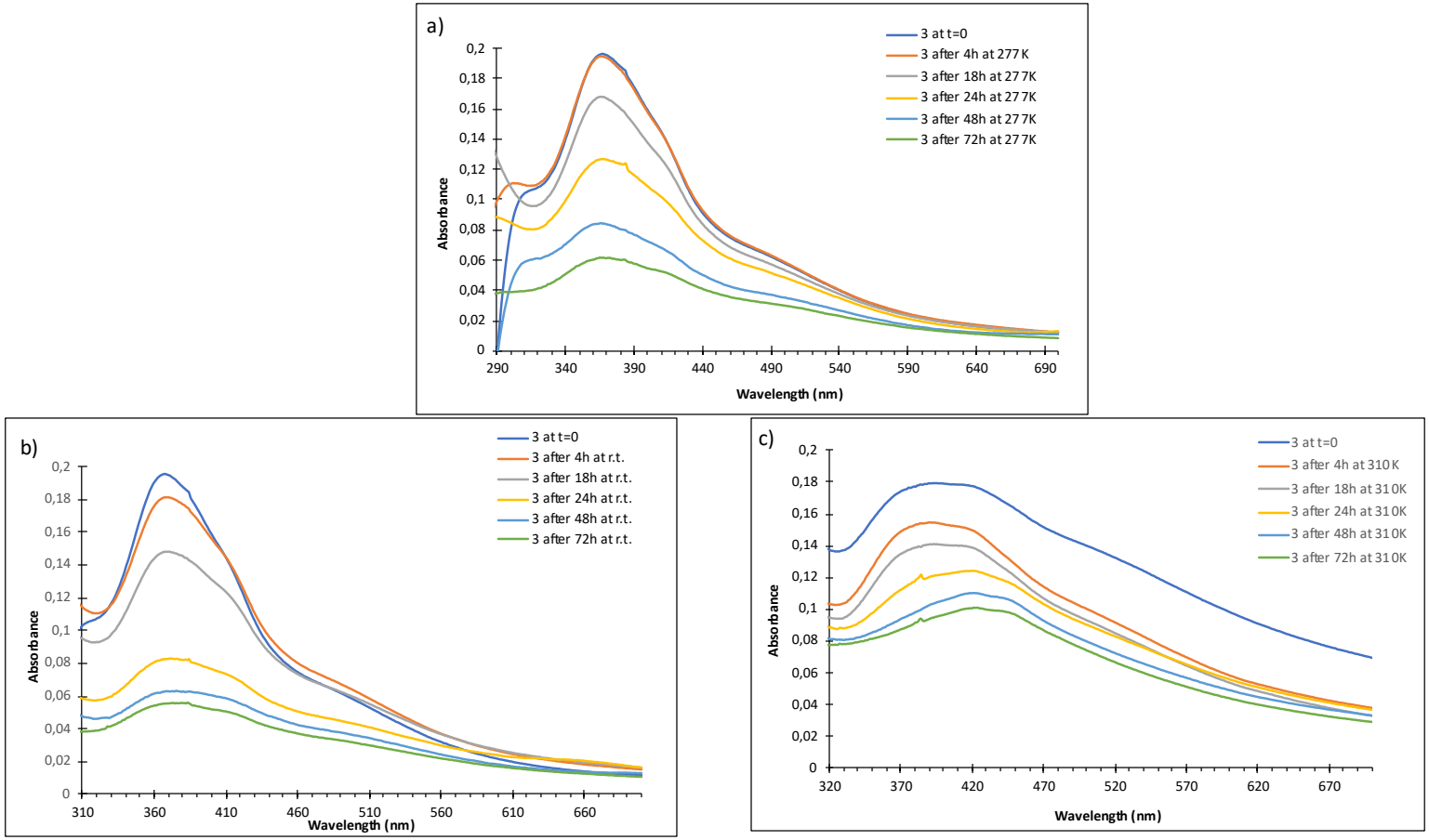

Figure S49. UV-vis spectrum of **3** in DMSO-PBS (5%) at : 277 K (**a**), room temperature (**b**) and 310 K(**c**).

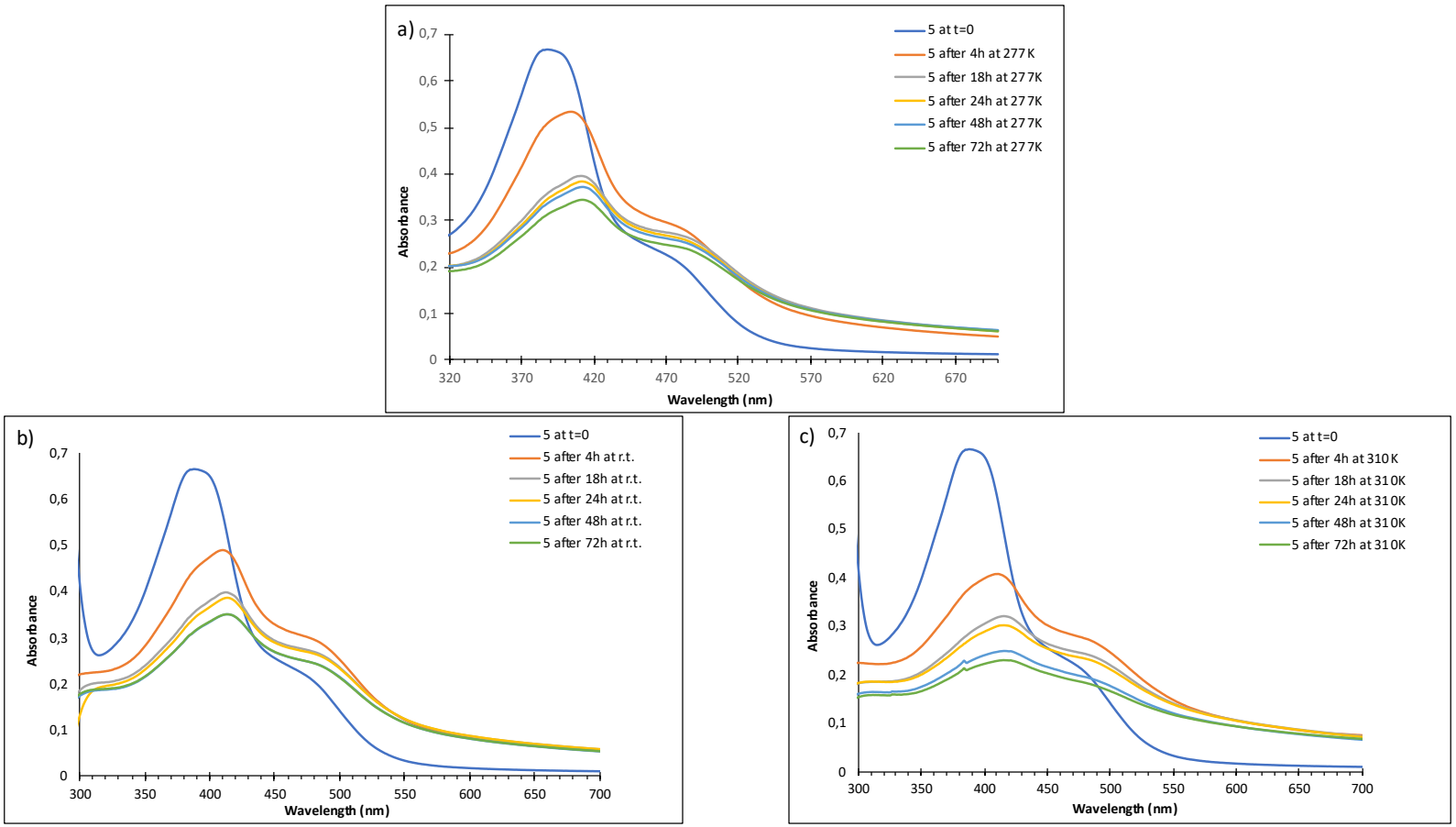

Figure S50. UV-vis spectrum of **5** in DMSO-PBS (5%) at : 277 K (**a**), room temperature (**b**) and 310 K(**c**).

	Compound	A2780	A2780cis	HEK 293T
Ref. [1]	[Ru(cym)(bdcurc)(PTA)]PF_6	0.14 ± 0.05	0.51 ± 0.10	2.0 ± 0.1
4	[Os(cym)(p-bdcurc)Cl]	0.4 ± 0.1	>50	>50
Ref. [1]	[Ru(cym)(curc)(PTA)]SO_3CF_3	0.39 ± 0.16	0.36 ± 0.02	4.5 ± 0.5
2	[Ru(cym)(p-bdcurc)Cl]	0.5 ± 0.2	6.3 ± 7.7	>50
Ref. [1]	[Ru(cym)(bdcurc)(PTA)]SO_3CF_3	0.81 ± 0.14	0.95 ± 0.21	22 ± 4.0
Ref. [1]	[Ru(cym)(curc)(PTA)]PF_6	1.15 ± 0.05	1.18 ± 0.02	30 ± 1.0
Ref. [2]	[Os(cym)(bdcurc)(PTA)]SO_3CF_3	1.9 ± 0.3	2.9 ± 0.2	34±4.0
8	[Os(cym)(p-bdcurc)(PTA)]SO_3CF_3	3.7 ± 2.2	2.3 ± 0.4	3.7 ± 0.8
5	[Ru(cym)(p-curc)(PTA)]SO_3CF_3	6.1 ± 1.7	11.2 ± 0.6	24 ± 80
7	[Os(cym)(p-curc)(PTA)]SO_3CF_3	10.3 ± 2.9	14.9 ± 2.6	21 ± 10
6	[Ru(cym)(p-bdcurc)(PTA)]SO_3CF_3	11.8 ± 2.6	14.4 ± 5.7	21 ± 19
Ref. [3]	[Ru(cym)(curc)Cl]	23.38 ± 3.334	-	-
Ref. [2]	[Os(cym)(curc)(PTA)]SO_3CF_3	32±2.0	35±2.0	69±7.0
Ref. [2]	[Os(cym)(curc)Cl]	36±3.0	39±3.0	70±9.0
3	[Os(cym)(p-curc)Cl]	49 ± 6.0	>50	>50
1	[Ru(cym)(p-curc)Cl]	43 ± 5.0	>50	>50
Ref. [2]	[Os(cym)(bdcurc)Cl]	169 ± 17.0	169 ± 17.0	>200
	RAPTA-C	>100	>100	>100
	Cisplatin	1.1 ± 0.5	7.7 ± 0.9	3.4 ± 1.7

Table S1. IC_{50} values of all curcuminoid complexes for A2780, A2780R and HEK

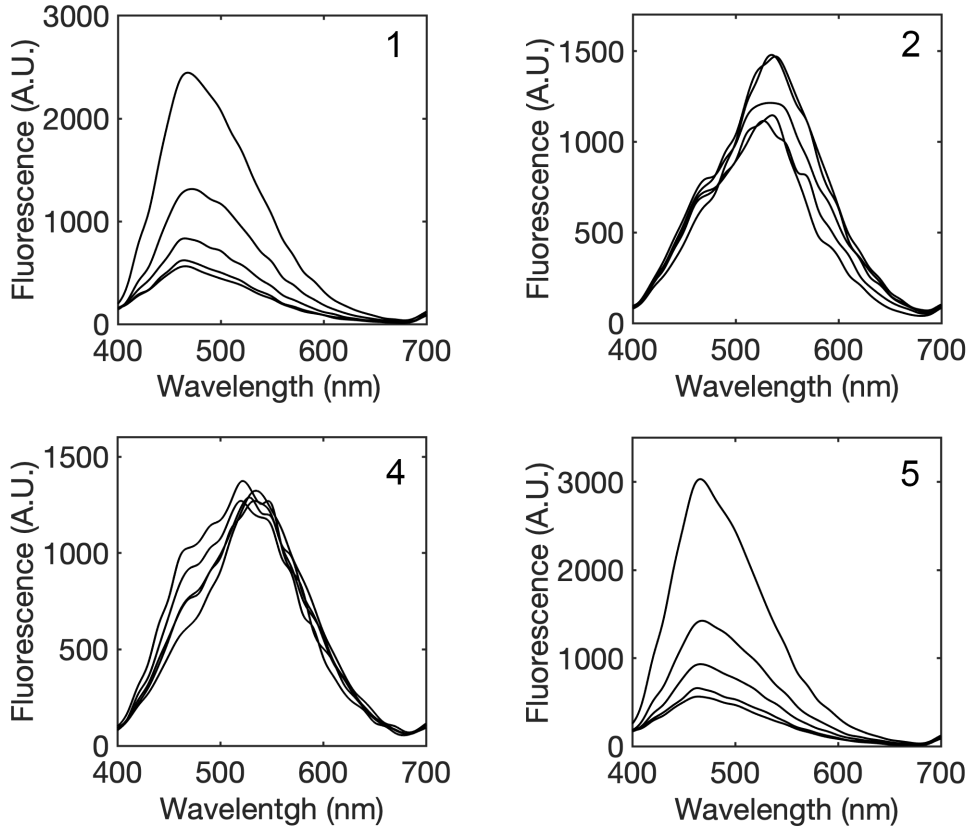

Figure S51. Changes in fluorescence emission spectra of DAPI-DNA complex upon excitation at 338 nm in the presence of increasing concentrations of complexes **1**, **2**, **4** and **5**.

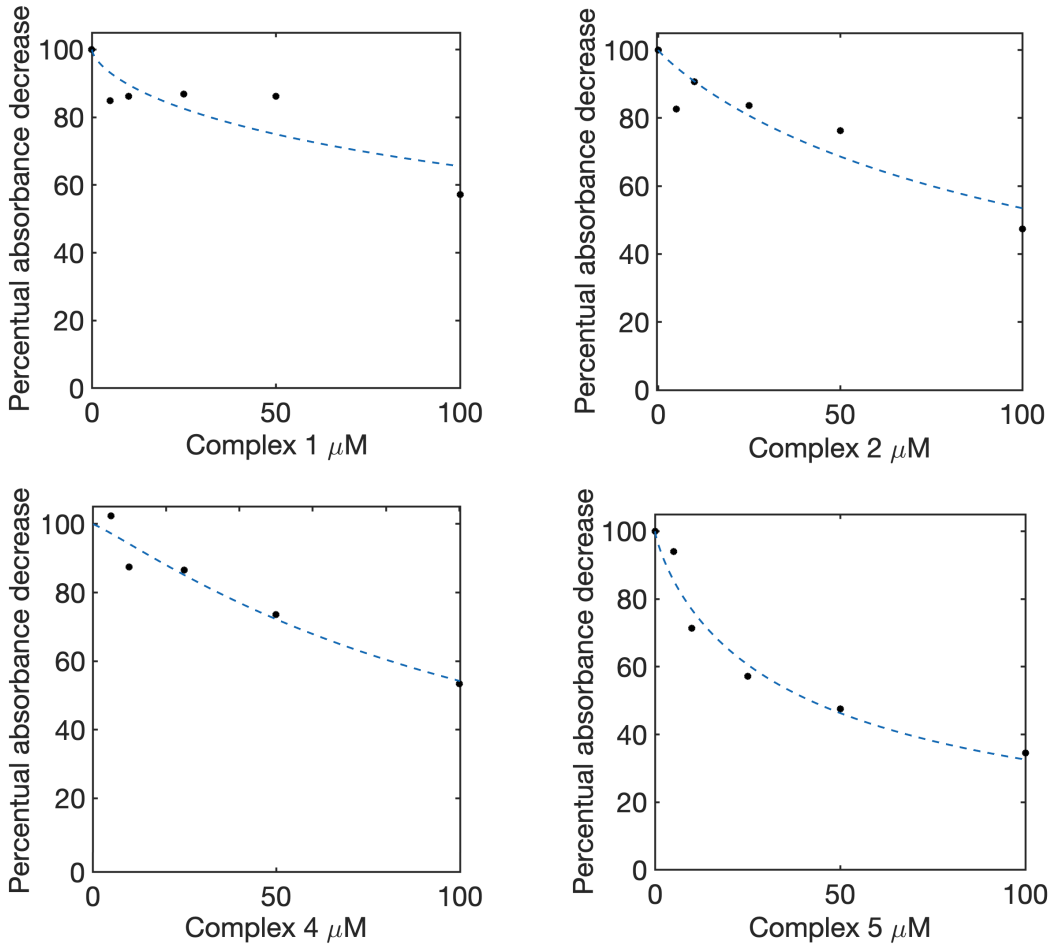

Figure S52. Decrease in absorbance at 600 nm of the MethylGreen-DNA complex in the presence of increasing concentrations of complexes **1**, **2**, **4** and **5**.

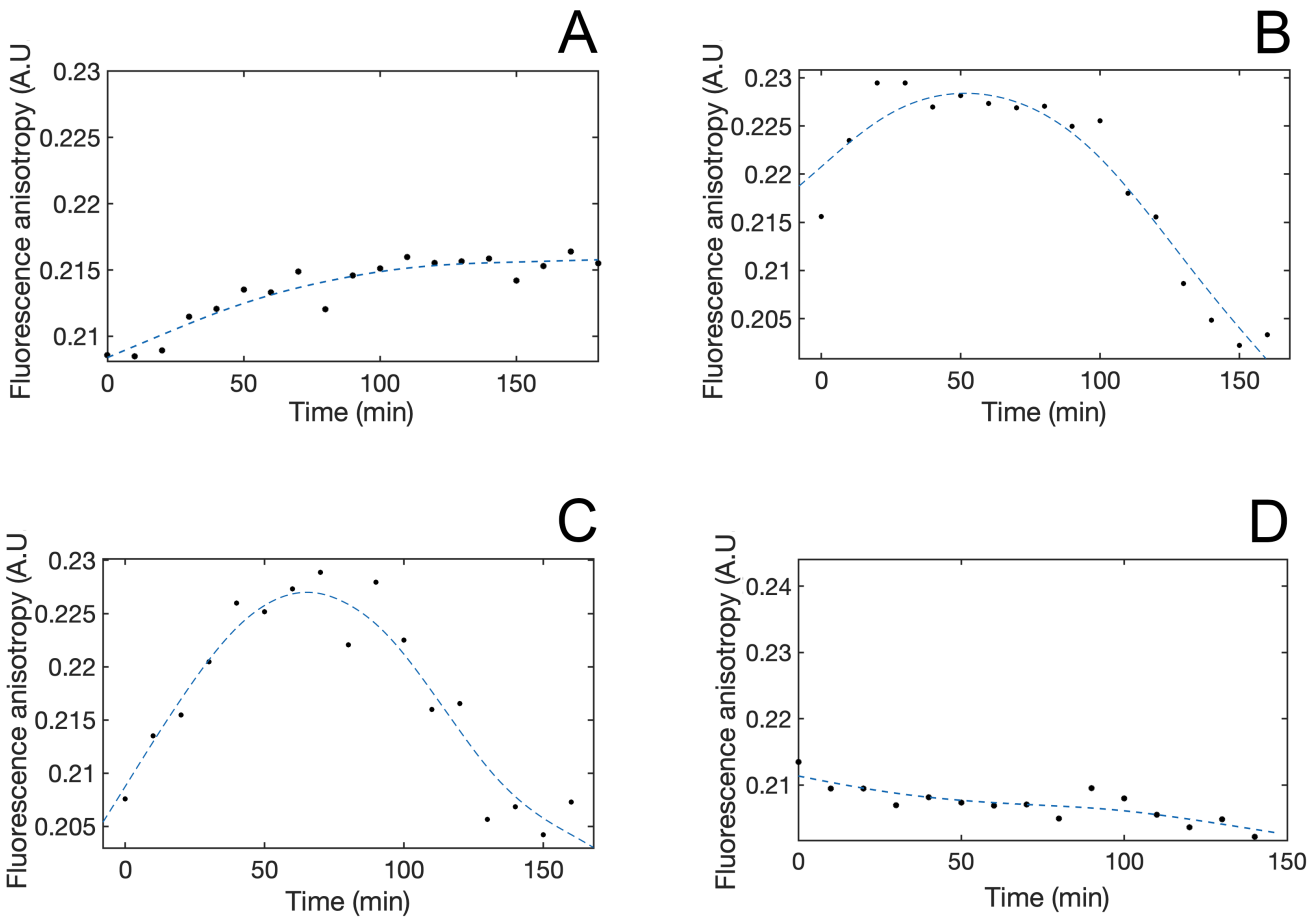

Figure S53. Comparative changes in emission anisotropy with time observed upon cell membrane passage of **1** (Panel A), **2** (Panel B), **4** (Panel C) and **5** (Panel D).

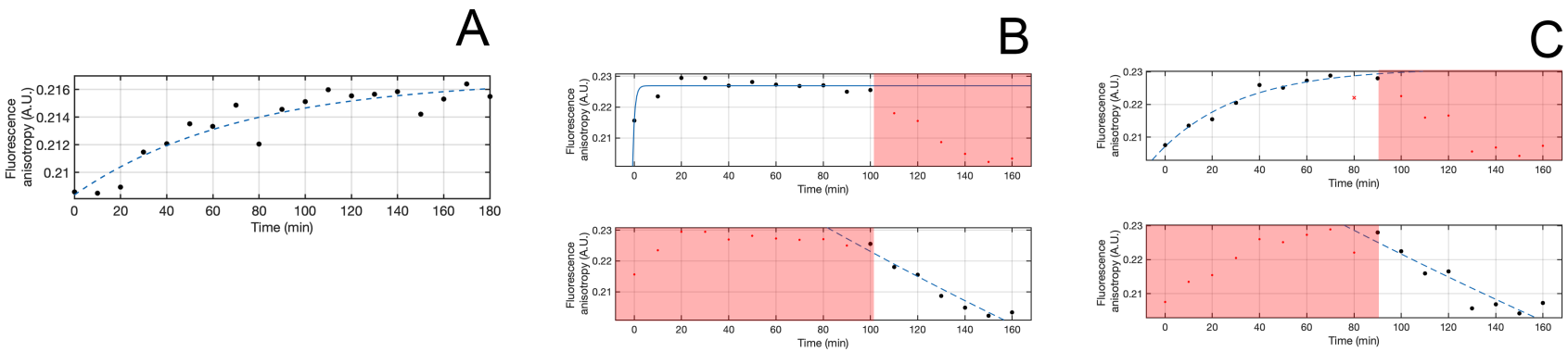

Figure S54. Detailed kinetic analyses of individual membrane entry/release stages of complex **1** (Panel A), complex **2** (Panel B) and complex **4** (Panel C).

	k_{in} (s^{-1})	k_{out} (s^{-1})
Complex 1	0.01 ± 0.005	n/a
Complex 2	0.16 ± 0.05	0.002 ± 0.001
Complex 4	0.03 ± 0.01	0.0015 ± 0.0008
Complex 5	n/a	n/a

Table S2 - Kinetic rate constants corresponding to the main steps of the drug internalization event for complexes **1**, **2**, **4** and **5**.

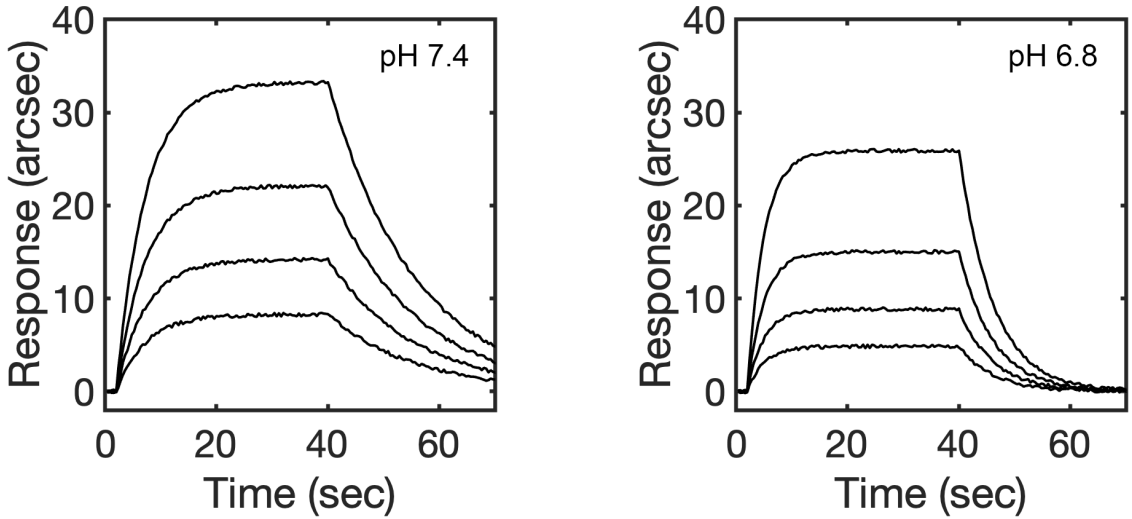

Figure S55. Effect of pH on the serum albumin binding. Representative comparison of the kinetics of binding of complex **5** to surface blocked BSA under different pH conditions.

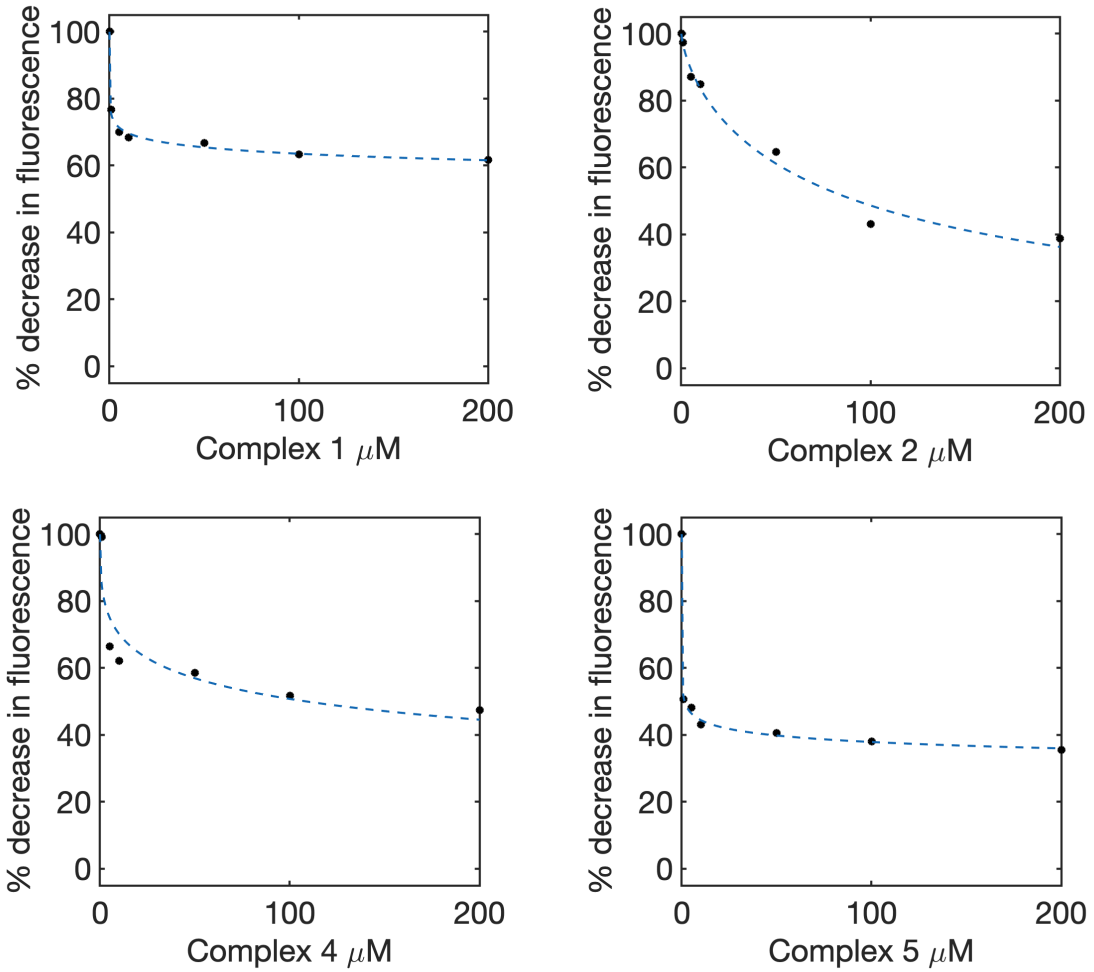

Figure S56. Decrease in intrinsic emission of BSA at 360 nm upon quenching of Trp fluorescence in the presence of increasing concentrations of complexes **1**, **2**, **4** and **5**.

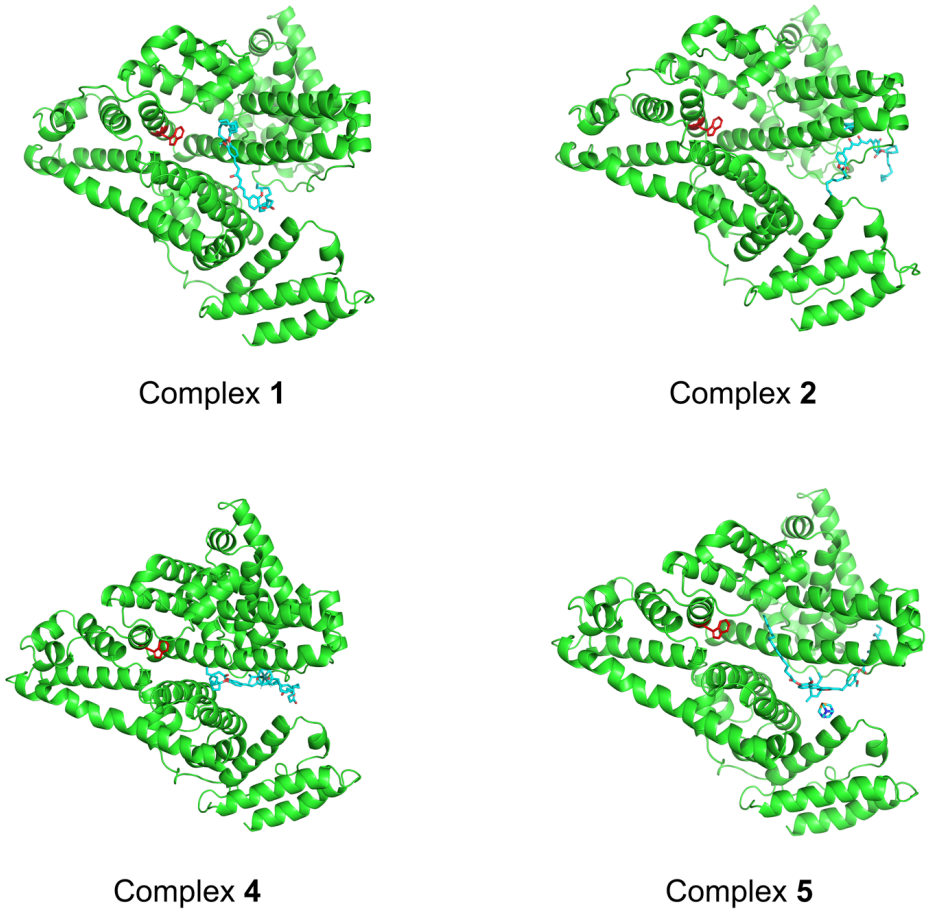

Figure S57. Comparison of the computed binding modes of complexes **1**, **2**, **4** and **5** to crystallographic structure of HSA. Trp residue responsible for the intrinsic fluorescence of HSA is rendered as red stick.

References

(1) Pettinari, R.; Marchetti, F.; Condello, F.; Pettinari, C.; Lupidi, G.; Scopelliti, R.; Mukhopadhyay, S.; Riedel, T.; Dyson, P. J. Ruthenium(II)-Arene RAPTA Type Complexes Containing Curcumin and Bisdemethoxycurcumin Display Potent and Selective Anticancer Activity. *Organometallics* **2014**, *33* (14), 3709–3715.

(2) Pettinari, R.; Marchetti, F.; Di Nicola, C.; Pettinari, C.; Cuccioloni, M.; Bonfili, L.; Eleuteri, A. M.; Therrien, B.; Batchelor, L. K.; Dyson, P. J. Novel Osmium(Ii)-Cymene Complexes Containing Curcumin and Bisdemethoxycurcumin Ligands. *Inorg. Chem. Front.* **2019**, *6* (9), 2448–2457.

(3) Caruso, F.; Rossi, M.; Benson, A.; Opazo, C.; Freedman, D.; Monti, E.; Gariboldi, M. B.; Shaulky, J.; Marchetti, F.; Pettinari, R.; Pettinari, C. Ruthenium-Arene Complexes of Curcumin: X-Ray and Density Functional Theory Structure, Synthesis, and Spectroscopic Characterization, in Vitro Antitumor Activity, and DNA Docking Studies of (p-Cymene)Ru(Curcuminato)Chloro. *J. Med. Chem.* **2012**, *55* (3), 1072–1081.